DOCTOR OF PHILOSOPHY

A transthyretin-related gene and a neuroligin-like gene prevent 6-hydroxydopamine-induced dopaminergic neurodegeneration in C. elegans

Offenburger, Sarah-Lena

Award date:
2016

A transthyretin-related gene and a neuroligin-like gene prevent 6-hydroxydopamine-induced dopaminergic neurodegeneration in *C. elegans*

Sarah-Lena Offenburger

September 2016

Submitted for the degree of Doctor of Philosophy at the University of Dundee

Declarations

I hereby declare that the following thesis is based on the results of work conducted by myself, and that the thesis is of my own composition. Work other than my own is clearly indicated in the text by reference to the relevant researchers or their publications. I conducted all the experiments described in this thesis myself except for the following ones that were done by internship students I supervised: the egg-laying assay and the basal slowing response were done by Eline Jongsma, and the double mutants *jnk-1;ttr-33* and *pmk-1;ttr-33* were created by Theresa Tachie-Menson. The experiments presented here have, to my best knowledge, never been presented for a higher degree or publication excluding where clearly stated and referenced.

Sarah-Lena Offenburger Date

I certify that Sarah-Lena Offenburger has spent eight semesters in research in the Wellcome Trust Centre for Gene Regulation and Expression, University of Dundee, and that she has fulfilled the conditions of Ordinance General No. 39 of the University of Dundee and is qualified to submit the accompanying thesis for the degree of Doctor of Philosophy.

Dr. Anton Gartner Date
Supervisor
University of Dundee

Table of Contents

Abbreviations

6-OHDA	6-Hydroxydopamine
ACh	Acetylcholine
ADE	Anterior deirid
bas	Biogenic amine synthesis related
bp	Base pairs
cat	Abnormal catecholamine distribution
CD	Cluster of differentiation
ced	Cell death abnormality
CEP	Cephalic sensilla
crt	Calreticulin
DA	Dopamine
dat	Dopamine transporter
dop	Dopamine receptor
EMS	Ethyl methanesulfonate
ER	Endoplasmic reticulum
ERAD	Endoplasmic reticulum-associated protein degradation
GABA	Gamma-aminobutyric acid
glit	Gliotactin (*Drosophila* neuroligin-like) homolog
gof	Gain-of-function
hsf	Heat shock factor
ire	IRE1 kinase related
jnk	Jun N-terminal kinase
kgb	Kinase, GLH-Binding
L-DOPA	Levodopa, L-3,4-dihydroxyphenylalanine
lof	Loss-of-function
MAPK	Mitogen-activated protein kinase
mtROS	Mitochondrial reactive oxygen species
NGM	Nematode growth medium
nlg	Neuroligin family
nrf	Nose resistant to fluoxetine
nrx	Neurexin related
PD	Parkinson's disease
pdr	Parkinson's disease related

PDZ	PSD95, Dlg1, Zo-1
pink	PINK (PTEN-induced kinase) homolog)
pmk	P38 MAPK family
PS	Phosphatidylserine
psr	Phosphatidylserine receptor family
ROS	Reactive oxygen species
SEM	Standard error of the mean
skn	Skinhead
SNP	Single nucleotide polymorphism
StDev	Standard deviation
SWIP	Swimming-induced paralysis
tat	Transbilayer amphipath transporters (subfamily IV P-type ATPase)
tsp	Tetraspanin
TTR	Transthyretin
ttr	Transthyretin-related
UPR	Unfolded protein response

Acknowledgements

First and foremost I would like to thank my supervisor Anton Gartner for his encouragement and his support throughout my PhD.

I would also like to thank current members of the Gartner lab – Bin Wang, Simone Bertolini, Bettina Meier, Ye Hong, Victor González-Huici, Federico Pelisch, Remi Sonneville and Yasir Malik – for providing help, for scientific and non-scientific discussions and for making me feel at home. I also want to thank the excellent internship students I supervised – Eline Jongsma and Theresa Tachie-Menson – for their contributions to my project. Furthermore, I thank Neda Masoudi for teaching me when I joined the lab.

I would like to thank my friends for their support, especially Martina and Olesja for the weekly coffee parties.

Also, I want like to thank my committee members Gordon Simpson and Ian Ganley for their suggestions, the Wellcome Trust and Parkinson's UK for funding and Mei Zhen for sharing the mutant strain *nrx-1(wy778).*

Finally, I would like to thank my family for supporting my career and, most importantly, Johannes for sharing the journey.

Abstract

The loss of dopaminergic neurons is a hallmark of Parkinson's disease, the aetiology of which is thought to encompass increased levels of oxidative stress and protein misfolding. We used *C. elegans* to screen for genes that protect dopaminergic neurons from oxidative stress inflicted by 6-hydroxydopamine (6-OHDA) uptake and isolated the neuroligin-like gene *glit-1* and the transthyretin-related gene *ttr-33.* Neuroligins are transmembrane proteins involved in the development and function of synapses. We provide evidence that *glit-1* and the previously identified tetraspanin *tsp-17* are associated with the regulation of dopamine turnover, impacting on 6-OHDA uptake into the neurons: *glit-1* and *tsp-17* mutant sensitivities to 6-OHDA are not additive and both mutants exhibit signs of increased dopamine signalling. A P*glit-1*::GFP transcriptional reporter is expressed in the pharynx, intestine and possibly dopaminergic neurons. The second isolated mutant *ttr-33* in contrast does not display dopamine-related behavioural defects. TTR-33 is likely secreted from the posterior arcade cells in the head and might play a role in cell engulfment, similar to another member of the *C. elegans* transthyretin-related protein family. *C. elegans* dopaminergic neurons seem to be phagocytosed after 6-OHDA intoxication as mutations in the engulfment pathway largely suppress neuronal loss. Before being engulfed, dopaminergic neurons likely undergo a necrosis-like cell death − since mutations in apoptosis pathway genes do not prevent, but rather increase neurodegeneration. In addition, the mutated TTR-33 protein might be more prone to aggregation, similar to its human orthologue transthyretin which is associated with amyloid diseases. Indeed, inhibition of the *C. elegans* unfolded protein response partly alleviates dopaminergic neurodegeneration in the *ttr-33* mutant. On the organismal level, *glit-1, tsp-17* and *ttr-33* mutations cause oxidative stress sensitivity but resistance to protein folding stress. In summary, we think that *tsp-17*, *glit-1* and *ttr-33* play a role in the organismal defence against environmental stress.

1 GENERAL INTRODUCTION

1.1 Dopamine function and signalling

Dopamine is a neurotransmitter that functions in distinct parts of the brain to control diverse behaviours such as movement, attention, cognition and motivation (Schultz, 2007). Dopaminergic signalling parallels classical neurotransmission (**Figure 1**): After production in dopaminergic neurons, dopamine is stored in presynaptic vesicles and released into the synaptic cleft upon intracellular calcium stimulation (Standaert and Galanter, 2008). Upon synaptic release, the neurotransmitter binds to postsynaptic excitatory or inhibitory receptors which stimulate or prevent influx of extracellular Ca^{2+} into the postsynaptic neuron, respectively (Lodish et al., 2000). Dopamine is taken back up into the presynaptic neuron via the dopamine transporter for recycling or degradation (Standaert and Galanter, 2008). Erroneous dopamine signalling is associated with distinct disorders such as Parkinson's disease (PD), attention deficit hyperactivity disorder (ADHD) and Schizophrenia (Schultz, 2016).

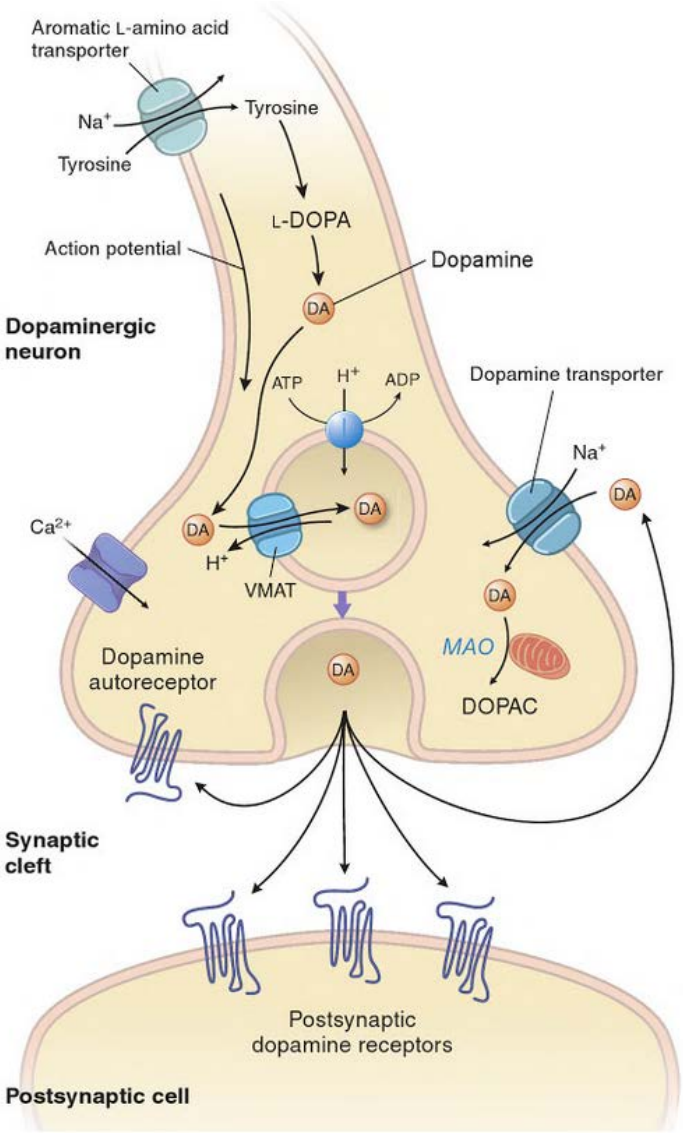

Figure 1: Dopaminergic metabolism, recycling and degradation – from (Standaert and Galanter, 2008).
Dopamine (DA) synthesis starts with the amino acid tyrosine and produces the intermediate product L-3,4-dihydroxyphenylalanine (L-DOPA). Dopamine is packed into secretory vesicles by the vesicular monoamine transporter (VMAT), an antiporter which requires the action of a proton ATPase to establish a gradient of protons in the vesicle. When an action potential arrives, the influx of Ca^{2+} triggers dopamine vesicle release into the synaptic cleft where dopamine can bind to postsynaptic receptors or presynaptic autoreceptors. Most of the dopamine is then taken up into the dopaminergic neuron again via the dopamine transporter which co-transports Na^{+}. Back inside the neuron, dopamine can be degraded to 3,4 – dihydroxyphenylacetic acid (DOPAC) by monoamine oxidases (MAO).

1.2 Pathophysiology of Parkinson's disease

1.2.1 Parkinson's disease symptoms and occurrence

Parkinson's disease (PD) is the second most common neurodegenerative disorder and has a prevalence of 1% in the population over 60 (Lau and Breteler, 2006). The characteristic motor symptoms of PD – resting tremor, poor balance, rigidity and slow involuntary movement – are caused by the progressive loss of dopaminergic neurons in the substantia nigra (Duda et al., 2016). In addition, neurodegeneration also occurs in other parts of the brain, relating to some of the non-motor symptoms of the disorder (Chaudhuri et al., 2011). There is no cure for PD to date and even the 'gold standard' treatment, the supply of the dopamine precursor L-DOPA (L-3,4-dihydroxyphenylalanine), leads to severe side effects (Sarkar et al., 2016). To improve therapy or even prevent disease onset, the molecular mechanisms of PD need to be better understood.

The aetiology of PD is multifactorial with the majority of disease cases being evoked by the interplay of one or multiple genetic defects and environmental factors (Klein and Westenberger, 2012). Less than 10% of PD patients report a positive family history while the majority of instances are sporadic (Thomas and Beal, 2007). Furthermore, single gene mutations only account for about 30% of familial and 3-5% of sporadic PD incidences (Klein and Westenberger, 2012). Among these monogenetic PD loci there are recessive ones such as PINK1, parkin and DJ-1 – for which both gene copies need to be mutated to evoke a phenotype and which are therefore associated with gene loss-of-function. In addition, there are dominant PD loci such as α-synuclein and LRRK2 – for which a single mutant copy is sufficient to induce a phenotype (Klein and Westenberger, 2012). A dominant phenotype can be provoked by a) haploinsufficiency, i.e. a single copy of the gene is not enough to provide function, b) a dominant negative effect, i.e. the mutant allele interferes with the normal allele, or c) a gain-of-function mutation that makes the gene product adopt an abnormal function (Klein and Westenberger, 2012). In addition to genetic causes, rare cases of sporadic PD incidences can

be purely connected to environmental exposure, such as the accidental ingestion of 1-methyl-4-phenyl-1,2,3,6-tetrahydropyridine (MPTP) (Duda et al., 2016). Since there is a substantial overlap of clinical features between genetic and sporadic PD, common pathophysiological mechanisms might underlie neurodegeneration in both forms of the disease (Haddad and Nakamura, 2015). Shared factors such as mitochondrial and lysosomal dysfunction, metabolic stress and impaired Ca^{2+} homeostasis are thought to reinforce each other and trigger PD (Duda et al., 2016).

PD is discussed to reflect a form of accelerated aging (Duda et al., 2016). Hallmarks of aging such as mitochondrial dysfunction and loss of proteostasis (López-Otín et al., 2013) also represent risk factors for PD (Duda et al., 2016). Furthermore, aging itself increases the chances to develop PD, and neurons vulnerable to degeneration with age are also vulnerable to degeneration in PD (Duda et al., 2016).

1.2.2 Oxidative stress in Parkinson's disease

Dopaminergic neurons, especially those in the substantia nigra, seem to be particularly sensitive to PD risk factors and one reason for this could be dopamine metabolism itself (Caudle et al., 2008). Cytosolic dopamine can auto-oxidise to highly neurotoxic compounds and reactive oxygen species (ROS) such as $OH\cdot$,$O\cdot^-_2$ and H_2O_2 (Caudle et al., 2008). Synaptic vesicle storage of dopamine can prevent cellular damage, but this safe-keeping seems diminished in neurons in the substantia nigra and is further disrupted by PD risk factors (Caudle et al., 2008). In addition, the enzymatic degradation of dopamine results in the production of H_2O_2 and this additional source of ROS might increase the vulnerability of dopaminergic neurons even further (Caudle et al., 2008).

An imbalance between the production of ROS and the endogenous defence against these molecules leads to 'oxidative stress' (Finkel and Holbrook, 2000), a major risk factor for PD (Duda et al., 2016). ROS can damage proteins, lipids and mitochondria, leading to a self-

accelerating loop of cellular damage and ultimately cell death (Duda et al., 2016). Oxidative stress defence systems have evolved to prevent damage to the cell and the sulphur-containing amino acids cysteine and methionine form part of important antioxidants (Kim et al., 2014; Lu and Holmgren, 2014). Consistent with the idea that increased levels of oxidative stress are a major component in the pathogenesis of PD, the substantia nigra of PD patients was reported to contain decreased levels of the cysteine-containing antioxidant glutathione (Sian et al., 1994). In addition, mutation of DJ-1, a protein which acts as a redox sensor or antioxidant protein, is associated with the development of PD (Abou-Sleiman et al., 2006). Finally, oxidative stress induced by the herbicide paraquat (Tanner et al., 2011; Wang et al., 2011) and exposure to pesticides is associated with a higher incidence of PD (Priyadarshi et al., 2001). In summary, there is evidence that increased oxidative damage raises the risk to develop PD (Haddad and Nakamura, 2015).

1.2.3 Mitochondrial dysfunction in Parkinson's disease

The mitochondrial electron transport chain is one of the main energy sources and is assumed to generate most of the reactive oxygen species (ROS) in the cell (Hekimi et al., 2011; Sena and Chandel, 2012). Mitochondrial stress – induced by excessive demand for mitochondrial functions or by mitochondrial damage – is discussed to contribute to PD (Haddad and Nakamura, 2015). Dysfunction of mitochondria leads to decreased cellular energy production (Haddad and Nakamura, 2015). However, the substantia nigra population of dopaminergic neurons might have unusually high energy requirements − since they target more neurons than neighbouring dopaminergic neurons that are unaffected by PD (Haddad and Nakamura, 2015). In addition, dopaminergic neurons in the substantia nigra use an unusual and energy-intensive Ca^{2+} gradient to exert their pacemaking activity (Haddad and Nakamura, 2015) – a regular and intrinsically generated firing pattern with low frequency (Duda et al., 2016). Remarkably, the redox sensor DJ-1, which is linked to the development of PD, was reported to attenuate oxidative stress evoked by this pacemaking function (Guzman et al., 2010). In

addition to reducing cellular energy production, interference with the mitochondrial electron transport chain also leads to the leakage of electrons and subsequently to increased generation of ROS (Haddad and Nakamura, 2015). Several lines of evidence directly link inhibition of the electron transport chain to the development of PD (Haddad and Nakamura, 2015). A metabolite of the drug MPTP inhibits complex I of the electron transport chain (Nicklas et al., 1985) and induces selective dopaminergic neurodegeneration in the substantia nigra as well as PD symptoms (Duda et al., 2016). Another complex I inhibitor, rotenone, leads to PD-like symptoms (including Lewy body-like aggregates) in rats (Betarbet et al., 2000). Finally, a complex I deficiency was identified in the substantia nigra of PD patients (Schapira et al., 1989).

Apart from their function in energy production, mitochondria are involved in the regulation of calcium signalling and cell death (Kroemer et al., 2007). Intact mitochondria maintain their membrane potential and sustain cellular calcium homeostasis (Haddad and Nakamura, 2015). In apoptotic and necrotic cells, however, the mitochondrial membrane potential is lost, the mitochondrial permeability transition pores open and apoptogenic proteins and Ca^{2+} are released (Brenner and Moulin, 2012).

Damaged mitochondria display a loss of membrane potential and can be disposed of by a specific form of autophagy termed mitophagy (Kazlauskaite and Muqit, 2015; Pickrell and Youle, 2015; Ploumi et al., 2016). The autosomal recessive PD loci PINK1 and parkin (Kitada et al., 1998; Valente et al., 2004) mediate mitophagy and a malfunction of this process seems to contribute to PD (Kazlauskaite and Muqit, 2015; Pickrell and Youle, 2015; Ploumi et al., 2016). Mitochondrial membrane depolarisation activates the kinase PINK1, which then phosphorylates ubiquitin (Kane et al., 2014; Kazlauskaite et al., 2014a; Koyano et al., 2014), as well as parkin within its autoinhibitory ubiquitin-like domain (Kondapalli et al., 2012; Shiba-Fukushima et al., 2012). Both phosphorylation events stimulate parkin E3 ubiquitin ligase

activity (Kazlauskaite et al., 2014a, 2014b, 2015; Koyano et al., 2014; Ordureau et al., 2014), leading to the ubiquitination of mitochondrial substrates to trigger mitophagy (Kazlauskaite and Muqit, 2015).

Drosophila was the first model organism in which PINK1 or parkin mutants were shown to possess severe mitochondrial defects (Clark et al., 2006; Park et al., 2006). Inhibition of the parkin-antagonising deubiquitinase USP30 reduces mitochondrial and behavioural defects of PINK1 or parkin-deficient flies (Bingol et al., 2014). Furthermore, USP30 knockdown specifically in dopaminergic neurons protects flies against toxicity of the mitochondrial toxin paraquat (Bingol et al., 2014). A connection between mitochondrial damage and the generation of oxidative stress is supported by data showing that neurodegeneration in parkin null flies is enhanced in glutathione S-transferase null mutants (Whitworth et al., 2005). In addition, parkin null flies exhibit increased oxidative damage and a higher innate immune response signalling (Greene et al., 2005). Remarkably, *Drosophila* with a mutation in the PD risk gene and redox sensor DJ-1 show similar defects as PINK1 and parkin mutants and upregulation of DJ-1 can ameliorate PINK1 mutant phenotypes (Hao et al., 2010).

More recently, also *C. elegans* PINK1/*pink-1* and parkin/*pdr-1* mutants have been shown to exhibit defects in mitophagy and a compromised stress resistance (Palikaras et al., 2015). Inhibition of *C. elegans* mitophagy leads to increased production of mitochondrial ROS and higher levels of cytoplasmic calcium (Palikaras et al., 2015). These results from the *C. elegans* mitophagy model further support the link between mitochondrial damage and oxidative stress production.

In mice, parkin deficiency results in reduced mitochondrial respiratory capacity and increased oxidative damage, but does not lead to neurodegeneration on its own (Abou-Sleiman et al., 2006). Therefore, even in the background of compromised mitochondrial function, additional insults might be needed to trigger PD-like symptoms (Abou-Sleiman et al., 2006).

1.2.4 Calcium homeostasis in Parkinson's disease

Environmental toxins that cause mitochondrial dysfunction can worsen defects in mitochondrial Ca^{2+} buffering capacity (Wojda et al., 2008). Remarkably, age-related Ca^{2+} dyshomeostasis has been proposed to be the dominant condition causing neurodegeneration in sporadic PD (Wojda et al., 2008). In support of a damaging effect of cytosolic Ca^{2+}, L-type calcium channel blockers that inhibit cellular Ca^{2+} entry reduce the risk of developing PD (Duda et al., 2016). In addition, neurons that are vulnerable in PD express lower levels of the cytosolic Ca^{2+}-binding protein calbindin (Duda et al., 2016). Thus, in the substantia nigra Ca^{2+} needs to be mainly buffered via uptake into mitochondria, lysosomes or the endoplasmic reticulum (ER), and this likely imposes additional stress on these organelles (Duda et al., 2016).

1.2.5 Protein folding and degradation in Parkinson's disease

A common hallmark for sporadic and familial cases of PD is the observation of Lewy bodies – abnormal intracellular protein aggregates in surviving dopaminergic neurons (Spillantini et al., 1997). The main component of Lewy bodies is α-synuclein (Spillantini et al., 1997), a protein which is encoded by an autosomal dominant PD locus (Polymeropoulos et al., 1997). α-synuclein has been shown to prevent neurodegeneration (Chandra et al., 2005) and mutations are thought to increase the propensity of the protein to polymerise and form fibrils (Bertoncini et al., 2005). Hence, PD might be triggered by reduced α-synuclein protection or by a gain-of-function mechanism based on α-synuclein aggregation. If the second scenario is the case, Lewy bodies may represent an attempt to encapsulate these toxic α-synuclein derivates in the cell (Chen and Feany, 2005). Furthermore, dopamine was shown to modulate α-synuclein aggregation, providing an explanation for the selective dopaminergic neurodegeneration in an α-synuclein mutant background (Conway et al., 2001).

Generally, the imbalance of protein synthesis and protein degradation may cause accumulation of defective proteins, leading to cell damage and ultimately cell death (Hipp et

al., 2014). If there is an accumulation of unfolded or misfolded proteins in the ER – the major site for protein synthesis and maturation – the unfolded protein response (UPR) is triggered to prevent detrimental cellular effects (Urra et al., 2013). The UPR first increases protein folding and clearance capacity to reduce the amount of misfolded proteins and to restart translation (Urra et al., 2013). However, under chronic 'ER stress', the UPR triggers apoptosis to eliminate irreversibly damaged cells, possibly by controlling cellular ROS production and ER calcium release (Urra et al., 2013). The E3 ubiquitin ligase parkin tags proteins for proteasomal degradation, therefore a mutation in the autosomal recessive PD locus is expected to exacerbate ER stress (Varma and Sen, 2015). In addition to the cellular protection conferred by the UPR, the autophagy and the proteasome pathway survey for and eliminate aggregated or dysfunctional proteins (Charmpilas et al., 2015). Several PD risk genes are associated with the autophagy-lysosome pathway, including the lysosomal glucocerebrosidase (GBA), and likely lead to defects in intracellular protein degradation (Duda et al., 2016). In addition, several pro-apoptotic proteins are normally degraded by the proteasome; thus, if proteasomal function is inhibited, cell death can be triggered (Abou-Sleiman et al., 2006).

1.2.6 Interplay of Parkinson's disease mechanisms

Besides α-synuclein, LRRK2 (Leucine-rich repeat kinase 2) is the second confirmed autosomal dominant PD locus for which a gain-of-function mechanism would be expected. Indeed, one of the LRRK2 disease mutations was shown to stimulate kinase activity in vitro (Jaleel et al., 2007), as well as in heterozygous and homozygous mutant mice (Yue et al., 2015). Furthermore, the *Lrrk2* mutant mice exhibited mitochondrial abnormalities and a reduction in induced dopamine release (Yue et al., 2015). The physiological and pathological roles of LRRK2 are still unclear, but accumulating evidence suggests that LRRK2 mutations are linked to mitochondrial dysfunction and abnormal autophagy (Rosenbusch and Kortholt, 2016). In addition, it was reported that LRRK2 is highly expressed in immune cells and that stimulation

of the Toll-Like Receptor innate immune pathway leads to LRRK2 phosphorylation (Dzamko et al., 2012).

The mechanisms that are assumed to underlie PD − such as increased oxidative stress, protein misfolding and aggregation and Ca^{2+} dyshomeostasis − exacerbate each other during disease development (Duda et al., 2016). Primary and secondary roles can be difficult to disentangle: proteasomal stress in neurons for example can result in increased sensitivity to complex I inhibition, and complex I defects can result in decreased proteasome activity (Höglinger et al., 2003; Sullivan et al., 2004). There is also a connection between oxidative stress and ER stress, and both can lead to increased Ca^{2+} leakage from the ER (Malhotra and Kaufman, 2007). Furthermore, autophagy seems required to overcome oxidative stress conditions (Filomeni et al., 2015) − whereas dysfunctional autophagy can lead to the accumulation of damaged mitochondria (Lee et al., 2012).

In summary, the loss of dopaminergic neurons is very likely due to a combination of exogenous stressors and genetic predisposition that renders the cells less capable of dealing with the stress (Abou-Sleiman et al., 2006).

1.3 *C. elegans* 6-OHDA-induced dopaminergic neurodegeneration as a Parkinson's disease model

Experimental approaches to investigate dopaminergic neurons in humans are limited to non-invasive methods and post-mortem samples. For molecular investigations in vivo, animal models are needed. There are genetic and neurotoxic models of PD; however, they all have their own advantages and no animal model fully represents the pathophysiology and the progressive nature of the disease (Le et al., 2014).

1.3.1 The 6-OHDA toxin model of Parkinson's disease

A classic toxin to model PD is 6-hydroxydopamine (6-OHDA), a hydroxylated analogue of dopamine which acts by inducing intracellular oxidative stress (Bové and Perier, 2012). 6-OHDA was found in human brain samples (Curtius et al., 1974) and in higher concentrations in the urine of PD patients (Andrew et al., 1993). 6-OHDA is structurally highly similar to dopamine and norepinephrine and exhibits high affinity to the receptors of these neurotransmitters (Kostrzewa and Jacobowitz, 1974). In line with this, 6-OHDA was shown to accumulate and act selectively in dopaminergic and noradrenergic neurons (Kostrzewa and Jacobowitz, 1974). Inside the neurons, 6-OHDA leads to reactive oxygen species (ROS) formation and inhibits complex I of the mitochondrial electron transport chain (Kostrzewa and Jacobowitz, 1974; Schober, 2004). ROS production and the depletion of neuronal energy stores is assumed to underlie 6-OHDA-induced neurodegeneration (Glinka et al., 1997). In *C. elegans,* noradrenaline and adrenaline cannot be detected (Horvitz et al., 1982; Sanyal et al., 2004), so it is expected that 6-OHDA specifically targets dopaminergic neurons.

1.3.2 *C. elegans* as a model organism for dopaminergic cell death

The nematode *Caenorhabditis elegans* was introduced as an experimental model organism by Sydney Brenner (Brenner, 1974). *C. elegans* follows a well-defined and largely invariant life cycle which makes it possible to trace the fate of every cell (Sulston and Horvitz, 1977; Sulston et al., 1983). Starting from the embryo, there are four larval stages (L1-L4) before the worm reaches adulthood (Sulston and Horvitz, 1977; Sulston et al., 1983). The transparency and genetic malleability of *C. elegans*, as well as sophisticated molecular tools made it possible to uncover basic mechanism of cell death and neurobiology (Kaletta and Hengartner, 2006). Despite the worms' small nervous system, most of the known dopamine signalling components are conserved between *C. elegans* and mammals (Nass et al., 2001). Dopaminergic neurons in *C. elegans* are not essential for viability or overt movement but are,

similar to their human counterparts, required to mediate subtle behaviours that are often connected to motion (Nass et al., 2001). *C. elegans* hermaphrodites possess eight ciliated and mechanosensory dopaminergic neurons – four CEP (cephalic sensilla) and two ADE (anterior deirids) neurons in the head and two PDE (posterior deirids) neurons in the midbody (Sulston et al., 1975) (**Figure 3A**). Specific fluorescent in vivo labelling of dopaminergic neurons is achieved by using the promoter of the dopamine transporter to drive GFP expression (BY200 strain, Nass et al., 2002) (**Figure 2A**).

1.3.3 *C. elegans* 6-OHDA model

After exposure to 6-OHDA, *C. elegans* dopaminergic neurons – mainly the CEPs and ADEs in the head – display blebbed processes, dark and rounded cell bodies and are eventually completely lost (Nass et al., 2002). Chromatin condensation, a feature reminiscent of apoptotic cell death, is evident; however, interference with the classical apoptosis pathway does not prevent dopaminergic neurodegeneration (Nass et al., 2002). Intriguingly, typical signs of necrotic cell death such as membranous whorls, swollen organelles or cell bodies are absent as well (Nass et al., 2002). However, autophagy seems to play a role in 6-OHDA-induced neurodegeneration since mutations of autophagy genes reduce neuronal loss (Tóth et al., 2007). In line with studies in other model organisms, 6-OHDA seems to be taken up by the dopamine transporter and compete with dopamine for entry, as overexpression of the dopamine synthesis enzyme CAT-2 protects against 6-OHDA toxicity in *C. elegans* (Masoudi et al., 2014). However, in the absence of 6-OHDA exposure – and in line with a detrimental effect of high intracellular concentration of dopamine – overexpression of the key dopamine synthesis enzyme CAT-2 was shown to induce age-dependent dopaminergic cell death (Cao et al., 2005; Masoudi et al., 2014).

Using the *C. elegans* 6-OHDA model of dopaminergic cell death, previous work from our lab showed that the tetraspanin *tsp-17* acts in dopaminergic neurons and alleviates 6-OHDA-induced neurodegeneration (Masoudi et al., 2014).

Aim

To find and characterise genes that prevent the loss of dopaminergic neurons after exposure to 6-hyroxydopamine (6-OHDA), I will extend the genetic screen that led to the isolation of *tsp-17*. Firstly, I aim to isolate and map novel gene mutations that render *C. elegans* susceptible to 6-OHDA-induced neurodegeneration. Secondly, I want to determine the mechanisms by which the identified genes normally prevent dopaminergic neurodegeneration in *C. elegans*.

2 RESULTS GLIT-1, TTR-33 AND TSP-17 MUTANTS

2.1 Premature 6-OHDA-induced neurodegeneration in *glit-1* and *ttr-33* mutants

C. elegans worms with mutations in genes necessary for neuronal survival are expected to exhibit increased neuronal loss when exposed to a low dose of a neurodegenerative drug. To find genes that prevent dopaminergic neuron death, worms with GFP-labelled dopaminergic neurons (**Figure 2A, B**) were mutagenised with ethyl methanesulfonate (EMS). This population of worms was then screened for mutants that lost their fluorescent dopaminergic head neurons upon intoxication with 6-Hydroxydopamine (6-OHDA) at a concentration that did not lead to neuronal loss in wild-type animals (**Figure 2B**). 6-OHDA is a neurodegenerative drug that is taken up specifically into dopaminergic neurons and that is assumed to cause intracellular oxidative stress (Kostrzewa and Jacobowitz, 1974). With this screen we expected to reveal mutations in genes that have a role in drug uptake, oxidative stress response or cell death.

The mutagen EMS produces random mutations in the genome; hence a mapping procedure is needed to identify the mutations that lead to premature neurodegeneration. For mapping, we selected mutant lines that developed dopaminergic neurons normally but exhibited strong degeneration after treatment with 6-OHDA. These strains were backcrossed and retested to eliminate mutations that are not linked to 6-OHDA sensitivity. The mutations in the two lines with the strongest 6-OHDA sensitivity, *gt1981* and *gt1983*, behaved in a recessive fashion and therefore result likely in a loss-of-function of the affected genes: In contrast to *gt1981*/*gt1981* and *gt1983*/*gt1983* homozygous mutants (**Figure 2B**), *gt1981*/*wild-type* and *gt1983*/*wild-type* heterozygous mutants did not exhibit neurodegeneration upon treatment with 6-OHDA (data not shown). In addition, we tested complementation of the mutations. If *gt1981* and *gt1983* would affect the same gene product, worms carrying one mutation each are expected to be still sensitive to 6-OHDA. However, *gt1981*/*gt1983* transheterozygotes behaved like wild-type

animals in the 6-OHDA assay (data not shown). Finally, to identify the genes that are mutated in *gt1981* and *gt1983*, we conducted whole-genome sequencing and single nucleotide polymorphism mapping (Doitsidou et al., 2010; Minevich et al., 2012). Using this strategy, mutations in the genes *glit-1* and *ttr-33* were determined for the lines carrying *gt1981* and *gt1983,* respectively. A fosmid carrying the *glit-1* wild-type gene rescued the hypersensitivity of *glit-1*(*gt1981*) (Moerman fosmid library clone WRM0632dG03, data not shown). In addition, strains with a *glit-1* splice-site mutation (*glit-1*(*gk384527)* or *glit-1(splice)),* a *glit-1* promoter deletion (*glit-1(ok237)* or *glit-1(Δ))* (**Figure 2D**) and a *ttr-33* point mutation (*ttr-33*(*gk567379) or ttr-33*(L72F)) (**Figure 2E**) were acquired from public strain collections and were confirmed to be hypersensitive to 6-OHDA (**Figure 2B**). The shared phenotype between mutants carrying a *glit-1* promoter deletion and mutants with a *glit-1(gt1981)* point mutation further supported the idea that the point mutation leads to a loss-of-function of *glit-1*. We crossed the new alleles to the isolated mutants to confirm that they affect the same gene. Indeed, the mutations did not complement each other since *glit-1*(*gt1981)/glit-1(splice), glit-1(gt1981)/glit-1(Δ)* and *ttr-33*(*gt1983)/ttr-33(L72F)* transheterozygous mutants were still hypersensitive to 6-OHDA (data not shown). We conclude that mutations in *glit-1* or *ttr-33* cause premature degeneration of dopaminergic neurons after 6-OHDA intoxication, likely due to reduced gene function.

So far, it has not been determined at which developmental stages *glit-1* and *ttr-33* act, but oxidative stress assays are usually performed at the L1 larval stage. When intoxicating later larval stages with 6-OHDA, the sensitivity of *glit-1* and *ttr-33* mutants was decreasing and adults were not sensitive (**Figure 2F**). The *ttr-33* phenotype is lost even earlier in development than the *glit-1* phenotype. In summary, the first two larval stages are most strongly affected by a mutation in *glit-1* or *ttr-33*.

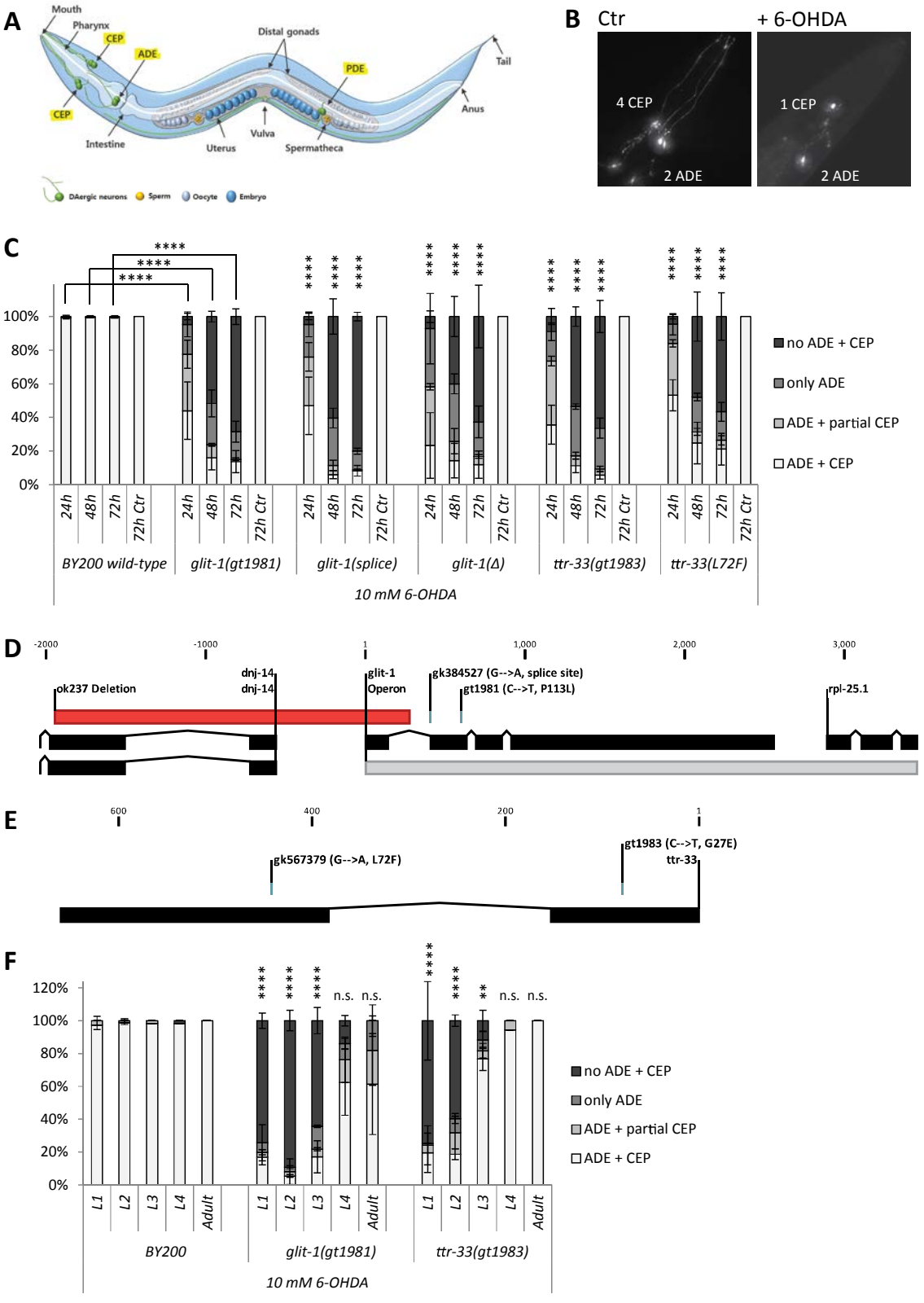
A
Mouth
Pharynx
CEP
ADE
CEP
Intestine
Uterus
Vulva
Distal gonads
PDE
Spermatheca
Tail
Anus
DAergic neurons
Sperm
Oocyte
Embryo
B
Ctr
+ 6-OHDA
4 CEP
2 ADE
1 CEP
2 ADE
C
100%
80%
60%
40%
20%
0%
no ADE + CEP
only ADE
ADE + partial CEP
ADE + CEP
24h
48h
72h
72h Ctr
BY200 wild-type
glit-1(gt1981)
glit-1(splice)
glit-1(Δ)
ttr-33(gt1983)
ttr-33(L72F)
10 mM 6-OHDA
D
-2000
-1000
1
1,000
2,000
3,000
ok237 Deletion
dnj-14
dnj-14
glit-1
Operon
gk384527 (G-->A, splice site)
gt1981 (C-->T, P113L)
rpl-25.1
E
600
400
200
1
gk567379 (G-->A, L72F)
gt1983 (C-->T, G27E)
ttr-33
F
120%
100%
80%
60%
40%
20%
0%
n.s.
n.s.
n.s.
n.s.
no ADE + CEP
only ADE
ADE + partial CEP
ADE + CEP
L1
L2
L3
L4
Adult
BY200
glit-1(gt1981)
ttr-33(gt1983)
10 mM 6-OHDA

Figure 2: Mutations in *glit-1* or *ttr-33* cause premature dopaminergic neurodegeneration after intoxication with 6-OHDA.
A) Cartoon of basic *C. elegans* anatomy and position of dopaminergic neurons: 4 CEP, 2 ADE and 2 PDE neurons (highlighted in yellow). Adapted from (Chege and McColl, 2014).
B) GFP-labelled *C. elegans* dopaminergic head neurons – 4 CEP neurons and 2 ADE neurons – (upper image, 'Ctr') and exemplary picture of neurodegeneration after intoxication with 6-hydroxydopamine (lower image, '+6-OHDA').
C) Remaining *C. elegans* dopaminergic head neurons 24, 48 and 72 hours after intoxication with 10 mM 6-OHDA and 72 h after treatment with ascorbic acid only ('72h Ctr') for BY200 wild-type or *glit-1* and *ttr-33* mutant animals. Animals possessing all neurons were scored as 'ADE + CEP' (white bar), those with partial loss of CEP but intact ADE neurons as 'ADE + partial CEP' (light grey bar), those with complete loss of CEP but intact ADE neurons as 'only ADE' (dark grey bar) and those with complete loss of dopaminergic head neurons as 'no ADE + CEP' (black bar). Error bars = S.E.M. of 2 biological replicates for *glit-1(ok237)* and 3 biological replicates for all the other strains, each with at least 60 animals per strain and concentration. Total number of animals per condition n = 115-340 (****p<0.0001; G-Test comparing BY200 wild-type and mutant data of the same time point) − except for the '72h Ctr' experiment was tested once with n = 30-100.
D) *glit-1* gene structure with positions of the *glit-1(gt1981)* point mutation, the *glit-1(gk384527)* splice site mutation and the *glit-1(ok237)* deletion. For the point mutations the nucleotide and amino acid changes are indicated in brackets. The *ok237* deletion spans 5'UTR and first exon of *glit-1* and 5'UTR and first exons of *dnj-14* (*DNaJ domain (prokaryotic heat shock protein)*) and is indicated with a red bar. Also, *glit-1* lies in an operon (grey bar) and shares a promoter with the ribosomal protein *rpl-25.1 (Ribosomal Protein, Large subunit).*
E) *ttr-33* gene structure with positions of *ttr-33*(*gt1983)* and *ttr-33(gk567379)/ttr-33(*L72F) point mutations. The nucleotide and amino acid changes are indicated in brackets.
F) Dopaminergic head neurons in wild-type animals and *glit-1* and *ttr-33* mutants 48 h after intoxicating the indicated larval stages (L1-L4) or adult animals with 10 mM 6-OHDA. Error bars = SEM of 2 biological replicates, each with at least 25 animals per stage and strain. Total number of animals per condition n = 50-75 (****p<0.0001, **p<0.01, n.s. p>0.05; G-Test comparing BY200 wild-type and mutant animals data of the same lifecycle stages).

During 6-OHDA intoxication, the whole animal is exposed to the drug; hence it is possible that mutants with an increased organismal drug uptake exhibit higher susceptibility. Since 6-OHDA causes oxidative stress, a higher drug uptake would be expected to be detrimental for organismal health. However, the development of the mutant worms was not compromised or retarded after the 6-OHDA assay: *glit-1* mutants grew markedly and *ttr-33* mutants slightly slower than wild-type animals, but this delay was not enhanced by intoxication with 6-OHDA (**Figure 3A**). We noted that mutants with a *glit-1* deletion grew much slower than mutants carrying *glit-1* point mutations. This growth delay could be caused by defects in neighbouring genes *rpl-25.1 (Ribosomal Protein, Large subunit)* and *dnj-14 (DNaJ domain (prokaryotic heat*

shock protein)) that are also affected by the deletion (**Figure 2D**). There is further support that the mutants are not generally sensitive to 6-OHDA, since preventing neuronal drug uptake also prevented neuronal loss: a deletion in *dat-1*, the *C. elegans* dopamine transporter that shuttles 6-OHDA into the neurons, rescued dopaminergic neurodegeneration of wild-type worms (Nass et al., 2002) and *glit-1(gt1981)* and *ttr-33(gt1983)* mutants (**Figure 3B**). In summary, it is unlikely that an increased organismal drug uptake is the mechanism by which the mutants are rendered hypersensitive – and *glit-1* and *ttr-33* mutations are expected to interfere with processes that occur after 6-OHDA enters dopaminergic neurons.

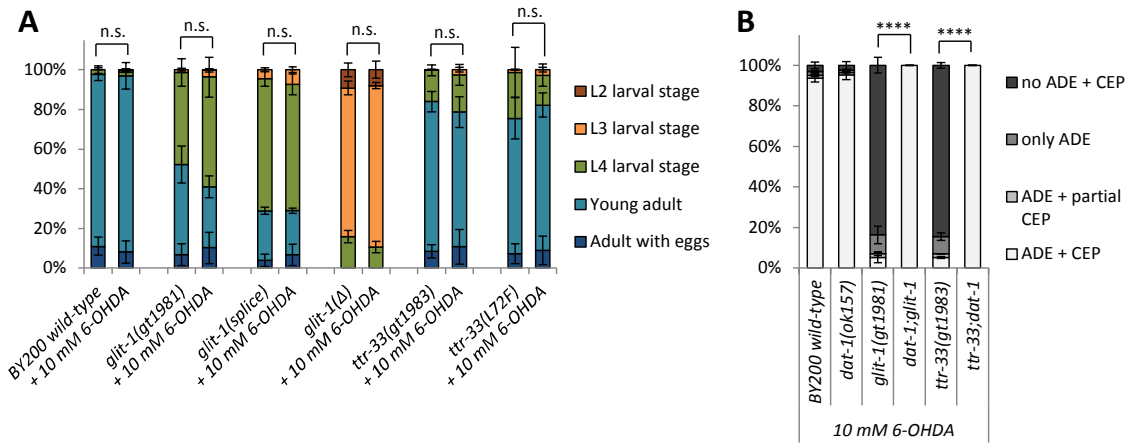

Figure 3: The mutants are unlikely to exhibit increased organismal drug uptake and 6-OHDA must enter dopaminergic neurons to cause dopaminergic neurodegeneration.
A) Developmental stages of wild-type and mutant L1 stage larvae 48 h after treatment without and with 6-OHDA. Worms developed via the L1, L2 (in red), L3 (in orange), L4 (green) and young adult stage (in light blue) into adults (in dark blue). Error bars = SEM of 3 biological replicates, each with at least 60 animals per concentration and strain. Total number of animals per condition n = 200-350 (n.s. $p>0.05$; G-Test).
B) Scoring of *C. elegans* dopaminergic head neurons 72 hours after intoxication with 10 mM 6-OHDA. Error bars = SEM of 2 experiments, each with at least 50 animals per strain. Total number of animals per strain n = 100-400 (****$p<0.0001$; G-Test).

2.2 *tsp-17, glit-1* and *ttr-33* are sensitive to oxidative stress and short-lived, but resistant to endoplasmic reticulum stress

Oxidative stress elicited by 6-OHDA led to premature death of dopaminergic neurons in *glit-1* and *ttr-33* mutants and we wanted to determine if oxidative stress also affects the mutants at an organismal level. We also included the tetraspanin mutant *tsp-17,* which was previously shown to be sensitive to 6-OHDA, in the characterisation (Masoudi et al., 2014). We treated worms with paraquat, an herbicide which elicits reactive oxygen species (ROS) and which is linked to the development of Parkinson 's disease (Tanner et al., 2011; Wang et al., 2011)**.** Paraquat however is not specifically taken up into dopaminergic neurons like 6-OHDA. Remarkably, paraquat exposure did not elicit dopaminergic neurodegeneration (data not shown), so it is possible that the neurons only die when accumulating high levels of intracellular ROS. However, in line with a higher sensitivity to organismal oxidative stress, *glit-1*, *tsp-17* and *ttr-33* showed a reduced survival after paraquat exposure. *glit-1* and *tsp-17* exhibited a very strong defect with equal severity, which was more pronounced than the *ttr-33* phenotype (**Figure 4A**). Hence, *glit-1*, *ttr-33* and *tsp-17* show increased sensitivity to 6-OHDA-induced oxidative stress on the neuronal and to paraquat-induced oxidative stress on the organismal level.

Increased oxidative stress has been implicated with premature aging (Lionaki and Tavernarakis, 2013), therefore we determined the lifespan of *glit-1* and *ttr-33* mutants. We found that *glit-1*, *tsp-17* and *ttr-33* exhibited shortened lifespans (**Figure 4B**), indicating that the mutants might suffer from malfunctioning stress response pathways on the organismal level.

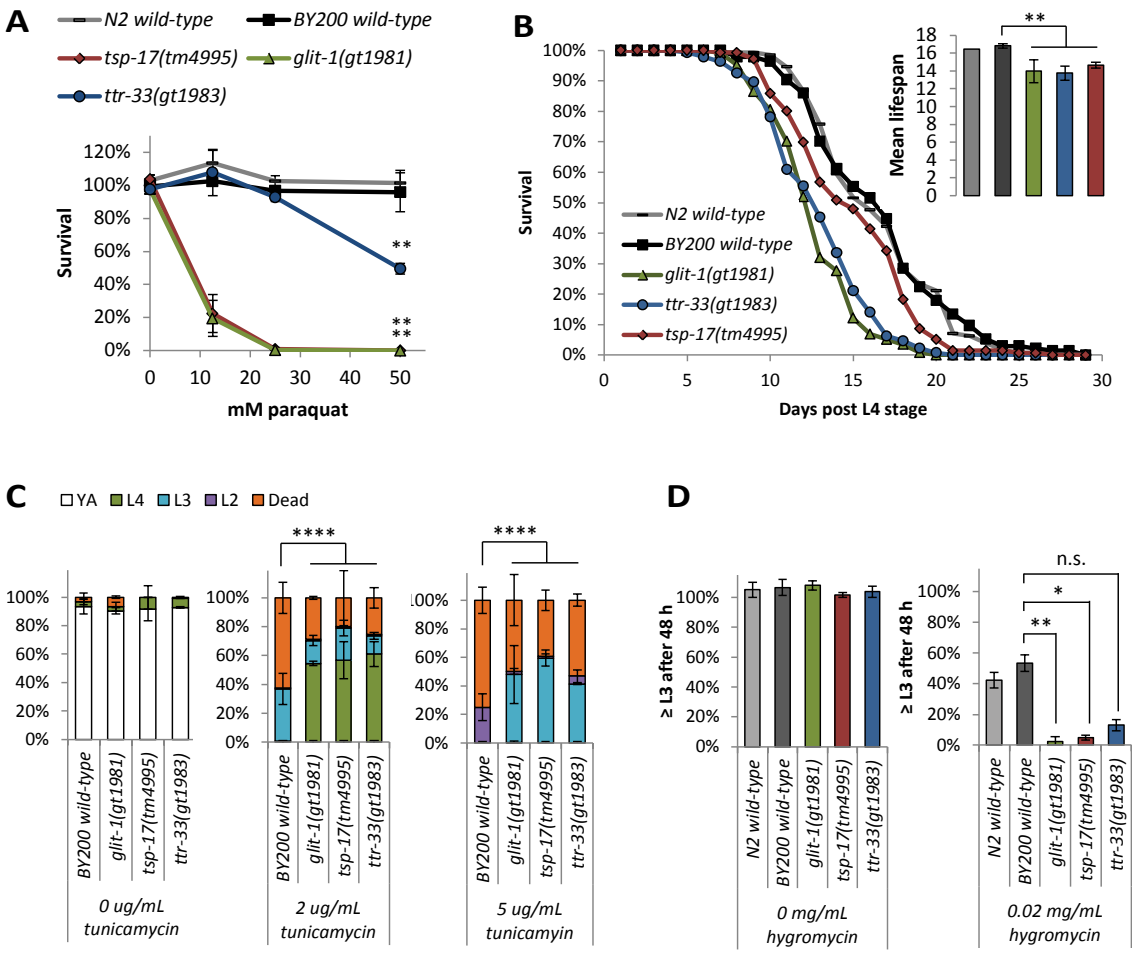

Figure 4: *glit-1*, *tsp-17* and *ttr-33* are sensitive to oxidative stress, short-lived and resistant to ER stress.

A) Oxidative stress assay: Survival of L1 larvae 24 h after 1 h incubation with indicated concentration of paraquat. At 100 mM paraquat, 50% of wild-type animals were dead (data not shown). Error bars = SEM of 3 biological replicates, each with at least 80 animals per strain and concentration. Total number of animals per condition n = 350-650 (**p<0.02; two-tailed t-test comparing data of BY200 wild-type and mutant animal data at 50 mM paraquat).

B) Lifespan assay: Lifespan data shown for second biological replicate. Inset depicts mean lifespan and SEM based on 2 biological replicates, each with at least 100 animals. Total number of animals per strain n = 200-230 (**Bonferroni p<0.01; Log-Rank Test), except for N2 wild-type which was tested once with n = 110.

C) ER stress assay: Development of embryos after 48 h into young adults (YA), L4, L3 or L2 stage larvae on plates with indicated concentration of tunicamycin. Only dead L1 stage larvae could be detected 48 h after egg-laying and were therefore included in the 'dead' category. Error bars = SEM of 2 biological replicates, each with at least 50 animals per strain and concentration. Total number of animals per condition n = 210-400 (****p<0.0001; G-Test)

D) Hygromycin B assay: Development of L1 larvae 48 h after plating on indicated concentration of hygromycin B. Error bars = SEM of 2 biological replicates, each with at least 60 animals per strain and concentration. Total number of animals per condition n = 120-330 (**p<0.02, *p<0.05, n.s. p>0.05; two-tailed t-test).

Changes in oxidative stress response pathways can lead to defects in protein metabolism; hence, we analysed if *glit-1*, *ttr-33* and *tsp-17* are sensitive to protein folding stress. The antibiotic tunicamycin inhibits N-glycosylation of proteins in the ER (Heifetz et al., 1979) and triggers the unfolded protein response (UPR) which in turn induces cell cycle arrest. Therefore, *C. elegans* worms grow slower when exposed to tunicamycin. Surprisingly, we found that all three mutants were resistant to tunicamycin-induced protein folding stress as the animals grew faster than wild-type worms (**Figure 4C**). Thus, a decrease in oxidative stress resistance goes along with an increase in ER stress resistance in *glit-1*, *ttr-33* and *tsp-17* mutant animals.

glit-1, *ttr-33* and *tsp-17* mutants are sensitive to oxidative stress and resistant to ER stress, thus they might exhibit an altered oxidative stress or ER stress response. There are two possible explanations why the mutants show resistance to ER stress: 1) The ER UPR could be working less efficiently in the mutants, leading to less growth inhibition, or 2) the mutants might be pre-conditioned, exhibiting a higher baseline level of the ER UPR and therefore be adapted to better deal with additional stress. These two possibilities can be distinguished by determining baseline stress response levels using transcriptional reporter lines. Preliminary experiments indicated lower expression of the oxidative stress reporter P*gst-4*::gfp and higher expression of the ER UPR reporter P*hsp-4*::gfp in *glit-1* mutant animals under basal conditions (**Figure 5**). These results indicate the oxidative stress response might be down- and the ER UPR stress response upregulated in *glit-1* mutants. However, the stress reporter experiments have to be repeated for quantification. One of the outcomes of the ER UPR is the inhibition of translation. If the UPR is upregulated, a slower organismal growth is expected and we detected that *glit-1* and *ttr-33* mutants are indeed developing slower than wild-type worms (**Figure 3A**). In addition, we tested the reaction to the translation inhibitor hygromycin B, which should lead to bigger effects in worms that already exhibit a reduced basal translation rate. We found that *glit-1*, *tsp-17* and *ttr-33* are more affected by an inhibition of protein translation than wild-type worms (**Figure 4D**), indicating that the UPR might indeed be upregulated in the mutants. In

summary, a downregulated or malfunctioning oxidative stress response might render the mutants more sensitive to ROS exposure and an upregulated UPR could prepare them for additional ER stress under basal conditions.

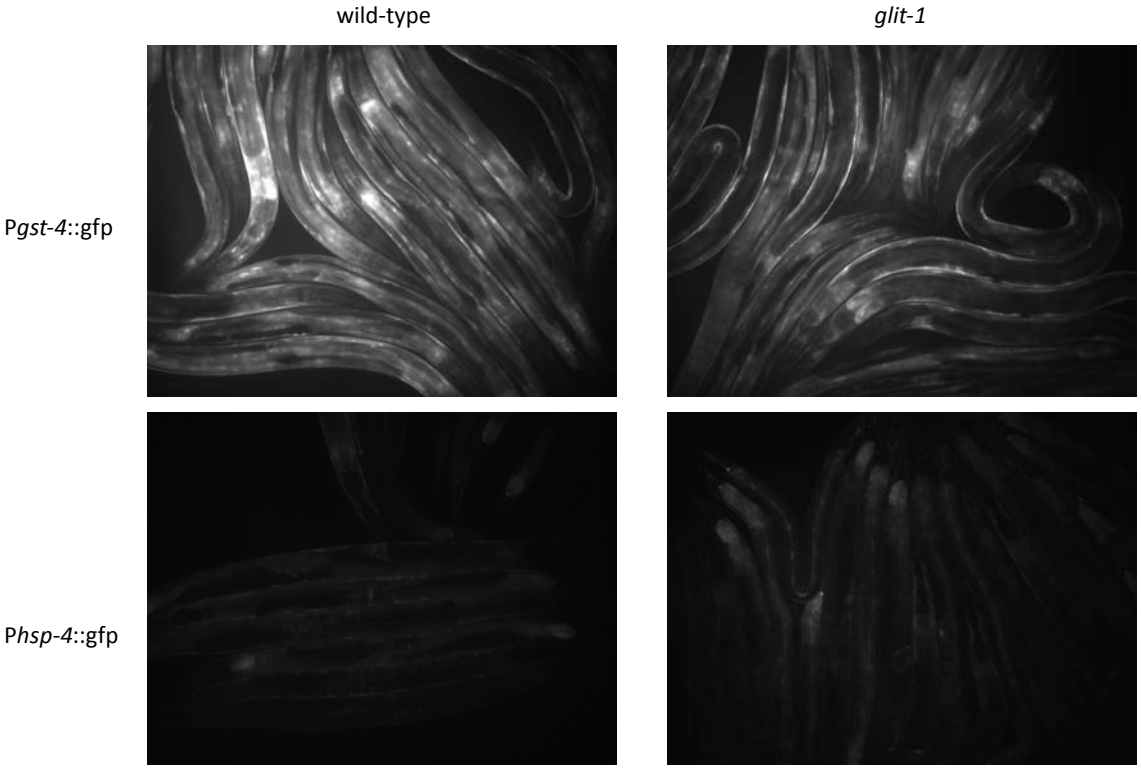

Figure 5: Indication for reduced basal expression of oxidative stress reporter and elevated basal expression of ER UPR stress reporter in *glit-1* mutants .
Preliminary results of oxidative stress reporter P*gst-4*::gfp and ER UPR stress reporter P*hsp-4*::gfp expression in wild-type and *glit-1* mutant animals at L4 stage at basal conditions.

2.3 Known stress response pathways influence 6-OHDA-induced dopaminergic neurodegeneration

glit-1, *ttr-33* and *tsp-17* mutants exhibit altered organismal stress responses. To determine if known *C. elegans* stress response pathways influence the 6-OHDA-induced neurodegeneration of the mutants, we turned to a candidate approach.

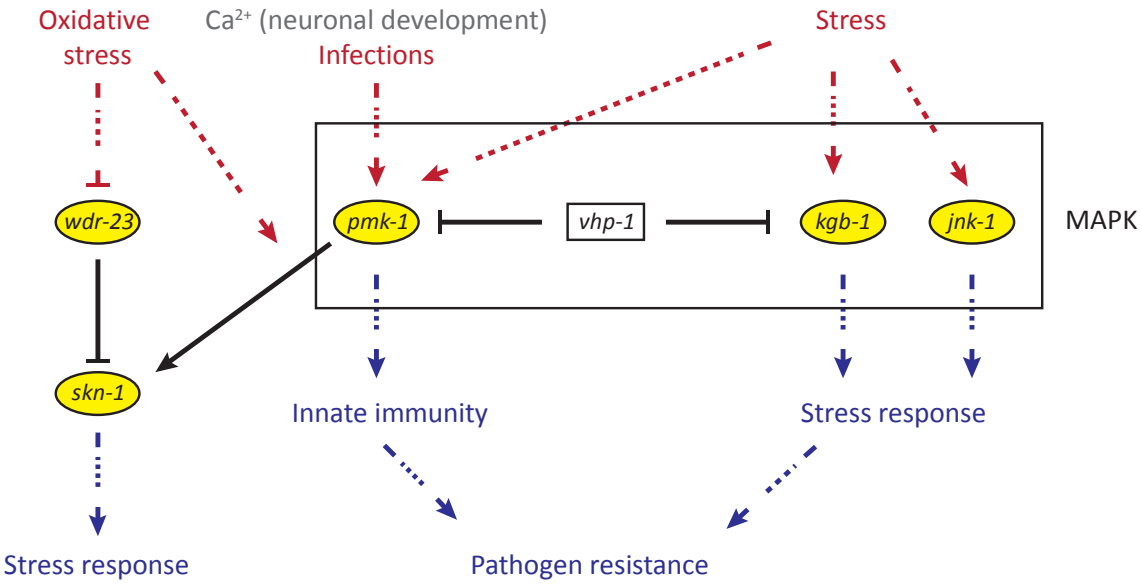

Figure 6: Interactions of *C. elegans* skn-1/Nrf and MAPK stress response pathways tested in this study – adapted from (Ewbank, 2006; Inoue et al., 2005).
Tested genes are shaded in yellow. Stimuli of stress response pathways are shown in red and grey and responses of stress response pathways in blue. The MAPKs (mitogen-activated protein kinases) *pmk-1*, *kgb-1* and *jnk-1* are shown, but not the upstream MAPK kinases and the MAPK kinase kinases.

The Nrf (nuclear factor E2-related factor) transcription factor family regulates an oxidative stress response in mammals (Sykiotis and Bohmann, 2010) and the *C. elegans* Nrf orthologue *skn-1 (SKiNhead)* similarly promotes oxidative stress resistance and longevity (An and Blackwell, 2003). If *skn-1* regulates the stress response after 6-OHDA exposure, the *skn-1/Nrf loss-of-function* mutation *zu67* is expected to render dopaminergic neurons hypersensitive to the drug. However, a *skn-1(zu67)* mutation neither led to increased dopaminergic neurodegeneration (**Figure 7A**), nor altered the phenotype of *glit-1* mutants after 6-OHDA intoxication (**Figure 7B**). In *C. elegans*, the abundance of SKN-1 is negatively regulated by the CUL-4/DDB-1 ubiquitin ligase substrate targeting protein WDR-23 (WD Repeat protein) (**Figure 6**) (Choe et al., 2009; Staab et al., 2013). Hyperactivation of *skn-1* activity – conferred by a *gain-of-function (GOF)* mutation in *skn-1* or by loss of the *skn-1* repressor *wdr-23* (Choe et al., 2009) – led to reduced dopaminergic neurodegeneration in *glit-1* mutants (**Figure 7F**), but also

in wild-type worms (**Figure 7E**). The effect of the *wdr-23(tm1817)* repressor mutation seemed to be stronger than the *skn-1(lax120)* stimulation alone. In summary, *skn-1* hyperactivation seems to improve the general organismal stress response, but loss-of-function of *skn-1* does not lead to increased 6-OHDA-induced neurodegeneration.

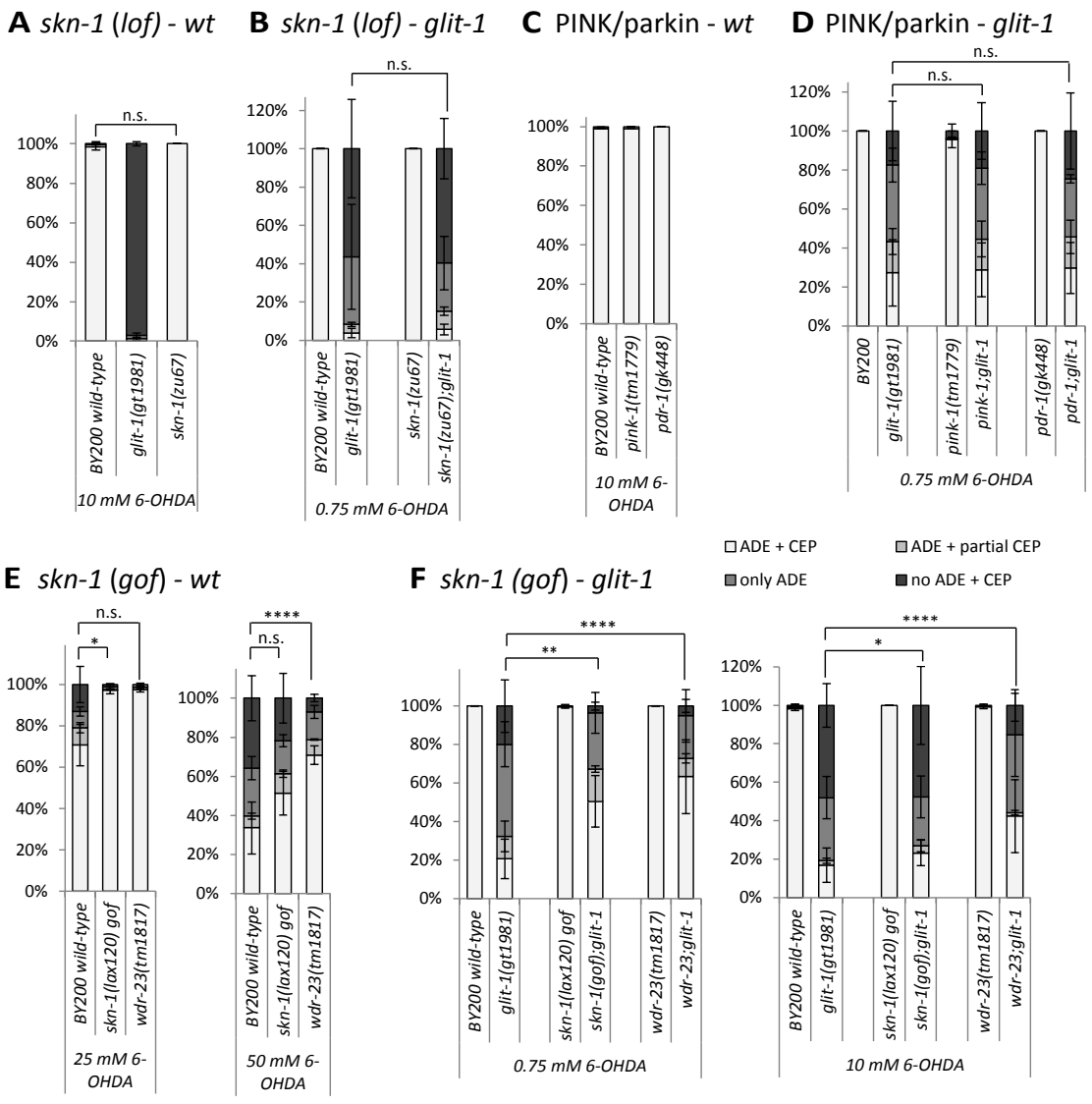

Figure 7: Boosting the *skn-1* oxidative stress pathway alleviates neurodegeneration.
Dopaminergic neurons were scored 72 h after intoxication with indicated concentration of 6-OHDA.
A) and **B)** Experiment were done with unstarved, filtered L1 larvae since an insufficient amount of *skn-1(zu67)* mutants could be gained in liquid culture. Unstarved worms show a higher degree of degeneration.
A) Effect of *skn-1 loss-of-function (lof)* allele *zu67* in a wild-type background. Error bars = SEM of 3 biological replicates, each with at least 30 animals per strain. Total number of animals per strain n = 160-270 (n.s. p>0.05; G Test).
B) Effect of *skn-1 loss-of-function (lof)* allele *zu67* in the *glit-1* mutant background. Error bars = SEM of 3 biological replicates with each 40-100 scored worms per condition. Error bars = SEM of 3 biological replicates, each with at least 40 animals per strain. Total number of animals per strain n = 190-310 (n.s. p>0.05; G Test).
C) Effect of PINK homologue mutation *pink-1* and parkin homologue mutation *pdr-1* in a wild-type background. 1 experiment was conducted with a total number of animals per strain n = 50.
D) Effect of PINK homologue mutation *pink-1* and parkin homologue mutation *pdr-1* in the *glit-1* mutant background. Error bars = SEM of 2 biological replicates, each with at least 60 animals per strain. Total number of animals per strain n = 120-210 (***p<0.0001, **p<0.01, *p<0.05; G-Test).
E) Effect of *skn-1 gain-of-function (gof)* mutations *skn-1(lax120) and wdr-23(1817)* in a wild-type background. Error bars = SEM of at least 3 biological replicates, each with at least 60 animals per strain and concentration. Total number of animals per condition = 240-430 (****p<0.0001, *p<0.05, n.s. p>0.05; G-Test).
F) Effect of *skn-1 gain-of-function (gof)* mutations *skn-1(lax120) and wdr-23(1817)* in the *glit-1* mutant background. Error bars = SEM of at least 3 biological replicates, each with at least 60 animals per strain and concentration. Total number of animals per condition n = 180-420 (****p<0.0001, **p<0.01, *p<0.05; G-Test).

Mitophagy, the removal of damaged mitochondria is important for cellular stress resistance and the kinase PINK1/*pink-1* and the E3 ubiquitin ligase Parkin/*pdr-1* initiate *C. elegans* mitophagy in a pathway parallel to *skn-1* (Palikaras et al., 2015). In addition, PINK1/*pink-1*- and Parkin/*pdr-1*-mediated mitophagy is activated in response to mitochondrial stress (Schiavi et al., 2015). We used strains carrying *pink-1* or *pdr-1* mutations to test if the compromise of mitophagy leads to an altered 6-OHDA response. However, *pink-1* or *pdr-1* mutations did not lead to premature loss of dopaminergic neurons (**Figure 7C**) and did not alter the *glit-1* mutant phenotype (**Figure 7D**). Therefore, mitophagy does not seem to have a role in 6-OHDA-induced neuronal death.

The unfolded protein response of the ER (ER UPR) appears upregulated in the mutants, so we aimed to investigate if this pathway influences 6-OHDA-induced dopaminergic neurodegeneration in *C. elegans*. IRE1 (inositol-requiring enzyme 1) is a UPR sensor and mediates the most conserved branch of the UPR (Urra et al., 2013). Upon ER stress, IRE1 dimerises, autophosphorylates and activates XBP-1 (X box-binding protein 1) by intron excision (Duda et al., 2016). XBP-1 in turn is a transcription factor that mediates the expression of proteins involved in folding, ER entry, ER-associated degradation, and ER and Golgi biogenesis (Duda et al., 2016). IRE1 has a pro-survival role, sustained IRE1 signalling however might also trigger cell death (Urra et al., 2013). The switch between pro-survival and pro-apoptotic phases of UPR likely depends on the duration and intensity of the stress stimuli (Urra et al., 2013). We find that a mutation in *ire-1* did not cause premature dopaminergic neurodegeneration (**Figure 8A, B**) and alleviated neurodegeneration in *ttr-33* mutants (**Figure 8A**). In the *glit-1* mutant it seemed that inhibition of the ER UPR led to slight alleviation of neurodegeneration at a low, but not at a higher concentration of 6-OHDA (**Figure 8B**). Therefore, the unfolded protein response seems to be involved in mediating 6-OHDA-induced neurodegeneration in the *ttr-33*, but not in the *glit-1* mutant.

c-Jun N-terminal Kinases (JNKs) and p38 can be activated by cellular stress and are part of the mitogen-activated protein kinase (MAPK) superfamily, which plays a central role in immune cell activation (Huang et al., 2009). Pro- and anti-apoptotic roles for JNK have been proposed (Liu and Lin, 2005), including sustained JNK activation via IRE1 upon ER stress (Tabas and Ron, 2011) and the promotion of apoptosis after 6-OHDA exposure in a cell-based model of PD (Wilhelm et al., 2007). In addition to its role in cell death regulation, JNK might be involved in intercellular adhesion (You et al., 2013).

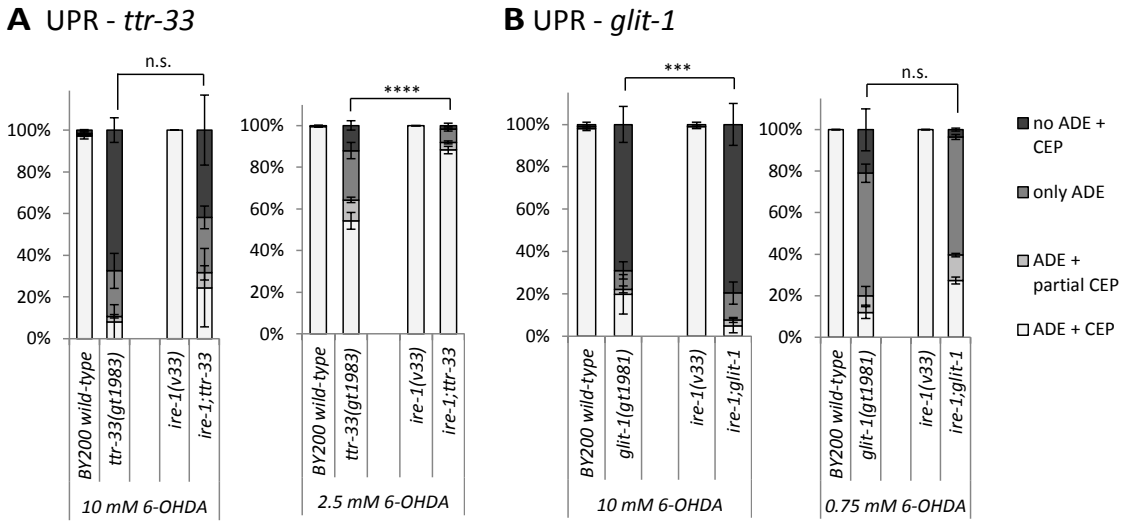

Figure 8: Abolishing the unfolded protein response alleviates neurodegeneration.
Dopaminergic neurons were scored 72 h after intoxication with indicated concentration of 6-OHDA.
A) Effect of unfolded protein response (UPR) gene mutation *ire-1* in the *ttr-33* mutant background. Error bars = SEM of at least 2 biological replicates, each with at least 50 animals per strain and concentration. Total number of animals per condition n = 100-320 (****p<0.0001, n.s. p>0.05; G-Test).
B) Effect of unfolded protein response (UPR) gene mutation *ire-1* in the *glit-1* mutant background. Error bars = SEM of at least 2 biological replicates, each with at least 50 animals per strain and concentration. Total number of animals per condition n = 190-320 (***p<0.001, n.s. p>0.05; G-Test).

The *C. elegans* JNK family members *jnk-1* (Jun N-terminal Kinase) and *kgb-1* (Kinase, GLH-Binding) are involved in the response to organismal stressors. JNK-1 (Jun N-terminal Kinase) is needed for a normal oxidative stress response (Oh et al., 2005) and is required for mitochondrial proliferation (Artal-Sanz and Tavernarakis, 2009). JNK-1 is expressed solely in neurons (Kawasaki et al., 1999), in contrast to KGB-1, which is expressed ubiquitously (Gerke et al., 2014; Uno et al., 2013). The *kgb-1* mutant exhibits increased sensitivity to protein folding stress (Mizuno et al., 2008). In addition, a recently discovered surveillance system – which interprets interruption of translation and protein transport as a pathogen attack – depends on *kgb-1* and inhibits the ER UPR (Runkel et al., 2013).

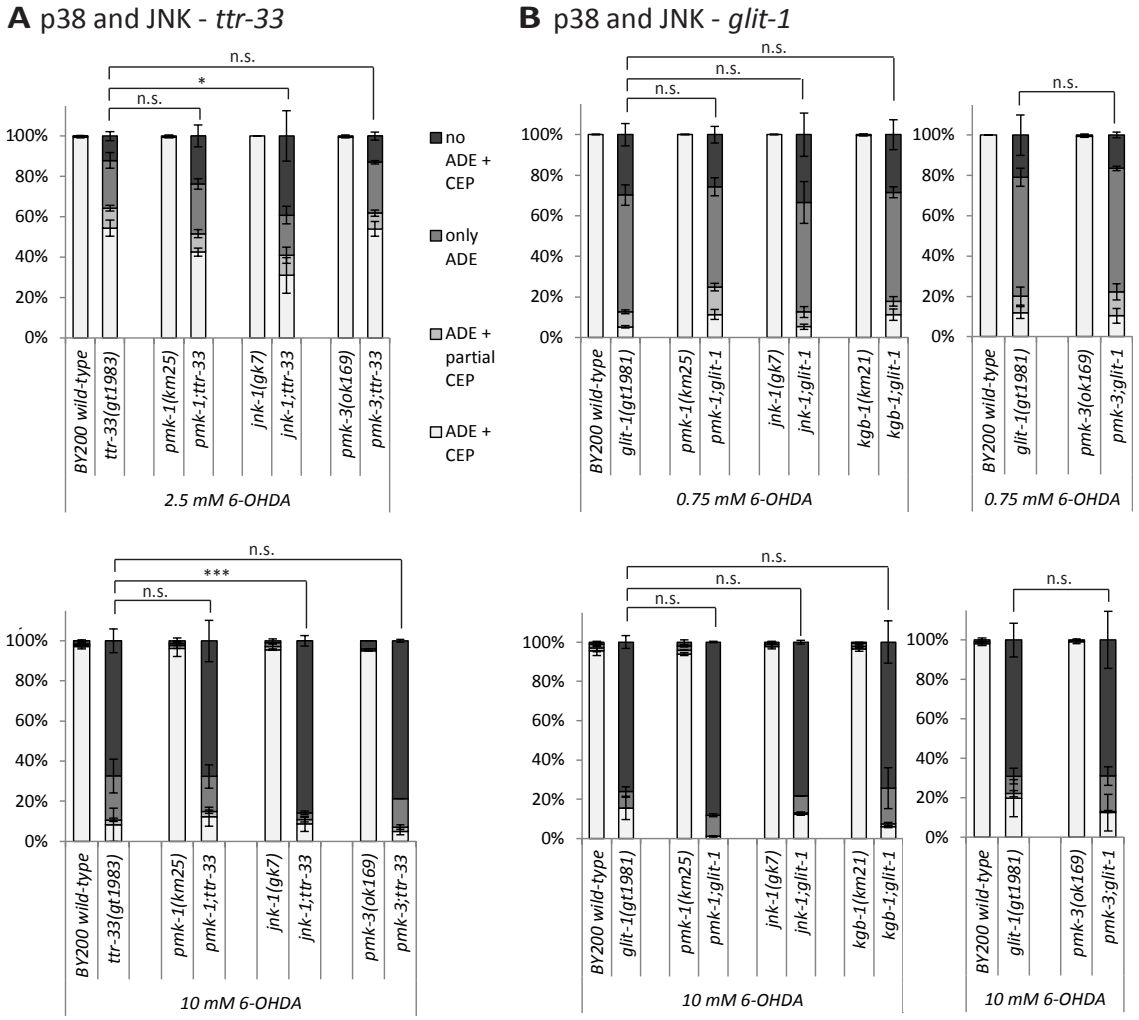

Figure 9: Loss of *jnk-1* stress response signalling worsens neurodegeneration in *ttr-33* mutants.
Dopaminergic neurons were scored 72 h after intoxication with indicated concentration of 6-OHDA.
A) Effect of p38 and JNK stress response pathway mutations in the *ttr-33* mutant background. Error bars = SEM of at least 2 biological replicates, each with at least 100 animals per strain and concentration. Total number of animals per condition n = 200-430 (***p<0.001, *p<0.05, n.s. p>0.05; G-Test).
B) Effect of p38 and JNK stress response pathway mutations in the *glit-1* mutant background. Error bars = SEM of at least 2 biological replicates, each with at least 50 animals per strain and concentration. Total number of animals per condition n = 140-330 (n.s. p>0.05; G-Test).

pmk-1 (p38 MAP Kinase family) and *pmk-3* each form a p38 MAPK pathway in *C. elegans*. *pmk-1* mediates resistance to bacterial pathogens as part of the innate immune response (Aballay et al., 2003; Bolz et al., 2010; Kim et al., 2002; Shivers et al., 2010; Troemel et al., 2006). In addition, *pmk-1* is needed for ER resistance (Judy et al., 2013; Richardson et al., 2011). Finally,

pmk-1 has been shown to stimulate *skn-1* activity (Inoue et al., 2005), and a crosstalk between the *pmk-1* p38 MAPK and the JNK-like *kgb-1* pathway has been shown in *C. elegans* (Kim et al., 2004; Mizuno et al., 2004). *pmk-3* in contrast is needed for axon regeneration (El Bejjani and Hammarlund, 2012) and prevents excessive germ cell apoptosis (Lettre et al., 2004).

MAPK response pathway single mutants (*jnk-1, kgb-1, pmk-1, pmk-3*) did not lead to premature dopaminergic neurodegeneration when intoxicated with 10 mM 6-OHDA (**Figure 9A, B**). Therefore, these pathways do not seem to mediate protection against 6-OHDA in the wild-type background. However, mutation of *jnk-1* led to increased neurodegeneration at both tested concentrations in *ttr-33* (**Figure 9A**), but not *glit-1* mutants (**Figure 9B**). Therefore, the JNK kinase JNK-1 – for which roles in the defence against oxidative stress have been reported – protects *ttr-33* mutants from further neurodegeneration.

In summary, we tested mutants from several *C. elegans* stress response pathways for their role in 6-OHDA-induced neurodegeneration. However, none of the tested mutants – *skn-1* being part of an oxidative stress response, *ire-1* mediating an unfolded protein response and MAP kinases regulating diverse stress responses – exhibited an increased sensitivity to 6-OHDA similar to *glit-1*, *ttr-33* or *tsp-17*. Hence, either the genes we identified are involved in previously unidentified pathways providing protection against 6-OHDA or alternatively, the pathways might act in a redundant manner.

2.4 *glit-1* and *tsp-17* might act in the same pathway

Mutations in *glit-1*, *ttr-33* or *tsp-17* render *C. elegans* dopaminergic neurons hypersensitive to 6-OHDA, so we asked if the genes could act in the same pathway. Double and triple mutants were generated to test epistasis, i.e. to determine if the hypersensitivity phenotypes of the single mutants would add up – as expected for different pathways – or if the dopaminergic neurons degenerate to a similar extent in the single, double and triple mutants – as predicted if the genes were in the same pathway. We found that *glit-1* and *tsp-17* might act in the same

pathway since the *glit-1;tsp-17* double mutant was equally hypersensitive as the *glit-1* and *tsp-17* single mutants (**Figure 10**). Reminiscent of the previously described paraquat oxidative stress assay (**Figure 4B**), *glit-1* and *tsp-17* mutants were equally sensitive and both showed a much stronger phenotype than *ttr-33* mutants. g*lit-1* and *tsp-17* mutants also showed a very similar extent of neurodegeneration when distinct developmental stages of *C. elegans* worms were intoxicated – except that *tsp-17* mutants at the L4 stage seemed to be equally sensitive as the L3 stage (**Figure 2F**)(Masoudi et al., 2014). *ttr-33* mutants instead only showed very little degeneration at the concentration at which *glit-1* and *tsp-17* mutants had their highest sensitivity window, so additive effects between the *ttr-33* and *glit-1* or *tsp-17* mutations cannot be unequivocally distinguished from phenotypic fluctuations. Increasing the concentration would lead to full degeneration in *glit-1* and *tsp-17* mutants, so again additive effects with a *ttr-33* mutation would not be visible. We conclude that *glit-1* and *tsp-17* likely act in a single genetic pathway.

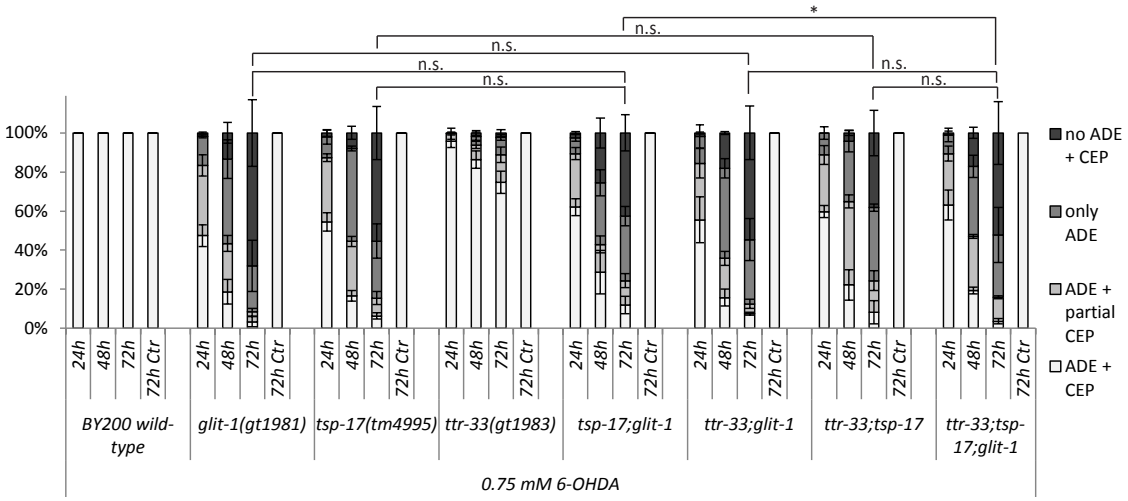

Figure 10: Interplay between *glit-1, tsp-17* and *ttr-33* mutations and sensitivity of different larval stages.
Dopaminergic head neurons scoring in wild-type and *glit-1*, *tsp-17* and *ttr-33* single, double and triple mutants 24, 48 and 72 h after intoxication with 0.75 mM 6-OHDA and 72 h after treatment with ascorbic acid only ('72 h Ctr'). Error bars = SEM of 3 biological replicates, each with at least 60 animals per strain. Total number of animals per condition n = 180-350 (*p<0.05, n.s. p>0.05; G-Test) − except for the '72 h Ctr' which was conducted twice with 30 worms per strain, resulting in a total n = 60.

3 INTRODUCTION NEUROLIGIN-LIKE GLIT-1

3.1 Neuroligins

Neuroligins are postsynaptic cell adhesion proteins required for the correct maturation and function of synapses (Varoqueaux et al., 2006). The neuroligin family of proteins is defined by an extracellular carboxyesterase-like domain that is enzymatically inactive and that mediates binding to the presynaptic neurexins (Hu et al., 2015) (**Figure 11**). In mammals, neuroligin subtypes display unique localisations at excitatory and inhibitory synapses (Bemben et al., 2015) and neuroligins and neurexins influence the balance of these synapse types in neuronal circuits (Calahorro, 2014). Neuroligin and neurexin dysfunction leads to impairment of synaptic properties and disruption of neural networks, and neuroligin and neurexin mutations are associated with autism and other cognitive diseases (Südhof, 2008).

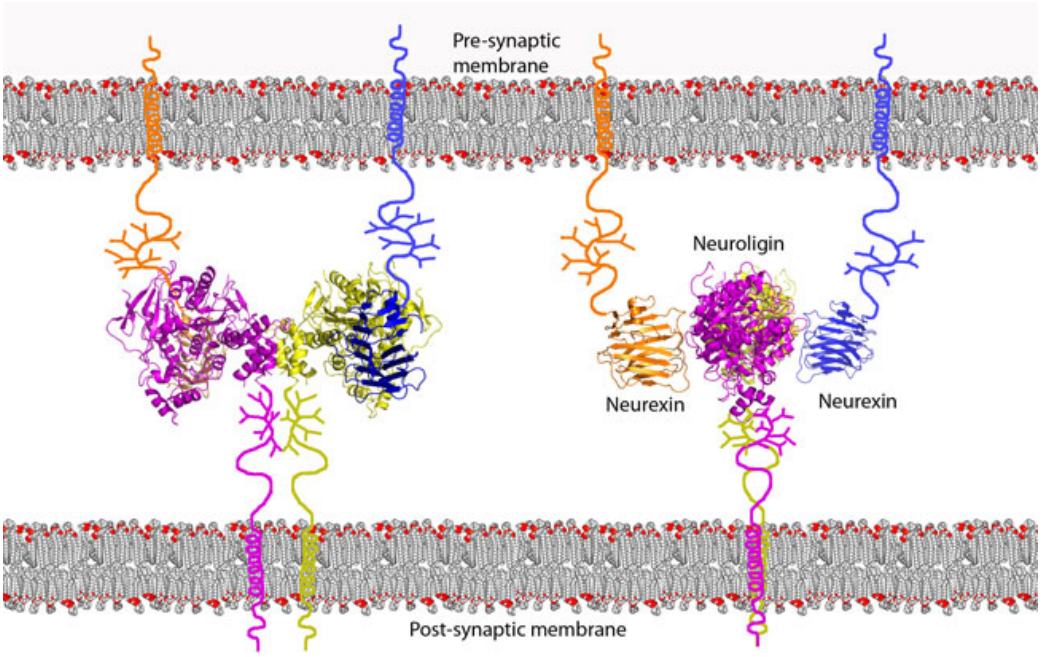

Figure 11: Model of neuroligin-neurexin interaction at the synapse – from (Araç et al., 2007)**.** A postsynaptic neuroligin dimer (in magenta and yellow) binds to a presynaptic neurexin dimer (in orange and blue). Two views of the interaction are shown with a 90° angle difference.

Neuroligins have a conserved WW-binding domain and a PDZ (PSD95, Dlg1, Zo-1) binding sequence at their C-terminus and occur as dimers, if not as higher-order oligomers (Bemben et al., 2015). There is evidence for direct interactions (Bemben et al., 2015), but the canonical model is that scaffolding molecules link neuroligin to receptors at the synapse – e. g. by binding via their PDZ domain. The neuroligin-neurexin junction based on PDZ domain protein binding resembles the architecture of tight junctions (Südhof, 2008).

The properties of neuroligins might be influenced by synaptic activity and the accompanying calcium signalling. Ca^{2+}-binding EF-hand motifs are common in neuroligins (Tsigelny et al., 2000) and Ca^{2+} influences synapse density via neuroligin-1 in mice (Bemben et al., 2015). Also, neuroligins and neurexins interact in a Ca^{2+}-dependent manner (Araç et al., 2007; Fabrichny et al., 2007; Ichtchenko et al., 1995; Nguyen and Südhof, 1997). Furthermore, neuroligin-1 can be cleaved in a Ca^{2+}-dependent manner, resulting in a reduction of synaptic transmission (Peixoto et al., 2012). Finally, neuroligin-1 activity-dependent cleavage by ADAM10 generates a secreted extracellular neuroligin form and an intracellular fragment which is subsequently cleaved by presenilin/γ-secretase (Suzuki et al., 2012).

3.2 *C. elegans* neuroligins

nlg-1 is the only reported *C. elegans* neuroligin and predominantly expressed in neurons (Hunter et al., 2010). NLG-1 acts at the synapse and influences behavioural phenotypes. At neuromuscular junctions, NLG-1 and the *C. elegans* neurexin NRX-1 mediate inhibition of neurotransmitter release (Hu et al., 2012) and control postsynaptic GABA receptor clustering together with MADD-4 (Muscle Arm Development Defective) (Maro et al., 2015; Tu et al., 2015). MADD-4 is a secreted protein with predicted metalloprotease activity and physically interacts with the extracellular domains of NLG-1 and NRX-1 (Maro et al., 2015; Tu et al., 2015). *nlg-1* mutants show defects in various behaviours, including the 'basal slowing response' that is mediated by dopamine (Calahorro et al., 2009; Hunter et al., 2010; Izquierdo

et al., 2013). *nlg-1* seems to act together with *nrx-1* to mediate some of its behavioural functions, as a *nlg-1* mutant defect could be rescued by *nrx-1* mutation (Calahorro et al., 2009). The conservation of neuroligins is emphasised by the fact that basal slowing response phenotype of the *nlg-1* mutant is alleviated by expression of human neuroligin-1 (Izquierdo et al., 2013).

C. elegans nlg-1 also forms part of an organismal stress response. The abundance of synaptic NLG-1 is transcriptionally induced by the oxidative stress 'master regulator' SKN-1 to promote organismal survival (Staab et al., 2014). In line with this, *nlg-1* mutants are short-lived (Hunter et al., 2010), sensitive to oxidative stress (Hunter et al., 2010; Staab et al., 2014) and possess higher levels of protein carbonylation, a phenotype which is increased by oxidative stress exposure (Hunter et al., 2010).

4 RESULTS GLIT-1

4.1 *glit-1* encodes a neuroligin-like gene

Mutations in the so far uncharacterised *C. elegans* neuroligin-like gene *glit-1* (*GLIoTactin (Drosophila neuroligin-like))* cause hypersensitivity to oxidative stress and resistance against ER stress. The predicted *GLIT-1* protein structure is similar to those of mammalian neuroligins and contains a single-pass transmembrane domain (**Figure 12A, B**) and an extracellular carboxyesterase-like domain. The carboxyesterase domain lacks the conserved catalytic triad residues characteristic of acetylcholinesterases but instead features two aspartates, a configuration reminiscent of aspartyl proteases (**Figure 12 B**). In *glit-1(gt1981)* mutants, a proline residue in the carboxyesterase domain is substituted by leucine (**Figure 13C**). This proline residue is conserved in neuroligins and acetylcholinesterases (**Figure 12 B**), hence the P113L substitution in the neuroligin-like *glit-1*(*gt1981)* likely interferes with an important protein function.

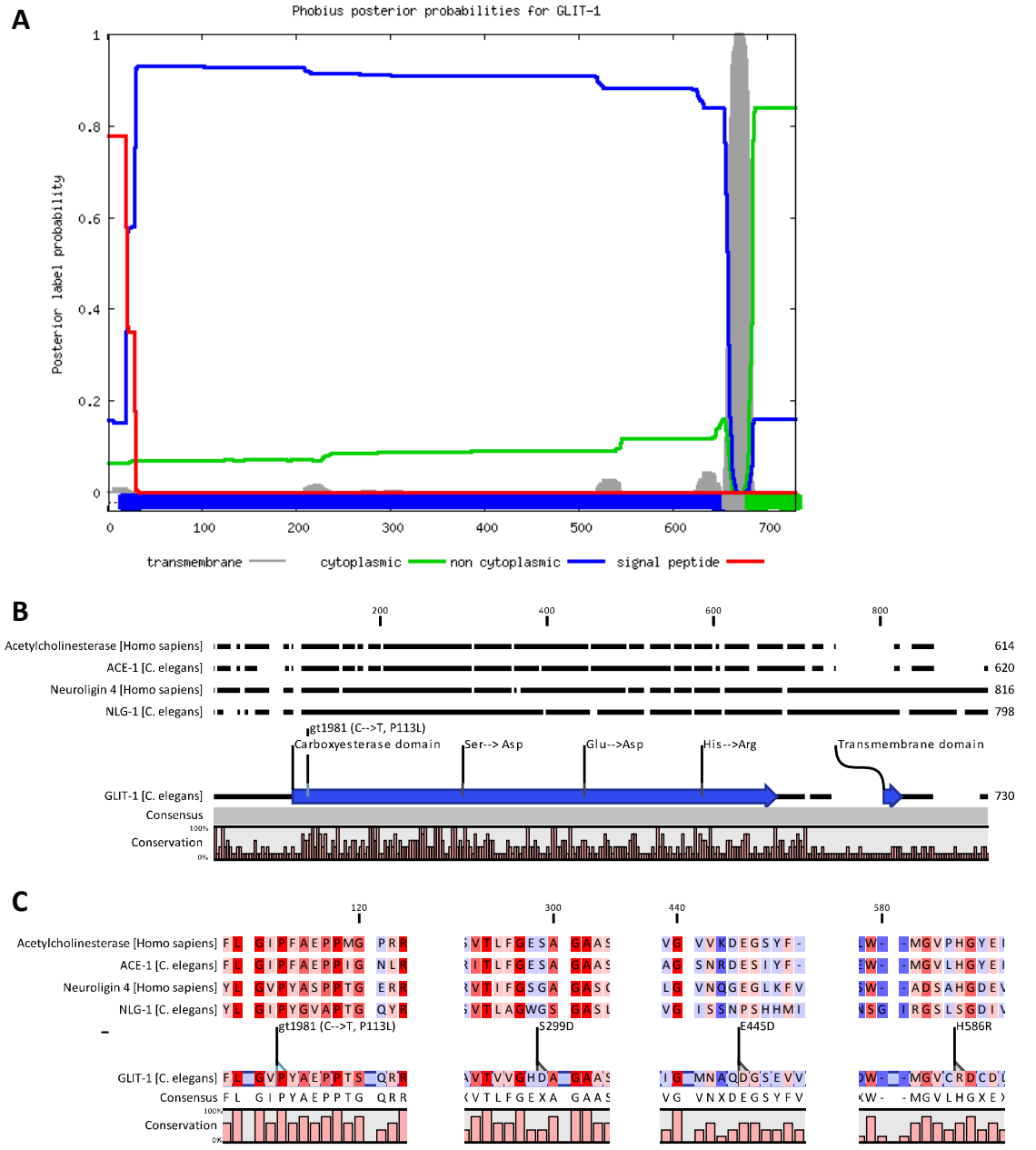

Figure 12: GLIT-1 protein architecture and conservation of residues.

A) GLIT-1 signal peptide (in red), transmembrane domain (in grey) and cytoplasmic/non-cytoplasmic part (in green and blue, respectively) prediction by Phobius (http://phobius.sbc.su.se/).

B)-C) Visualisation of conservation score is shown at the bottom of each alignment.

B) Alignment of the human acetylcholinesterase and neuroligin 4 and *C. elegans* acetylcholinesterase ACE-1, neuroligin NLG-1 and neuroligin-like GLIT-1. Carboxyesterase and transmembrane domain are indicated with an arrow.

C) Magnification of alignment in B) to show conservation of the proline residue mutated in *gt1981* (P113L) and non-conservation of the serine (S), histidine (H) and glutamate (E) residues that form part of the catalytic triad of acetylcholinesterases. High conservation is indicated in red and low conservation in blue.

Based on its categorisation as a neuroligin-like protein, GLIT-1 should be phylogenetically closer to neuroligins than to acetylcholinesterases. Indeed, in a phylogenetic tree based on human, mouse, *Drosophila* and *C. elegans* neuroligins and acetylcholinesterases, GLIT-1 groups with its *Drosophila* homologue gliotactin and close to invertebrate neuroligins (**Figure 13A, B**). The *glit-1 Drosophila* homologue gliotactin is localised at tricellular junctions (Schulte et al., 2006) and necessary for the development of septate junctions, an invertebrate analogue of tight junctions in epithelial cells (Genova and Fehon, 2003; Schulte et al., 2006). Thyroglobulin, a *glit-1* human orthologue according to Panther (Protein ANalysis THrough Evolutionary Relationships) also possesses a carboxyesterase domain and was included in the tree but does not group close to GLIT-1. This is not unexpected since thyroglobulin is a vertebrate-specific protein (Holzer et al., 2016). We note however that thyroglobulin is a precursor of thyroid hormones which are transported by transthyretin, an orthologue of *C. elegans ttr-33*. In addition, thyroglobulin folds an dimerises in the endoplasmic reticulum (ER) and a defect in ER export leads to ER storage disease (Kim et al., 1998). In summary, the phylogenetic analysis confirms the classification of GLIT-1 as a neuroligin-like protein.

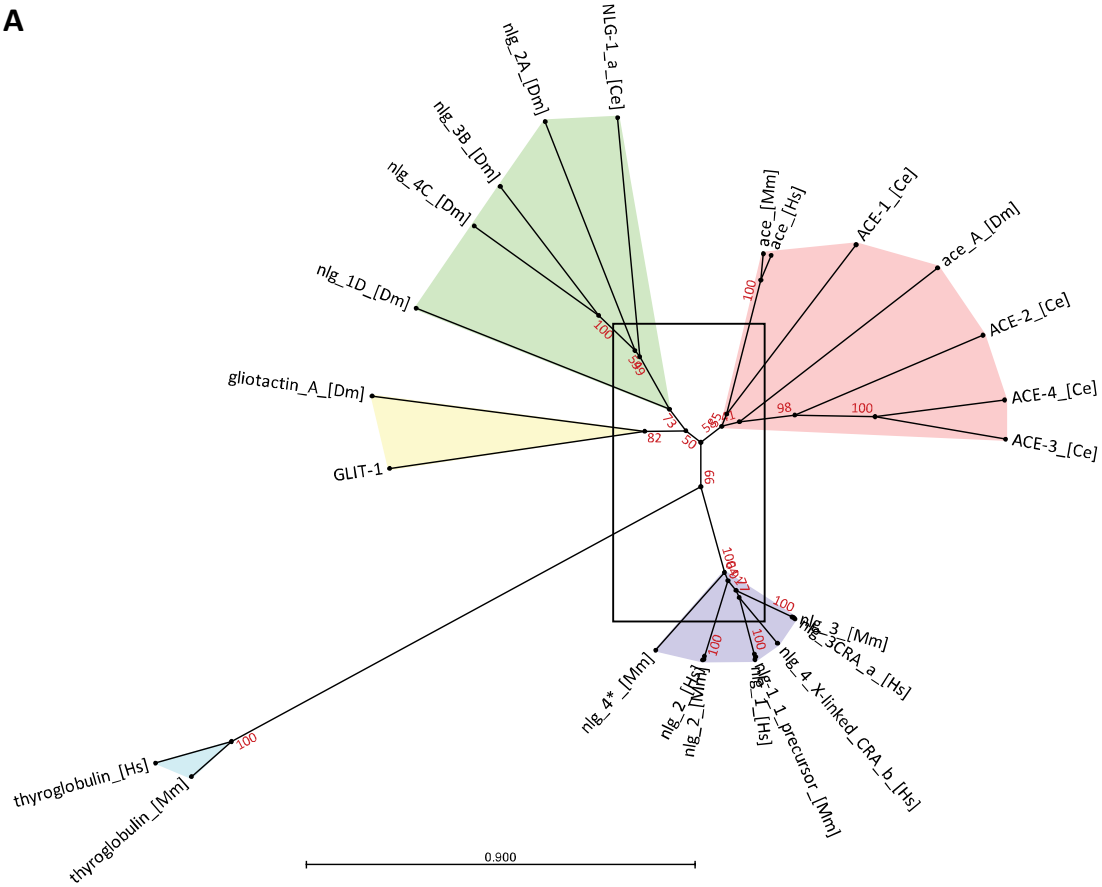
A
NLG-1_a_[Ce]
nlg_2A_[Dm]
nlg_3B_[Dm]
nlg_4C_[Dm]
nlg_1D_[Dm]
gliotactin_A_[Dm]
GLIT-1
thyroglobulin_[Hs]
thyroglobulin_[Mm]
ace_[Mm]
ace_[Hs]
ACE-1_[Ce]
ace_A_[Dm]
ACE-2_[Ce]
ACE-4_[Ce]
ACE-3_[Ce]
nlg_3_[Mm]
nlg_3CRA_a_[Hs]
nlg_4_X-linked_CRA_b_[Hs]
nlg_1_1_precursor_[Mm]
nlg_1_[Hs]
nlg_2_[Hs]
nlg_2_[Mm]
nlg_4*_[Mm]
0.900
B
0.150
C
R413
S276
Y531
D408

Figure 13: *gt1981* is located in the cholinesterase domain of the neuroligin-like protein *glit-1*.
A) Phylogenetic tree of acetylcholinesterases and neuroligins from *C. elegans*, *Drosophila,* mouse and human, gliotactin from *Drosophila* and thyroglobulin from mouse and human. Bootstrap values are indicated in red on top of the branches. ACE = Acetylcholinesterase, Ce = *C. elegans*, Dm = *Drosophila melanogaster*, Hm = *Homo sapiens*, Mm = *Mus musculus,* NLG = Neuroligin.
B) Enlargement of centre part of phylogenetic tree in A). Bootstrap values are indicated in red on top of the branches.
C) GLIT-1 protein structure prediction based on homology modelling with acetylcholinesterase (PDB ID: 2W6C). The *gt1981* point mutation leads to a proline to glycine conversion (P113G) and is indicated in red. The amino acids which now reside at the position of the previous catalytic triad are indicated in blue.

4.2 Genetically, *glit-1* does not act via neurexin but GLIT-1 PDZ domain interactors can be predicted

Neuroligins modulate signalling by contacting pre-synaptic neurexins (Südhof, 2008). Therefore we asked if the *C. elegans* neurexin *nrx-1* protects dopaminergic neurons from 6-OHDA-induced neurodegeneration as the neuroligin-like *glit-1.* In *C. elegans* and higher organisms there are many neurexin isoforms due to alternative splicing (Calahorro, 2014) (**Figure 14D**). We acquired two strains with deletions in the only *C. elegans* neurexin *nrx-1*, *ok1649* affecting only the long isoform and *wy778* affecting the long and short isoforms of the gene (**Figure 14D**). However, neither of the two *nrx-1* deletions led to premature loss of dopaminergic neurons after exposure to 6-OHDA (**Figure 14A**). The *nrx-1(ok1649)* mutation slightly alleviated neurodegeneration of *glit-1* mutants (**Figure 14A**), but also in wild-type worms (**Figure 14B**). Hence, *glit-1* is a neuroligin-like gene but does not seem to act with the neurexin *nrx-1* to prevent dopaminergic neuron death.

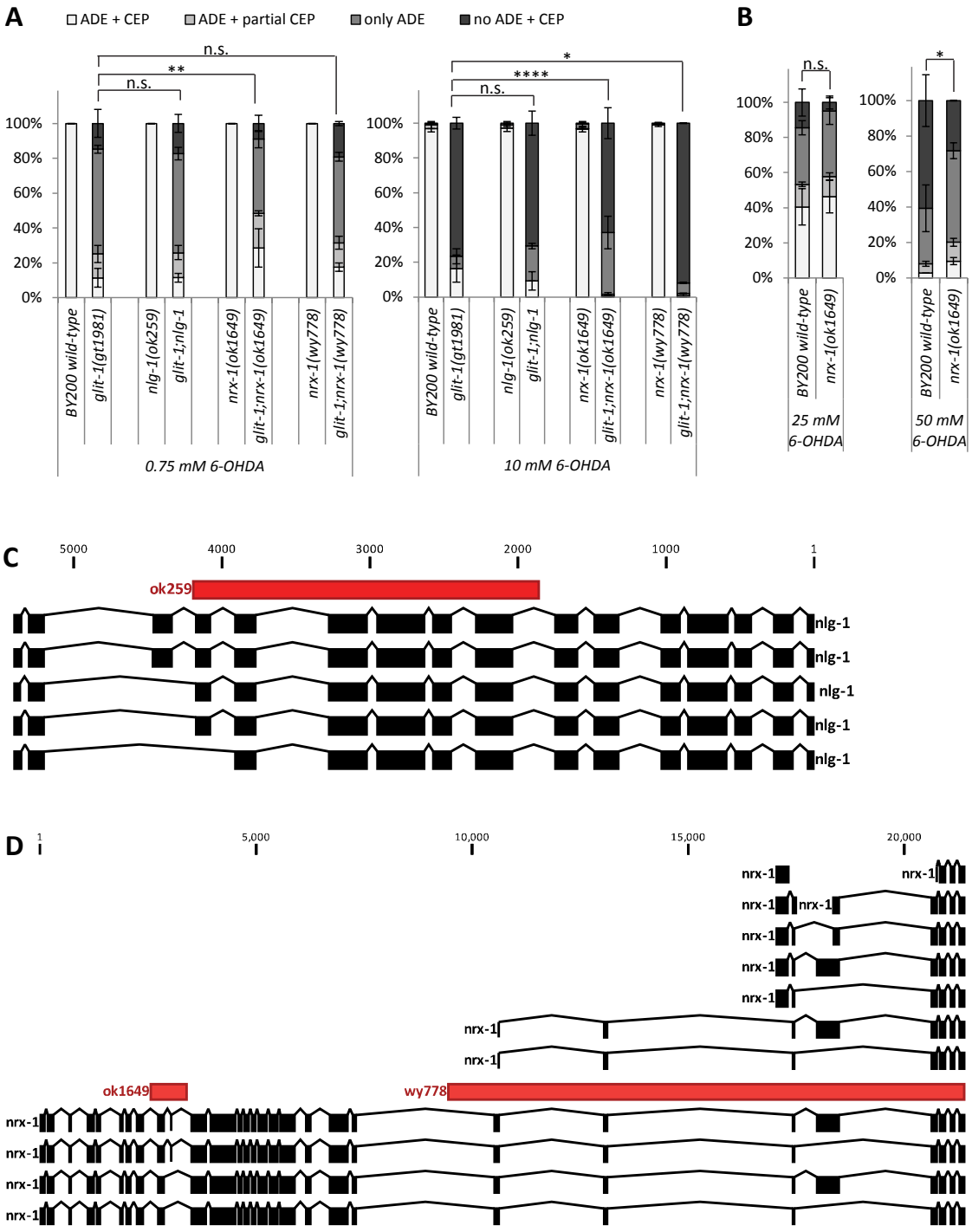
A
ADE + CEP
ADE + partial CEP
only ADE
no ADE + CEP
n.s.
**
n.s.
*
****
n.s.
100%
80%
60%
40%
20%
0%
BY200 wild-type
glit-1(gt1981)
nlg-1(ok259)
glit-1;nlg-1
nrx-1(ok1649)
glit-1;nrx-1(ok1649)
nrx-1(wy778)
glit-1;nrx-1(wy778)
0.75 mM 6-OHDA
10 mM 6-OHDA
B
n.s.
*
25 mM 6-OHDA
50 mM 6-OHDA
C
5000
4000
3000
2000
1000
1
ok259
nlg-1
D
1
5,000
10,000
15,000
20,000
nrx-1
ok1649
wy778

Figure 14: *C. elegans* neuroligin and neurexin mutations do not lead to premature dopaminergic neurodegeneration.
Dopaminergic head neurons were scored 72 h after intoxication with indicated concentration of 6-OHDA.
A) Effects of neuroligin and neurexin mutations on dopaminergic neurodegeneration in the *glit-1* mutant. Error bars = SEM of 2 biological replicates, each with at least 75 animals per strain and concentration. Total number of animals per condition n = 150-220 (****p<0.0001, **p<0.01, n.s. p>0.05; G-Test).
B) Effect of neurexin *nrx-1(ok259)* mutation on dopaminergic neurodegeneration in wild-type animals. Error bars = SEM of 2 biological replicates, each with at least 80 animals per strain and concentration. Total number of animals per condition n = 170-220 (*p<0.05, n.s. p>0.05; G-Test).
C) *C. elegans* neuroligin *nlg-1* gene structure with indicated *ok259* deletion site.
D) *C. elegans* neurexin *nrx-1* gene structure with indicated deletion sites *ok1649* and *wy778*.

Like mammalian neuroligins and *C. elegans* NLG-1, GLIT-1 contains a short intracellular domain (**Figure 12A**) with a C-terminal PDZ-binding motif, which might be bound by PDZ (PSD95, Dlg1, Zo-1) domain proteins. PDZ-domain containing interactors can be predicted based on the sequence and structure of the PDZ-binding motif (Hui and Bader, 2010; Hui et al., 2013). The sequence-based prediction was made by a machine-learning algorithm that was trained with large scale PDZ protein-binding data (Hui and Bader, 2010), whereas the algorithm was trained with PDZ domain structures and peptide sequence information for the structure-based prediction (Hui et al., 2013). Based on the last five amino acids of GLIT-1 (RITNL), potential GLIT-1 binding proteins were determined (**Table S 1, Table S 2**). Candidates include SHN-1 (SHANK (SH3/Ankyrin domain scaffold protein) related) − a mammalian homologue of which was proposed to form a complex with neuroligin and neurexin (Südhof, 2008)) − and DLG-1 (Drosophila Discs LarGe homolog) − the *Drosophila* homologue of which forms a complex with the GLIT-1 homologue gliotactin (Schulte et al., 2006) (Table S 1 and **Table S 2**). These PDZ domain-containing proteins are obvious candidates to test for their role in mediating GLIT-1 functions.

4.3 *glit-1* mutants show defects in dopamine-associated behaviours

The *C. elegans* neuroligin mutant *nlg-1* displays defects in dopamine-mediated behaviours (Izquierdo et al., 2013), so we aimed to analyse if a mutation in the neuroligin-like *glit-1* interferes with dopamine signalling (**Figure 15E**) as well.

To analyse if dopamine signalling is functional in the *glit-1* and *ttr-33* mutants, we turned to the basal slowing response assay. *C. elegans* worms slow down when encountering a lawn with bacterial food, a behaviour that is mediated by dopamine (Sawin et al., 2000). In contrast to the tyrosine hydroxylase mutant *cat-2 (abnormal catecholamine distribution)* which is defective in dopamine synthesis, *glit-1* and *ttr-33* mutants moved slower on plates with bacteria than on empty plates (**Figure 15D**) and the same has been shown before for *tsp-17* (Masoudi et al., 2014). Since *glit-1*, *ttr-33* or *tsp-17* mutants did not exhibit a compromised basal slowing response, dopamine signalling does not appear decreased in these strains.

In *C. elegans*, dopamine regulates acetylcholine release in motor neurons, which in turn stimulates muscle action (**Figure 15E**) (Chase and Koelle, 2007). Hence, when animals are exposed to increasing concentrations of exogenous dopamine in the 'dopamine paralysis assay', this eventually leads to inhibition of acetylcholine release and muscle paralysis (Sanyal et al., 2004). Animals with a higher level of intrinsic dopamine signalling are expected to paralyse at lower concentration of exogenous dopamine and vice versa. We found that *glit-1* and *tsp-17* mutants, but not *ttr-33* mutants, stopped moving at lower dopamine concentrations than wild-type animals (**Figure 15A**). In support of increased endogenous dopamine signalling, *glit-1* mutants showed reduced egg-laying (**Figure 15B**), a behaviour which is inhibited by dopamine (Schafer and Kenyon, 1995). A previous study showed increased dopamine uptake for neurons from *tsp-17* mutant neurons, suggesting that the accompanying higher 6-OHDA uptake causes hypersensitivity against the drug (Masoudi et al., 2014). Since a higher dopamine uptake might be a secondary effect of a higher dopamine

release, it is possible that *glit-1* and *tsp-17* act via a similar mechanisms. However, the *tsp-17* single mutant paralysed at a lower dopamine concentration than the *glit-1* single mutant (**Figure 15A**). In addition, the phenotype of the *glit-1*;*tsp-17* double mutant was stronger compared to the respective single mutants. Thus, there might be two at least partially additive mechanisms causing increased dopamine release in *glit-1* and *tsp-17* mutants.

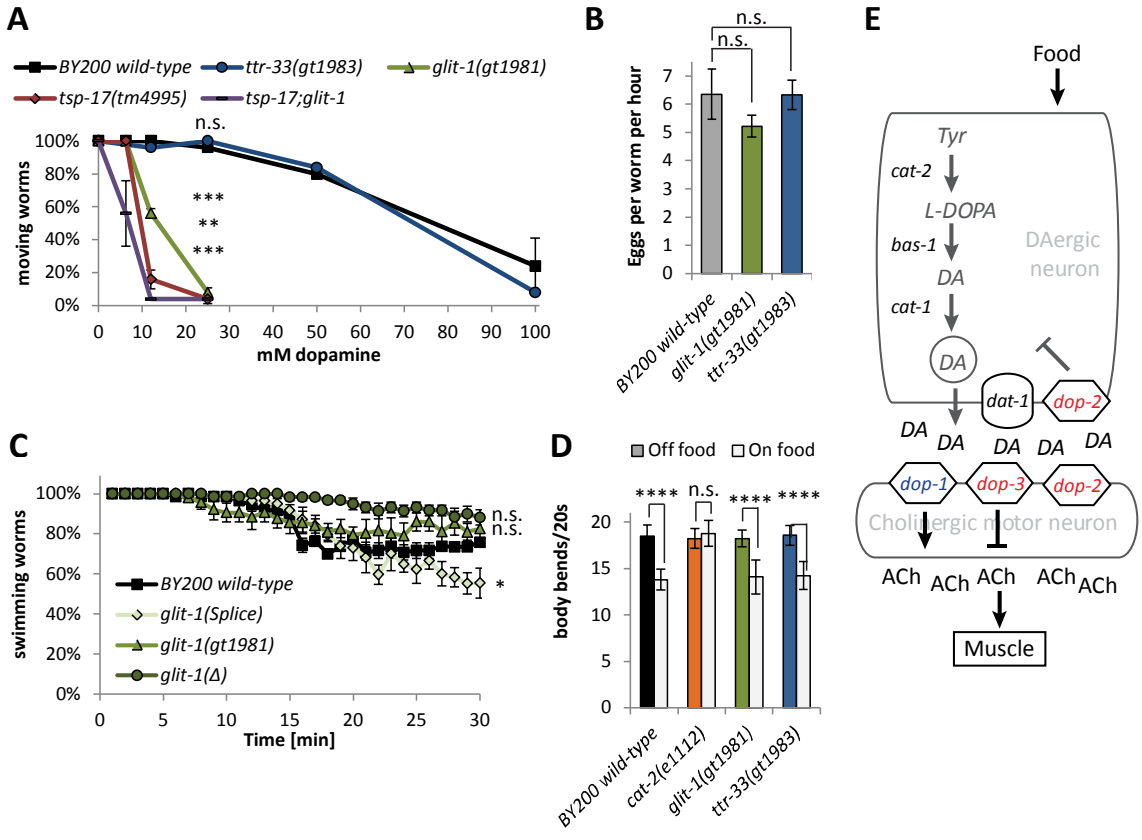

Figure 15: Dopamine-mediated behaviours are altered in *glit-1* and *tsp-17*, but not *ttr-33* mutants.
A) Dopamine paralysis assay: Ability of young adult animals to move on plates with indicated concentrations of dopamine. Error bars = StDev of 2 technical replicates, each with 25 animals per strain and condition. Total number of animals per condition n = 50 (***p<0.001, **p<0.02, n.s. p>0.05; two-tailed t-test comparing wild-type and mutant animal data at 25 mM dopamine).
B) Egg-laying assay (done by Eline Jongsma): Number of eggs per worm per hour. Error bars = StDev of 3 technical replicates, each with 3 animals laying at least 45 eggs. A total number of 9 animals laid a total number of eggs per strain n = 140-171 (n.s. p>0.05; two-tailed t-test).
C) Swimming-induced paralysis (SWIP) assay: Ability of L4 stage animals to swim in a drop of water. Error bars = SEM of at least 3 biological replicates with at least 12 animals per strain. Total number of animals per strain n = 50-60 (*p<0.05, n.s. p>0.05; two-tailed t-test comparing wild-type and mutant data at 30 min time point).
D) Basal slowing response (done by Eline Jongsma): Ability of young adult animals to slow down on a lawn of bacteria. The tyrosine hydroxylase mutant *cat-2 (abnormal catecholamine distribution)* is deficient of dopamine synthesis. Error bars = SEM of 2 biological replicates, each with 6 animals per strain and state. Total number of animals per condition n = 12 (****p<0.0001, n.s. p>0.05; two-tailed t-test).
E) Dopamine signalling cartoon. Dopaminergic (DAergic) neurons are stimulated by food. Dopamine synthesis starts with tyrosine (Tyr), which is converted to L-DOPA (L-3,4-dihydroxyphenylalanine) by the tyrosine hydroxylase *cat-2 (abnormal catecholamine distribution)* and then to dopamine (DA) by the aromatic amino acid decarboxylase *bas-1 (biotenic amine synthesis related).* Dopamine is packed into vesicles by the vesicular monoamine transporter *cat-1*. Postsynaptic dopamine signalling is stimulated by the the D1-like dopamine receptor *dop-1* and inhibited by the D2-like dopamine receptor *dop-3*. The D2-like receptor *dop-2* can also be postsynaptic or presynaptic and acts as an autoreceptor. The D1-like (stimulatory) and the D2-like (inhibitory) dopamine receptors are indicated in blue and red, respectively. Dopamine is transported back into the dopaminergic neurons via the dopamine transporter *dat-1*. Cholinergic neurons signal via the neurotransmitter ACh (acetylcholine) which in turn stimulates muscle action.

A second approach to test for excessive dopamine signalling is the swimming-induced paralysis (SWIP) assay. Here, worms are put in a drop of water to monitor their swimming behaviour. Mutants with higher extrasynaptic dopamine concentrations, like the dopamine transporter mutant *dat-1,* exhibit premature paralysis (McDonald et al., 2007). Also *tsp-17* mutants have been shown to exhibit premature paralysis (Masoudi et al., 2014), but *glit-1* mutants did not paralyse earlier than wild-type worms (**Figure 15C**). Animals with the *glit*-1(ok237) deletion seemed to swim even longer than wild-type animals; however, this mutation affects also two neighbouring genes that could cause these effects. Taken together, the dopamine paralysis assay and the SWIP assay suggest that the dopamine signalling defects in *glit-1* mutants might

be much smaller than in *tsp-17* mutants, and can therefore not be detected in the SWIP assay. Alternatively, *glit-1* and *tsp-17* might have different mechanisms of action to interfere with dopamine release.

4.4 Interference with dopamine metabolism increases *glit-1* dopaminergic neurodegeneration

glit-1 mutants showed signs of higher intrinsic dopamine signalling and we wanted to address if this could be the reason for their sensitivity to 6-OHDA. If a change in dopamine metabolism is the cause for *glit-1* mutant hypersensitivity, interference with dopamine metabolism (**Figure 15E**) is expected to alter the *glit-1* phenotype. We find that mutation of the tyrosine hydroxylase *cat-2* highly, and mutation of the vesicular monoamine transporter *cat-1* slightly augmented dopaminergic neurodegeneration of *glit-1* mutants (**Figure 16B**). This enhancement was specific for *glit-1*, since degeneration of wild-type animals was not increased by *cat-2*, and might even be decreased by *cat-1* (**Figure 16C**). Mutation of the aromatic amino acid decarboxylase *bas-1,* which is also part of the dopamine synthesis pathway, did not modulate *glit-1* sensitivity. Yet importantly, out of the three tested enzymes, *cat-2* is the one specific for dopamine synthesis since *bas-1* also functions in serotonin production and *cat-1* also mediates vesicle packing in serotonergic, tyraminergic and octopaminergic neurons (Chase and Koelle, 2007). CAT-1 mediates synaptic vesicle packing, thus a *cat-1* mutation might lead to increased cytosolic dopamine levels which were shown to be detrimental for dopaminergic neurons. A mutation in *cat-2* in contrast leads to decreased dopamine synthesis and as a result, a 6-OHDA/dopamine ratio should be tilted in favour of 6-OHDA. Since both dopamine and 6-OHDA compete for entry into dopaminergic neurons via *dat-1*, a higher proportion of 6-OHDA entering the cell could explain the increased sensitivity of *glit-1*;*cat-2* mutants. In line with this argument, CAT-2 overexpression was shown to diminish 6-OHDA-induced dopaminergic neurodegeneration, likely because of increased dopamine synthesis (Masoudi et al., 2014). Alternatively, defects in dopamine synthesis might

cause additional cellular stress, leading to decreased resistance to 6-OHDA. In summary, we find that a decrease in dopamine synthesis or vesicle packing leads to an increased loss of dopaminergic neurons in *glit-1* mutants.

Dopamine acts by binding to the D_1-type (stimulatory) dopamine receptor *dop-1* and the D_2-type (inhibitory) dopamine receptors *dop-2* and *dop-3* and we aimed to investigate if the downstream signalling mediated by these receptors affects the *glit-1* phenotype. We found that mutation of *dop-2* decreased the sensitivity of *glit-1* mutants (**Figure 16A**), however this is also true for wildtype worms (**Figure 16C**). Studies in mice and cell culture indicate that D_2-type receptors regulate activity and cell surface expression of the dopamine transporter (Bolan et al., 2007; Lee et al., 2007b) and pharmacological inhibition of D2 class dopamine receptors in rats was shown to inhibit dopamine transporter function (Cass and Gerhardt, 1994). Similarly, mutation of the *C. elegans* D_2-type dopamine receptor *dop-2* might lead to a decrease in dopamine transporter activity. This is expected to lead to decreased 6-OHDA uptake and thus reduced 6-OHDA toxicity in dopaminergic neurons. *C. elegans dop-2* was reported to act as a D_2-type presynaptic dopamine autoreceptor and to stimulate dopamine release (Suo et al., 2003; Voglis and Tavernarakis, 2008). This suggests an alternative explanation for the reduced 6-OHDA toxicity in *dop-2* mutant animals: decreased amounts of extracellular dopamine competing for cellular entry via the dopamine transporter would also lead to a higher amount of toxic 6-OHDA being able to enter the neuron.

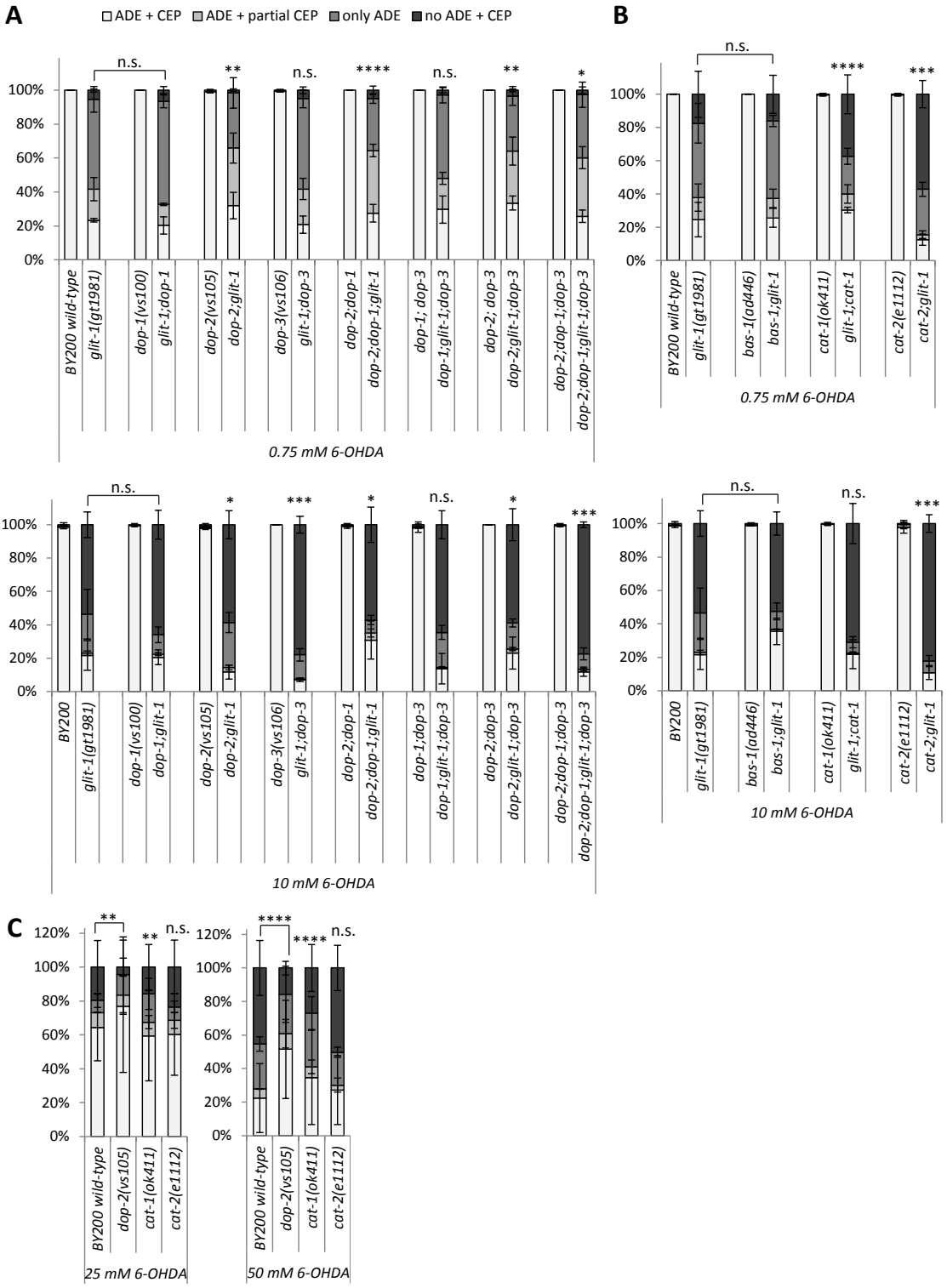
A
ADE + CEP
ADE + partial CEP
only ADE
no ADE + CEP
n.s.
**
n.s.
****
n.s.
**
*
BY200 wild-type
glit-1(gt1981)
dop-1(vs100)
glit-1;dop-1
dop-2(vs105)
dop-2;glit-1
dop-3(vs106)
glit-1;dop-3
dop-2;dop-1
dop-2;dop-1;glit-1
dop-1; dop-3
dop-1;glit-1;dop-3
dop-2; dop-3
dop-2;glit-1;dop-3
dop-2;dop-1;dop-3
dop-2;dop-1;glit-1;dop-3
0.75 mM 6-OHDA
B
n.s.
****
***
BY200 wild-type
glit-1(gt1981)
bas-1(ad446)
bas-1;glit-1
cat-1(ok411)
glit-1;cat-1
cat-2(e1112)
cat-2;glit-1
0.75 mM 6-OHDA
n.s.
*
***
n.s.
*
n.s.
*
***
BY200
glit-1(gt1981)
dop-1(vs100)
dop-1;glit-1
dop-2(vs105)
dop-2;glit-1
dop-3(vs106)
glit-1;dop-3
dop-2;dop-1
dop-2;dop-1;glit-1
dop-1;dop-3
dop-1;glit-1;dop-3
dop-2;dop-3
dop-2;glit-1;dop-3
dop-2;dop-1;dop-3
dop-2;dop-1;glit-1;dop-3
10 mM 6-OHDA
n.s.
n.s.
***
BY200
glit-1(gt1981)
bas-1(ad446)
bas-1;glit-1
cat-1(ok411)
glit-1;cat-1
cat-2(e1112)
cat-2;glit-1
10 mM 6-OHDA
C
**
n.s.
**
****
****
n.s.
BY200 wild-type
dop-2(vs105)
cat-1(ok411)
cat-2(e1112)
25 mM 6-OHDA
50 mM 6-OHDA

Figure 16: Interference with dopamine synthesis and vesicle packing increases *glit-1* dopaminergic neurodegeneration.
Dopaminergic neurons were scored 72 h after intoxication with indicated concentration of 6-OHDA.
A) Effect of dopamine receptor mutations on dopaminergic neurodegeneration in the *glit-1* mutant background. Error bars = SEM of 3 biological replicates, each with at least 60 animals per strain and concentration. Total number of animals per condition n = 180-330 (****p<0.0001, ***p<0.001, **p<0.01, *p<0.05, n.s. p>0.05; G-Test comparing *glit-1* mutant data to double and triple mutant data). A significant p-value is only indicated if all or all but one replicate were found to be significant.
B) Effect of mutations in dopamine metabolism genes on dopaminergic neurodegeneration in the *glit-1* mutant background.
Error bars = SEM of 3 biological replicates, each with at least 60 animals per strain and concentration. Total number of animals per condition n = 180-330 (****p<0.0001, ***p<0.001, n.s. p>0.05; G-Test comparing *glit-1* mutant data to double mutant data).
C) Effect of mutations in the dopamine receptor *dop-2* and the dopamine metabolism genes *cat-1* and *cat-2* on dopaminergic neurodegeneration in a wild-type background.
Error bars = SEM of 3 biological replicates, each with at least 60 animals per strain and concentration. Total number of animals per condition n = 180-330 (****p<0.0001, **p<0.02, n.s. p>0.05; G-Test comparing BY200 wild-type to mutant animal data). A significant p-value is only indicated if all or all but one replicate were found to be significant.
dop-1, dop-2, dop-3 = dopamine receptors, *bas-1* (biotenic amine synthesis related) = aromatic amino acid decarboxylase, *cat-1* (abnormal catecholamine distribution = the vesicular monoamine transporter, *cat-2* (abnormal catecholamine distribution) = tyrosine hydroxylase.

4.5 *glit-1* is expressed in pharynx, intestine and possibly dopaminergic neurons

glit-1 genetically interacts with *cat-2,* the key enzyme of dopamine synthesis, and mutation of *glit-1* partially phenocopies mutation of *tsp-17,* a gene shown to function in dopaminergic neurons (Masoudi et al., 2014). Several constructs were created to determine where *glit-1* acts. Unfortunately, a C-terminal CRISPR-Cas9 GFP insertion at the *glit-1* locus seemed to render the protein non-functional: No GFP expression was visible and the GFP-tagged gene was not able to rescue the *glit-1*(*gt1981*) mutant phenotype, *glit-1*(*gt1981*)/*glit-1*::gfp animals were still sensitive to 6-OHDA (data not shown). In parallel, a P*glit-1*::gfp transcriptional construct for targeted chromosomal insertion was made. In five independent lines, GFP expression was detected in animals carrying the non-integrated and therefore stochastically inherited PExglit-1::GFP construct. Expression was visible in the pharynx, intestine and possibly the neurons of L1 larvae – the developmental stage most sensitised to 6-OHDA in the *glit-1*

mutant (**Figure 17A, B**). In adult animals, dopaminergic neurons seemed to express the P*glit-1*::gfp construct (**Figure 17C, D**), however adults were not sensitive to 6-OHDA (**Figure 10B**). Importantly, *glit-1* is in an operon with *rpl-25.1* and shares its promoter region with *dnj-14,* which is situated on the other strand (**Figure 2D**). Therefore, a P*glit-1*::gfp transcriptional reporter construct automatically includes parts of those other promoters that could also drive expression, so only cautious interpretations can be made. In summary, GLIT-1 is expressed in pharynx and intestine and possibly in dopaminergic neurons.

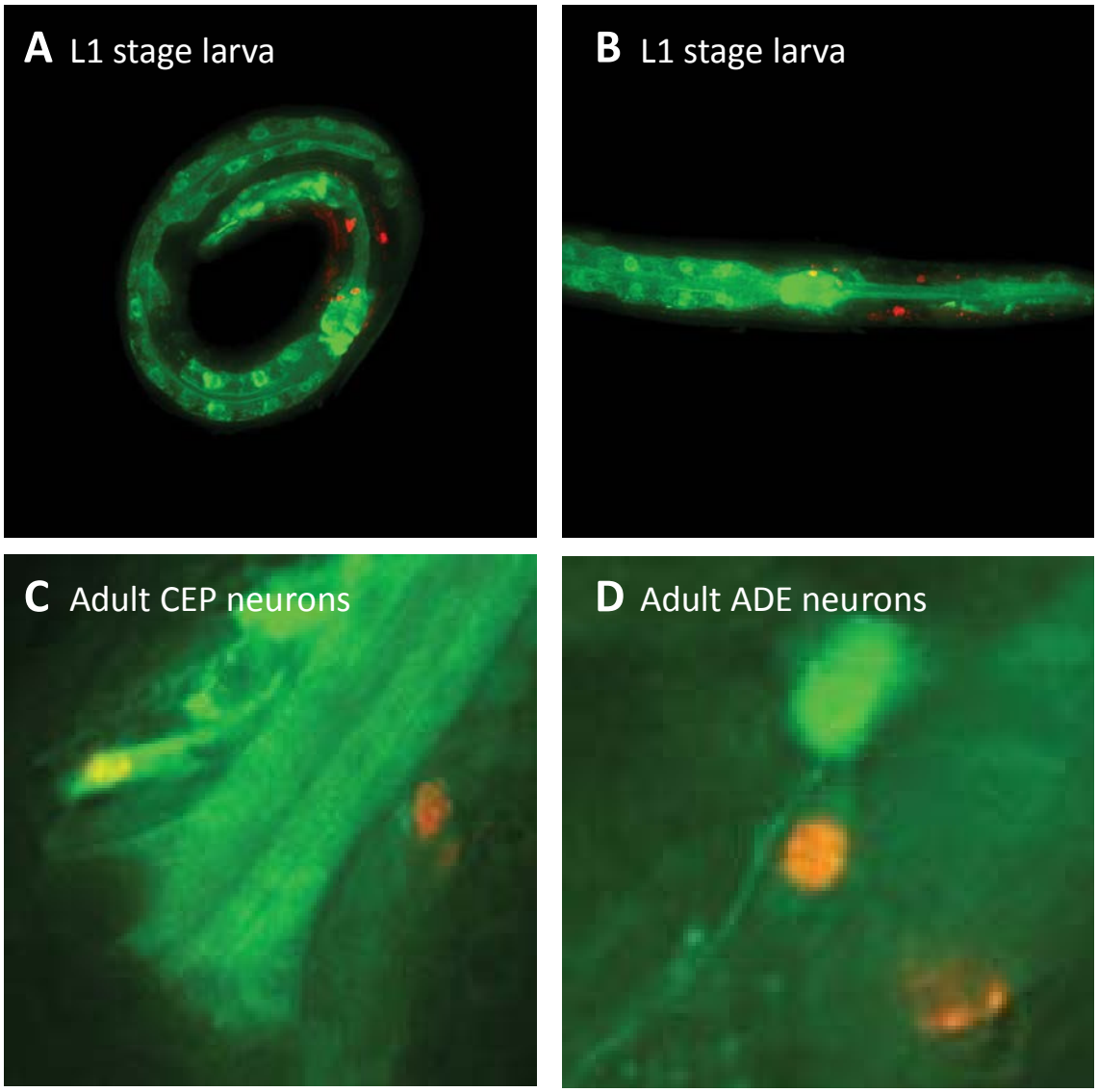

Figure 17: glit-1 is expressed in pharynx and intestine and might be expressed in dopaminergic neurons.
Animals expressing the extrachromosomal, transcriptional PExglit-1::GFP construct in the background of Pdat-1::RFP which labels nuclei of dopaminergic neurons.
A) L1 stage larva.
B) L1 stage larva.
C) CEP-neuron containing head region of adult animal.
D) ADE-neuron containing head region of same adult animal.

5 INTRODUCTION TRANSTHYRETIN-RELATED TTR-33

5.1 Transthyretin, transthyretin-like and transthyretin-related proteins

ttr-33 belongs to the nematode-specific family of transthyretin-related proteins, which likely arose from a duplication of an ancestral transthyretin-like family (Jacob et al., 2007), similar to the vertebrate-specific transthyretins (Richardson, 2015).

Transthyretin (transporter of thyroxine (T_4) and retinol) transports thyroid hormones and retinol, in the latter case through binding to retinol-binding protein, and is associated with amyloid diseases (Alshehri et al., 2015). The ancestral transthyretin-like family has characteristic residues to hydrolyse a product of uric acid oxidation, however these are lost in transthyretin (Richardson, 2015). Transthyretin is mainly synthesised in the liver and the choroid plexus of the brain (Alshehri et al., 2015) – a branching network of cells that produces the cerebrospinal fluid. The pathological deposition of transthyretin can cause amyloid diseases: wild-type transthyretin is connected to age-dependent senile systemic amyloidosis (SSA), whereas mutant transthyretin is associated with autosomal dominant familial amyloid polyneuropathy (FAP) which leads to axonal loss and neuronal death in peripheral nerves (Richardson and Cody (Eds.), 2009). FAP mutations destabilise the transthyretin homotetramer (McCutchen et al., 1993, 1995). However, there are protective 'trans-suppressor' transthyretin mutations that counteract this destabilisation (Hammarström et al., 2001) similarly to several inhibitors of transthyretin amyloidosis (Hammarström et al., 2003).

Apart from its role as a transport protein, additional transthyretin functions have been suggested. One lab proposed a protease activity (Liz et al., 2004) that seems important for the role of transthyretin as an enhancer of nerve regeneration (Fleming et al., 2007; Liz et al., 2009). Furthermore, in mice with a compromised heat-shock response (due to heterozygosity of the heat-shock transcription factor HSF1) TTR seems to contribute to control neuronal cell death and inflammation (Santos et al., 2010). In line with this, transthyretin seems to behave

as a neuronal stress protein regulated by HSF1 in human neuroblastoma cells and in an Alzheimer's disease mouse model (Wang et al., 2014). Finally, transthyretin may promote increase of glucose-induced cytoplasmic Ca^{2+} levels and insulin release in pancreatic β-cells (Refai et al., 2005).

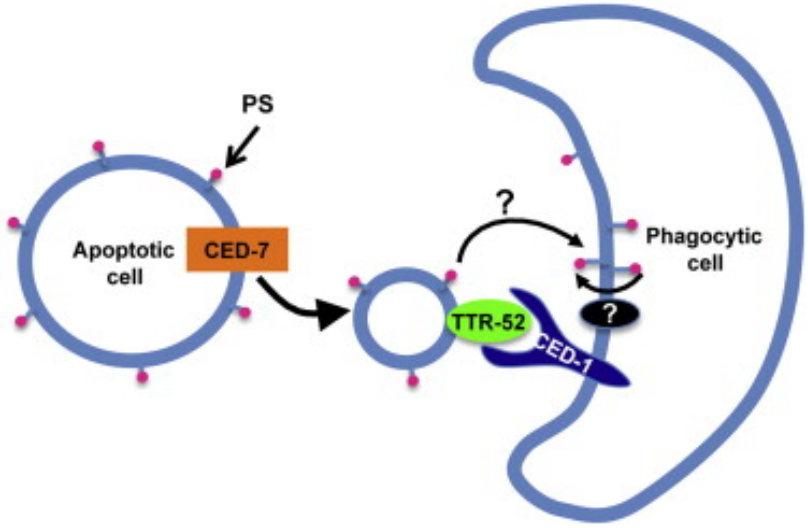

Figure 18: Model of TTR-52/CED-7 phosphatidylserine vesicle transfer – from (Mapes et al., 2012)**.**
The ATP binding cassette (ABC) transporter CED-7 mediates the exposure of phosphatidylserine (PS) on the surface of apoptotic cells which is bound by TTR-52. Both CED-7 and TTR-52 promote the generation of extracellular PS vesicles between apoptotic and engulfing cell. CED-7, TTR-52 and the TTR-52-binding phagocyte receptor CED-1 are necessary for the appearance of PS on the engulfing cell.

The *C. elegans* family of TransThyretin-Related genes consists of 59 members but only *ttr-52* has been characterised so far. TTR-52 is secreted and acts as a bridge between phosphatidylserine (PS) that is exposed on the surface of apoptotic cells and the phagocyte receptor CED-1/MEGF10 (Wang et al., 2010) (**Figure 18**, **Figure 23A**). Intriguingly, PS exposure becomes reduced in older or unengulfed apoptotic cells and is also detected on the surface of phagocytes (Mapes et al., 2012). It was proposed that TTR-52, CED-7 and NRF-5 (Nose Resistant to Fluoxetine) promote efflux of PS from apoptotic cells by generation of extracellular PS vesicles, thus leading to PS expression on phagocytes in the course of cell

corpse clearance (Mapes et al., 2012; Zhang et al., 2012)(**Figure 18**). TTR-52 is the first example of a molecule connecting an 'eat-me' signal on apoptotic cells to the CED-1 phagocyte receptor in *C. elegans;* however, TTR-52 is not known to have a role in the recognition of necrotic cells.

Surprisingly, it was found that *ttr-52* and other members of the engulfment pathway are also needed for regenerative axonal fusion (Neumann et al., 2014). To mediate the reconnection of two axon parts which have been cut by a laser, *ttr-52* acts together with the PS receptor *psr-1* upstream of the fusion facilitator *eff-1* (epithelial fusion failure) (Neumann et al., 2014). Hence, the same genes which mediate recognition and engulfment of apoptotic cells also mediate 'stitching' of neurons. It is not clear however how the decision between removal and regeneration is made.

5.2 Cell death and engulfment

Apoptosis, necrosis and autophagy are the three main morphologically distinct types of cell death. When cells undergo apoptosis, they shrink and when they undergo necrosis, they swell (**Figure 19**) (Kroemer et al., 2009). Cells that die via autophagy have little or no association with engulfing phagocytes (Kroemer et al., 2009) and exhibit extensive vacuolisation (Nikoletopoulou and Tavernarakis, 2014). However, it is not always possible to determine the type of cell death unequivocally, as some cell death markers might not be present and others might be shared between the different kinds of death (Syntichaki and Tavernarakis, 2002). Also, the same cell can undergo different types of cell death in response to different stimuli (Nikoletopoulou et al., 2013). The use of *C. elegans* as a model organism allowed to decipher molecular mechanisms of cell death and engulfment (Hall et al., 1997; Hengartner, 1997).

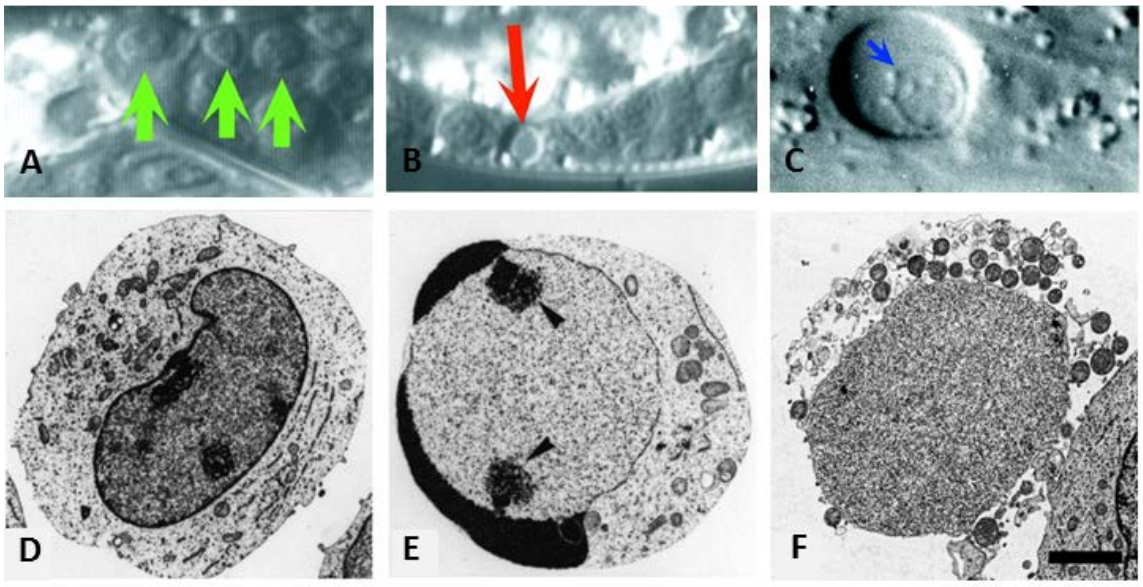

Figure 19: Morphological features of apoptotic and necrotic cells – adapted from (Syntichaki and Tavernarakis, 2002; Ziegler, 2004)**.**
A)-C) Differential interference contrast images of *C. elegans* cells – adapted from (Syntichaki and Tavernarakis, 2002).
A) Healthy cells marked with green arrows.
B) Apoptotic cell with compact, button-like appearance marked with red arrow.
C) Necrotic cell with swollen, vacuole-like appearance. Swollen nucleus marked with blue arrow
D)-F) Transmission electron microscope images of K562 cells – adapted from (Ziegler, 2004), Scale bar A, C = 3 µM, B= 2 µM
D) Healthy cell with normal morphology.
E) Apoptotic cell with condensed chromatin (electron dense, black structure along nuclear membrane) and fragmentation of the nucleus. Nucleoli marked with arrowheads.
F) Necrotic cell.

5.2.1 Apoptosis

Apoptosis is a genetically predetermined ('programmed') type of cell death. Apoptosis can be triggered extrinsically, by activation of cell surface death receptors, or intrinsically, via the mitochondrial signalling pathway (Kroemer et al., 2007). The most prominent morphological features of apoptotic cells include shrinkage and rounding-up, chromatin and nuclear fragmentation and condensation, plasma membrane blebbing, and little or no modification of cytoplasmic organelles (Kroemer et al., 2009) (**Figure 19B, E**). In *C. elegans,* apoptosis is driven

by the core apoptotic pathway consisting of the *cell death abnormality* genes *ced-9/*Bcl-2*, ced-4/*Apaf-1 and the caspase *ced-3* (Wang and Yang, 2016) (**Figure 23A**).

Apoptosis occurs in somatic and germline cells during development (Lettre and Hengartner, 2006) and is assumed to enhance the fitness of the whole organism (Aballay and Ausubel, 2001). Germ cell-specific apoptosis likely preserves the functionality of oogenesis and can be caused by different types of environmental stress (Gartner et al., 2008). DNA damage for example induces germ cell apoptosis via the p53 orthologue CEP-1 (*C. elegans* P-53-like protein), which activates the core apoptosis machinery via two BH3- only proteins, EGL-1 (Egg laying defective) and CED-13 (Derry et al., 2001; Gartner et al., 2000; Schumacher et al., 2001, 2005) (**Figure 23A**). Other types of environmental stress can induce germ cell apoptosis independently of *egl-1* and *cep-1*, but mostly dependent on p38 and JNK stress-activated MAP kinase pathways (Aballay and Ausubel, 2001; Aballay et al., 2003; Salinas et al., 2006).

5.2.2 Necrosis

Classically, necrosis was defined as the type of cell death lacking features of apoptosis or autophagy. However, research suggests that the occurrence and course of necrosis can be tightly regulated by a conserved set of mechanisms (Galluzzi et al., 2014; Vlachos and Tavernarakis, 2010). These mechanisms seem to be largely distinct from apoptosis, since necrotic-like deaths are not affected by mutations in the apoptotic core machinery (Reddien and Horvitz, 2004) and do not involve caspases (cysteine proteases) (Galluzzi et al., 2014).

There are a few necrotic-like cell deaths during *C. elegans* development (Nikoletopoulou and Tavernarakis, 2014) but most of the known necrotic cell deaths are based on extrinsic induction. Non-developmental necrotic cell death can be evoked by extreme environmental conditions – such as heat, hypoxia or hypo-osmotic shock – or by genetically encoded insults (Nikoletopoulou and Tavernarakis, 2014). Morphological features of necrosis are the distortion of the nucleus and the cell body, swelling of cells and organelles and the infolding and

internalisation of plasma membrane (Nikoletopoulou and Tavernarakis, 2014) (**Figure 19C, F**). In addition, increasingly translucent cytoplasm, and plasma membrane rupture with subsequent loss of intracellular contents have been suggested as features of necrotic cells (Nikoletopoulou and Tavernarakis, 2014). Morphological and mechanistic key features between necrotic cell death triggered by hyperactive ion channels in *C. elegans* and 'excitotoxic' cell death induced by hyperexcitation of postsynaptic cells in higher organisms are conserved (Nikoletopoulou and Tavernarakis, 2014).

In *C. elegans*, necrosis can be triggered by intracellular ionic imbalance – e.g. as a result of ion channel, neurotransmitter receptor or neurotransmitter transporter mutations (Vlachos and Tavernarakis, 2010). This imbalance results in Ca^{2+} dyshomeostasis, which is a key feature for necrosis in *C. elegans* (Xu et al., 2001) and neurodegeneration in higher organisms (Wojda et al., 2008). Cytosolic Ca^{2+} levels can rise via cellular influx or by release from the ER, the main intracellular calcium storage compartment (Nikoletopoulou and Tavernarakis, 2014). Ca^{2+} release from the ER is likely mediated by the calreticulin *crt-1* (Xu et al., 2001). Excessive cytoplasmic Ca^{2+} causes activation of Ca^{2+}-dependent calpain proteases (such as *clp-1* and *tra-3*) and lysosomal rupture, which in turn lead to the release of lysosomal cathepsin proteases (aspartyl proteases such as *asp-3* and *asp-4*) and the acidification of the cytoplasm (Artal-Sanz et al., 2006; Syntichaki et al., 2002, 2005) (**Figure 23A**). This 'calpain-cathepsin necrosis cascade' (**Figure 20**) also exists in primates (Yamashima, 2000). Autophagy, the degradation and recycling of cellular components, seems to synergise with lysosomal proteolytic mechanisms and endocytosis to mediate necrotic cell death (Samara et al., 2008; Troulinaki and Tavernarakis, 2011).

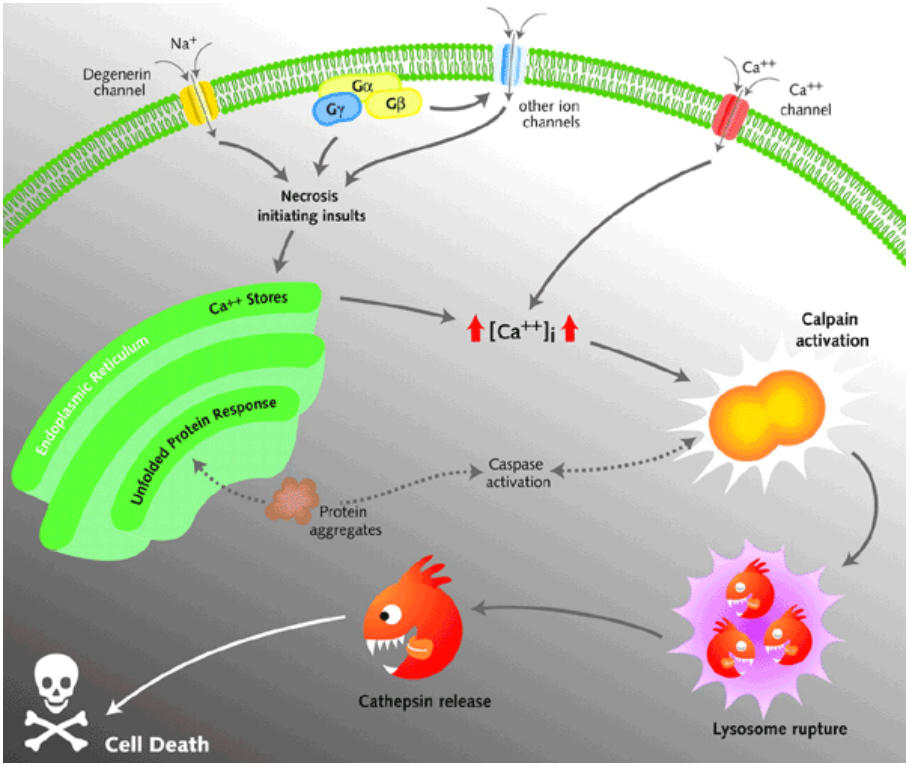

Figure 20: The proposed calpain-cathepsin necrosis cascade – from (Syntichaki and Tavernarakis, 2002)**.**
Necrosis can be triggered in many different ways, e.g. by hyperactive ion channels and Gαs proteins, and by protein aggregates. This leads to the increase in the intracellular cytoplasmic calcium concentration ($[Ca^{++}]_i$). Calcium can be mobilised from the endoplasmic reticulum store and/or through uptake from the extracellular space and can in turn activate Ca^{2+}-sensitive calpains, which provoke the release of lysosomal cathepsin proteases. This could ultimately lead to cell death.

5.2.3 Phagocytosis

The removal of dead cells by phagocytosis is important for tissue remodelling and the regulation of immune responses (Reddien and Horvitz, 2004). Active phagocytic cells in the brain are observed in almost all neurological diseases (Fu et al., 2014), as well as in 6-OHDA models of Parkinson's disease (Long-Smith et al., 2009). In contrast to mammals, there are no specialised phagocytes in *C. elegans*, but cells surrounding dying cells take on that role (Reddien and Horvitz, 2004). Furthermore, apoptotic and necrotic cells seem to be engulfed via distinct mechanisms in mouse cell culture (Krysko et al., 2006), however in *C. elegans,* all dead

cells seem to be eliminated by the same engulfment pathway (Chung et al., 2000; Li et al., 2015).

The recognition of the conserved 'eat-me' signal phosphatidylserine (PS) on the surface of apoptotic and necrotic cells triggers two partially redundant pathways in the engulfing cell (Conradt et al., 2016). In one pathway, the PS receptor *psr-1*/PSR or the integrin α *ina-1* signal to *ced-2*/CRKII, *ced-5*/DOCK180 and *ced-12*/ELMO, which in turn control the activation of the small GTPase *ced-10*/Rac1 (Conradt et al., 2016). *ced-10* activation leads to the reorganisation of the cytoskeleton needed for phagocytosis (Conradt et al., 2016). Apart from PSR-1 and INA-1, the *C. elegans* Frizzled homologue MOM-5 (more of MS) can also act as a receptor (Conradt et al., 2016). In the second pathway, PS is recognised by the two secreted proteins TTR-52 and NRF-5, and CED-7, CED-1/MEGF10 and CED-6 transduce the signal to also activate CED-10 (Conradt et al., 2016) (**Figure 23A**). In addition to the relay via TTR-52, CED-1 may also bind directly to PS (Li et al., 2015). Similarly, there are several known phagocytic receptors in mammals, some of which bind to PS or other 'eat-me' signals directly, whereas others recognise PS via extracellular, soluble bridging molecules (Ravichandran, 2011).

PS needs to be translocated from the inner to the outer leaflet of the plasma membrane to act as an 'eat-me' signal on the cell surface (Eroglu and Derry, 2016). In *C. elegans* apoptotic cells, there are several known mechanisms regulating extracellular phosphatidylserine (PS) exposure. Firstly, the aminophospholipid translocase TAT-1 (transbilayer amphipath transporters (subfamily IV P-type ATPase)) maintains plasma membrane asymmetry of PS (Darland-Ransom et al., 2008; Zullig et al., 2007): *tat-1* knockdown was reported to lead to abnormal PS exposure, triggering stochastic removal of living cells (Darland-Ransom et al., 2008) and to prevent PS exposure on apoptotic cells (Zullig et al., 2007). Secondly, it was proposed that the phospholipid scramblase SCRM-1 translocates PS from the inner to the outer leaflet of the plasma membrane after being activated by mitochondrial release of the

worm apoptosis-inducing (AIF) factor homologue WAH-1 (Wang et al., 2007). Thirdly, CED-8/Xkr8 is activated by caspase cleavage and mediates PS exposure during apoptosis (Chen et al., 2013; Suzuki et al., 2013). In summary, TAT-1, SCRM-1 and CED-8 have been shown control PS exposure on apoptotic cells.

Recently, several mechanisms regulating the exposure of PS on necrotic cells in *C. elegans* have been uncovered as well (Li and Zhou, 2015). Ca^{2+} influx – a key necrosis event – activates the neuronal PS-scramblase and TMEM16F homologue *anoh-1 (anoctamin (calcium-activated chloride channel) homolog),* which mediates cell surface exposure of PS (Li et al., 2015). In addition, *ced-7* also promotes PS exposure and removal of necrotic cells, most likely acting in a partially redundant pathway with *anoh-1* (Li et al., 2015). Lastly, *ced-8* has a modest role in the removal of necrotic cells and was also proposed to act in a partially redundant manner with *anoh-1* (Li et al., 2015). Remarkably, *ced-7* and *ced-8* have established roles in the removal of apoptotic cells, but *anoh-1* function seems to be specific for necrotic cells. Thus, there is likely a set of shared and specific mechanisms regulating PS exposure of apoptotic and necrotic cells.

Besides PS, the calcium-sensing chaperone calreticulin has been reported to act as a second general recognition ligand for engulfment receptors in human cell lines (Gardai et al., 2005). Remarkably, calreticulin only drives engulfment of apoptotic cells once ‘don’t eat me’ signals are inactivated (Gardai et al., 2005). Indeed, various types of ‘eat-me’ and ‘don’t eat me’ signals have been proposed to provide a combinatorial code for phagocytes (Zitvogel et al., 2010). It is conceivable that these codes could vary between different cell types and in response to different stimuli.

6 RESULTS TTR-33

6.1 *ttr-33* encodes a transthyretin-related gene

To determine why the isolated G27E or the L72F substitution in TTR-33 (TransThyretin-Related family domain) render *C. elegans* dopaminergic neurons susceptible to 6-OHDA, we first turned towards protein alignment and structural modelling methods. TTR-33, like the majority *C. elegans* transthyretin-related proteins (Wang et al., 2010), is predicted to be a secreted, non-cytoplasmic protein (**Figure 21A**). The putative N-terminal signal peptide part of *TTR-33* seems to fold into a helix, whereas the rest of the protein consists of beta sheets (**Figure 21b**).

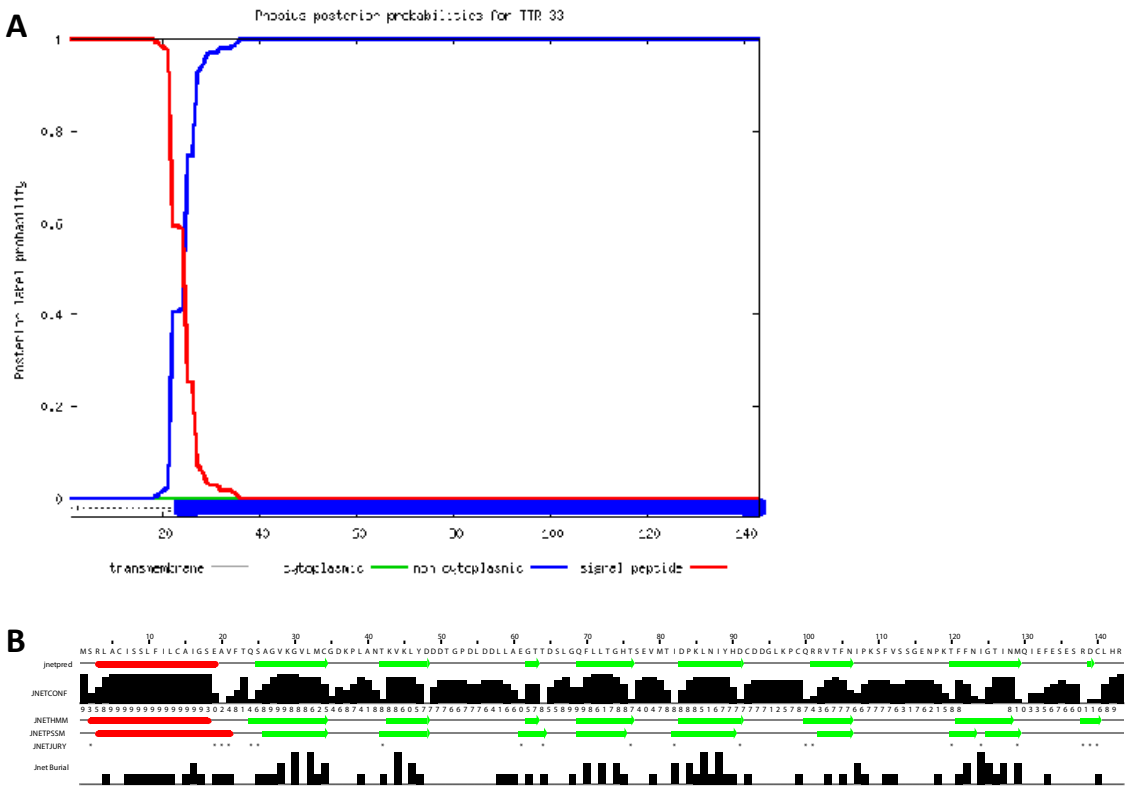

Figure 21: TTR-33 signal peptide prediction.
A) TTR-33 signal peptide (in red), transmembrane domain (in grey) and cytoplasmic/non-cytoplasmic part (in green and blue, respectively) prediction by Phobius (http://phobius.sbc.su.se/).
B) TTR-33 secondary structure prediction indicating helices (red tubes) and beta strands (green arrows) with JPred4

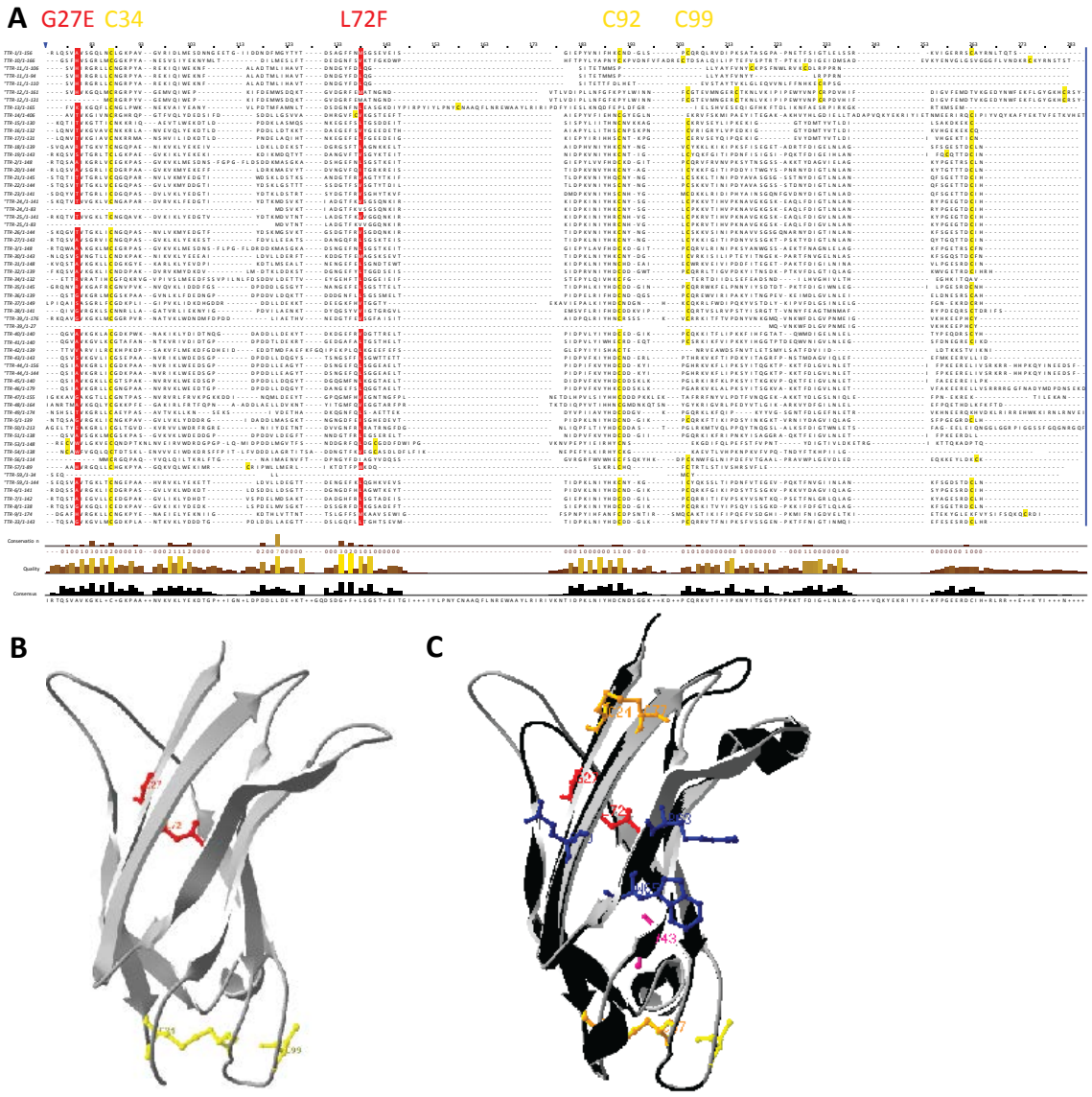

Figure 22: *gt1983* leads to a glycine to glutamate conversion (G27E) in the transthyretin-related protein TTR-33.

A) Alignment of all *C. elegans* TTR's with *TTR-33* (last row). The corresponding amino acids of the mutations in TTR-33 (G27 and L72) are highlighted in red and cysteines marked in yellow. The conservation score, quality and consensus of the alignment are each shown as a bar graph in the bottom of the alignment.

B) Predicted protein structure model of TTR-33 created with homology modelling based on the structure of TTR-52 (PDB ID: 3UAF). Mutated residues are indicated in red and conserved cysteines in yellow.

C) Predicted TTR-33 structure (grey with indicated mutated sites in red and cysteine bridges in yellow) with overlaid TTR-52 structure (black with indicated *sm211* mutation site in pink and cysteine bridges in orange). TTR-52 residues for which mutation leads to loss of dimerisation are marked in blue. Note that the TTR-52 α-helix which does not occur in TTR-33 is assumed to be an artefact due to mutations that were required for crystallisation (Kang et al., 2012).

Amino acids that are important for the protein family function are expected to be conserved and we found that this is the case for L72 but not G27 of *TTR-33* when aligning *C. elegans* (in red in **Figure 22A**). However, both residues were part of two neighbouring beta strands in the predicted TTR-33 3D protein structure (in red in **Figure 22B**). Since these beta strands form part of the dimer interface of the only other characterised *C. elegans* transthyretin-related protein, TTR-52 (Kang et al., 2012) (residues that interrupt the dimer interface in blue in **Figure 22C**), it is possible that the substitutions G27E and L72F interrupt dimerisation of TTR-33. In addition, we found conservation of 3 cysteine residues (in yellow in **Figure 22A, B**) that could potentially act as sensors or scavengers of reactive oxygen species.

TTR-33 is predicted to exhibit high structural similarity to the only characterised *C. elegans* transthyretin-related protein TTR-52 (**Figure 22C**), which bridges apoptotic cells to the engulfment machinery (Kang et al., 2012; Wang et al., 2010). Therefore, we aimed to investigate if phagocytosis could be involved in the mechanism causing premature dopaminergic neurodegeneration in *ttr-33*(*gt1983*).

6.2 Dopaminergic neurons are engulfed but do not undergo apoptosis upon intoxication with 6-OHDA

TTR-52 is the only characterised *C. elegans* transthyretin-related protein and was reported to bind to phosphatidylserine on the surface of apoptotic cells and to the phagocyte receptor CED-1/MEGF10 (Wang et al., 2010). It is not known how *C. elegans* dopaminergic die upon exposure to 6-OHDA, so we wanted to address if they might be engulfed. The two branches of the *C. elegans* engulfment pathway merge on *ced-10* (**Figure 23A**) and the *ttr-52/ced-1/ced-6* branch is also required for axon regeneration (Neumann et al., 2014). We found that neurodegeneration in the *ttr-33* mutant is slightly suppressed by mutation of *ced-2*, which is part of the *ced-2/ced-5/ced-12* branch, and highly suppressed by *ced-6*, which is part of the *ttr-52/ced-1/ced-6* branch (**Figure 23B**). Dopaminergic cell loss in the *ttr-33* mutants is largely

prevented when mutating the end point of the pathway, *ced-10*, so the two branches might act additively (**Figure 23B**). Importantly, a loss-of-function mutation in *ttr-52* did not confer hypersensitivity to dopaminergic neurons and did not influence the phenotype of *ttr-33* (**Figure 23B**). Therefore, in contrast to TTR-33, TTR-52 does not seem to have a role in 6-OHDA-induced neurodegeneration. To exclude that dopaminergic neurons are only engulfed in the *ttr-33* mutant background, we confirmed that mutations in *ced-6* or *ced-10* also alleviate dopaminergic neurodegeneration in a wild-type background (**Figure 23C**). We conclude that the 6-OHDA-induced dopaminergic cell death is alleviated by mutation of the phagocytosis genes *ced-6* and *ced-10*.

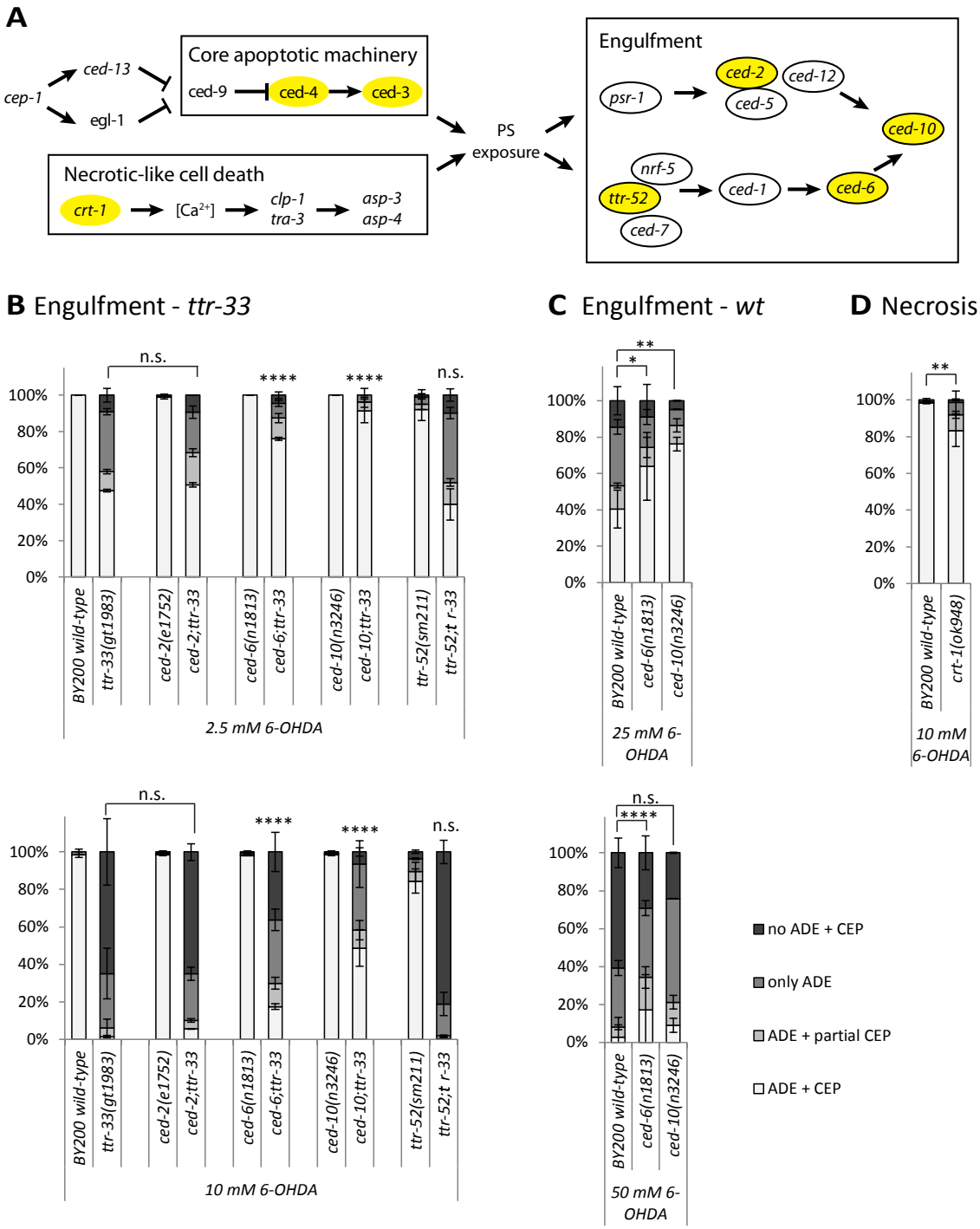
A
cep-1
ced-13
egl-1
Core apoptotic machinery
ced-9
ced-4
ced-3
Necrotic-like cell death
crt-1
[Ca2+]
clp-1
tra-3
asp-3
asp-4
PS exposure
Engulfment
psr-1
ced-2
ced-5
ced-12
ced-10
nrf-5
ttr-52
ced-7
ced-1
ced-6
B Engulfment - ttr-33
n.s.
****
****
n.s.
100%
80%
60%
40%
20%
0%
BY200 wild-type
ttr-33(gt1983)
ced-2(e1752)
ced-2;ttr-33
ced-6(n1813)
ced-6;ttr-33
ced-10(n3246)
ced-10;ttr-33
ttr-52(sm211)
ttr-52;t r-33
2.5 mM 6-OHDA
10 mM 6-OHDA
C Engulfment - wt
**
*
25 mM 6-OHDA
50 mM 6-OHDA
D Necrosis
**
crt-1(ok948)
10 mM 6-OHDA
no ADE + CEP
only ADE
ADE + partial CEP
ADE + CEP

Figure 23: Dopaminergic neurons are engulfed but do not undergo apoptosis after 6-OHDA intoxication.
A) Cartoon of apoptotic and necrotic-like cell death pathway and subsequent engulfment. Marked in yellow are the genes that were tested in this study.
B-D) Dopaminergic neurons were scored 72 h after intoxication with indicated concentration of 6-OHDA.
B) Effect of mutations in engulfment pathway and *ttr-52* in the *ttr-33* mutant background. Error bars = SEM of 2 biological replicates, each with at least 50 animals per strain and concentration. Total number of animals per condition n = 200-240 (****p<0.0001, n.s. p>0.05; G-Test comparing *ttr-33* mutant data to double mutant data), except for *ced-10*;*ttr-33* 10 mM with n = 70.
C) Effect of mutations in engulfment pathway on neurodegeneration in a wild-type (wt) background. Error bars = SEM of 2 biological replicates, each with at least 50 animals per strain and concentration. Total number of animals per condition n = 120-220 (****p<0.0001, **p<0.01, *p<0.05, n.s. p>0.05; G-Test), except for *ced-10* 50 mM which was tested once with n = 35.
D) Effect of mutations in calcium regulator calreticulin *crt-1* on neurodegeneration in a wild-type background. Error bars = SEM of at least 3 biological replicates with at least 90 animals per strain. Total number of animals per strain = 200-310 (** p<0.02; G-Test).

Before cells are engulfed, they commonly undergo apoptosis or a necrosis-type cell death (**Figure 23A**). To determine if any of these two cell death types occur during dopaminergic neurodegeneration, we first tested the caspases *ced-3* and *ced-4*, which are part of the canonical apoptosis pathway. In line with previous reports (Nass et al., 2002), we found that blocking the apoptosis pathway did not prevent dopaminergic cell death (**Figure 24A, B**). On the contrary, *ced-3* and *ced-4* seem to have a protective role as their mutation led to increased neurodegeneration (**Figure 24A, B**). In line with this, it has been reported that the apoptosis pathway can act protectively after sensing of mitochondrial reactive oxygen species (mtROS) (Yee et al., 2014). *ced-13* also influences the mtROS sensing pathway and we found that mutation of *ced-13* conferred slight hypersensitivity to dopaminergic neurons after intoxication with 10 mM 6-OHDA (**Figure 24B**). Since mutations in the apoptosis/mtROS-sensing pathway only conferred minor sensitivity to 6-OHDA, it is difficult to tell if there are additive effects in the *glit-1* mutant background (**Figure 24B**). However, a mutation in *ced-4* did not increase, but rather decrease neurodegeneration in the *ttr-33* mutant (**Figure 24A**). In summary, mutating the apoptosis genes *ced-3* and *ced-4* did not prevent 6-OHDA-induced

dopaminergic cell death, but instead increased neurodegeneration. We speculate that *ced-3* and *ced-4* might have a protective role based on their function as mtROS sensors.

Since dopaminergic neurons do not seem to die an apoptotic cell death, we aimed to determine if they die via necrosis. For this, we tested a strain with a mutation in the calreticulin *crt-1*, a Ca^{2+}-binding and Ca^{2+}-storing chaperone in the ER which mediates calcium release that is necessary for necrosis (Xu et al., 2001). A mutation in c*rt-1* mutation led to a minor increase in dopaminergic neuron loss in wild-type (**Figure 23D**), however the *crt-1;glit-1* double mutant appeared synthetic lethal (data not shown): We used a fluorescently labelled balancer chromosome to keep *crt-1* in a heterozygous state in a *glit-1* homozygous background. In the next generation, genetic segregation of the *crt-1* and the balancer chromosome is expected. However, we did not find any non-fluorescent animals, indicating that *crt-1* homozygosity is lethal in the *glit-1* homozygous background. In summary, it is possible that 6-OHDA triggers a necrosis-like cell death of dopaminergic neurons.

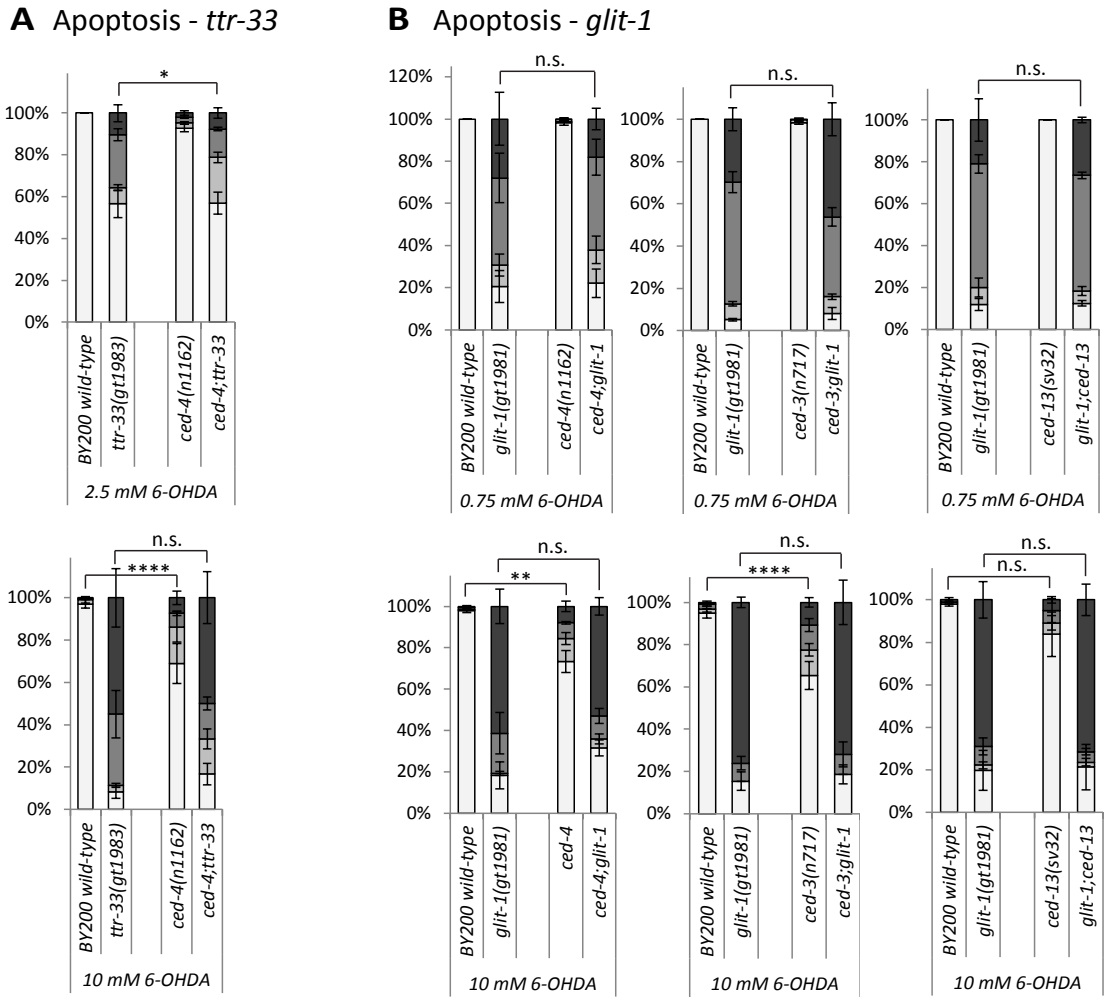

Figure 24: Dopaminergic neurons are engulfed but do not undergo apoptosis after 6-OHDA intoxication.

Dopaminergic neurons were scored 72 h after intoxication with indicated concentration of 6-OHDA.

A) Effect of apoptosis/mtROS pathway mutation on *ttr-33* neurodegeneration. Error bars = SEM of 3 biological replicates, each with at least 100 animals per strain and concentration. Total number of animals per condition n = 300-330 (****p<0.0001, *p<0.05, n.s. p>0.05; G-Test).

B) Effect of apoptosis/mtROS pathway mutations on *glit-1* neurodegeneration. Error bars = SEM of at least 3 biological replicates, each with at least 50 animals per strain and concentration. Total number of animals per condition n = 150-530 (****p<0.0001, **p<0.01, n.s. p>0.05; G-Test).

6.3 *ttr-33* is expressed in the posterior arcade cells

TTR-33 is predicted to be a secreted protein, so a transcriptional reporter might be needed to identify the location of protein production, and a translational reporter to identify its site of

action. We find that in five independent lines, an extrachromosomal transcriptional P*ttr-33*::gfp constructs exclusively labelled six cells in the head of L1 larvae, the stage most sensitive to 6-OHDA. Two cells were located next to the first pharyngeal bulb and four were situated halfway between mouth and first pharyngeal bulb and form protrusions towards the mouth of the larva (**Figure 25A, B**). The cells could already be detected as early as the embryonic pretzel stage (**Figure 25C**). Comparison with the cell atlas of *C. elegans* (www.wormatlas.org) revealed that these six cells are most likely the posterior arcade cells, which link the external epidermis and anterior pharynx/foregut (Portereiko and Mango, 2001). There is a specific promoter for these cells (P*bath-15*) which will be used to express TTR-33 only in the posterior arcade cells for tissue-specific rescue. A translational P*ttr-33*::*ttr-33*::gfp construct in contrast only weakly labelled several cells in the head (**Figure 25D**). By using different fluorophores, it will be addressed if the cells labelled by the transcriptional and translational reporter construct are identical − or if TTR-33 is secreted from the posterior arcade cells and then localises to other cells.

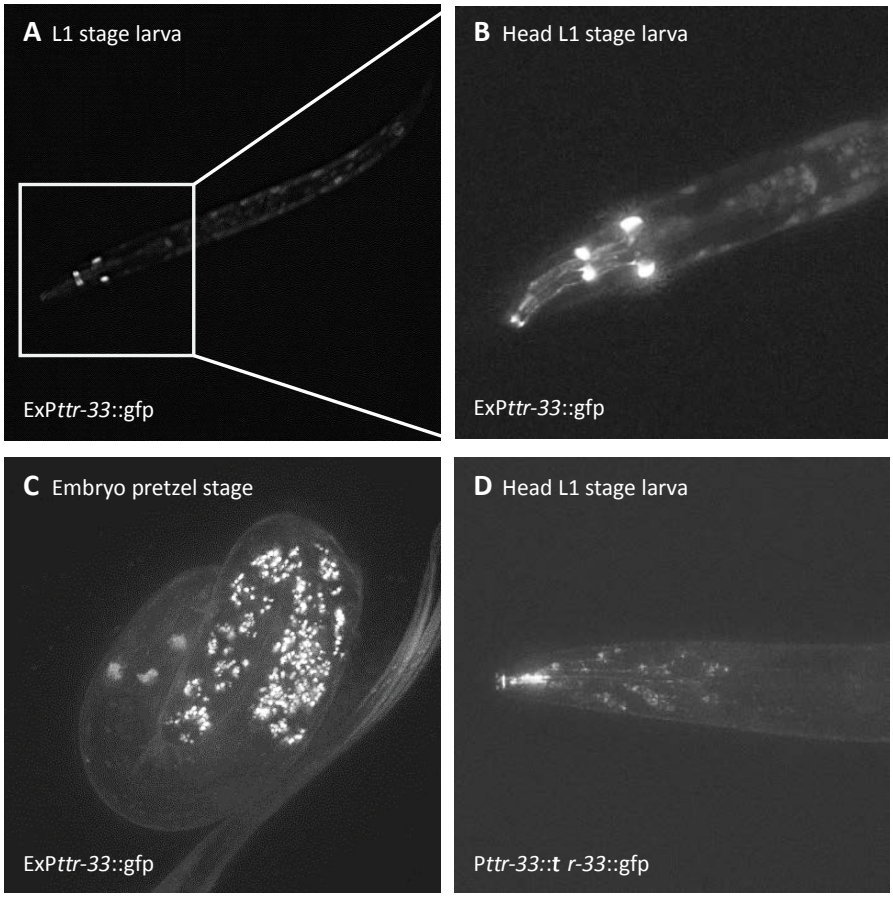

Figure 25: *ttr-33* is expressed in arcade cells.
A) Transcriptional reporter ExP*ttr-33*::gfp in L1 stage larva.
B) Magnified view of transcriptional reporter ExP*ttr-33*::gfp in L1 stage larva in A).
C) Transcriptional reporter ExP*ttr-33*::gfp in pretzel stage embryo, speckled signal is autofluorescence from the intestine.
D) Translational reporter P*ttr-33*::*ttr-33*::gfp in L1 stage larva.

7 DISCUSSION HYPERSENSITIVE MUTANTS

7.1 Oxidative stress sensitivity

We screened for genes that protect from 6-hydroxydopamine (6-OHDA)-induced dopaminergic neurodegeneration and isolated and mapped a mutation in the neuroligin-like gene *glit-1* and the transthyretin-like gene *ttr-33*. The tetraspanin *tsp-17* is sensitive to 6-OHDA as well and was characterised in a previous study (Masoudi et al., 2014). We could show that *glit-1*, *ttr-33* and *tsp-17* also exhibit reduced survival − but no dopaminergic neurodegeneration − after exposure to paraquat, another oxidative-stress inducing drug. To our knowledge, there is only one study that reported paraquat-induced loss of dopaminergic dendrites (González-Hunt et al., 2014), however worms were chronically exposed for 48 h without food, so additive effects conferred by starvation are possible. Even though both drugs are thought to act by inducing oxidative stress, it is likely that 6-OHDA – because of its specific uptake into dopaminergic neurons – leads to a higher intracellular concentration of damaging ROS than paraquat, and therefore dopaminergic neuron loss might occur well before the lethality threshold is reached.

The hypersensitivity to 6-OHDA and paraquat in L1 stage larvae might be caused by a reduced capacity to respond to oxidative stress, since preliminary experiments showed diminished P*gst-4*::gfp oxidative stress reporter expression in *glit-1* L4 stage mutants. This result will be followed up by measuring stress reporter fluorescence after oxidative stress induction in wild-type and mutant animals at different life cycle stages. As a complementary approach, we will determine transcription of the oxidative stress reporter by RT PCR. It is also possible to measure reactive oxygen species (ROS) more directly e.g. by staining *C. elegans* with Mitotracker Red (Schmeisser et al., 2013a), and to measure the effects of ROS on the worms e.g. by determining protein carbonylation (Hunter et al., 2010). In addition, we will also test if expression of *ttr-33* – and *glit-1* and *tsp-17* – is transcriptionally induced in response to oxidative stress. Finally, we aimed to determine if known stress response pathways confer

resistance to 6-OHDA in a similar manner as *glit-1*, *ttr-33* and *tsp-17*. Surprisingly, the oxidative stress 'master regulator' *skn-1* does not seem to mediate the response to 6-OHDA, since *skn-1* mutant worms are not sensitive to the drug. However, we note that hyperactivation of *skn-1* had a protective effect in wild-type and mutant worms alike. Therefore, *glit-1*, *ttr-33* and *tsp-17* are likely part of other another defence system that protects dopaminergic neurons from the effects of 6-OHDA.

7.2 ER stress resistance and unfolded protein response signalling

While being sensitive to oxidative stress, *glit-1*, *ttr-33* and *tsp-17* L1 stage mutants are resistant to protein folding stress. Remarkably, worms carrying a mutation in the Parkinson's disease gene *pink-1* were reported to share these phenotypes (Sämann et al., 2009), but they are not sensitive to 6-OHDA (our data). As preliminary results with *glit-1* L4 stage mutants suggest, the resistance to endoplasmic reticulum (ER) stress might be explained by an upregulation of the ER unfolded protein response (UPR) at basal conditions. These data need to be followed up by measuring P*hsp-4*::gfp UPR ER reporter levels after induction of ER stress in wild-type and mutant worms at different life cycle stages. In addition, transcription levels of the ER UPR reporter gene will be determined with and without induction in wild-type and mutant animals.

The UPR has two phases, a first phase for cellular protection and, if the cell cannot be saved, a second phase to trigger cell death (Urra et al., 2013). The primary phase of the UPR comprises a reduction of protein synthesis and indeed – as expected for worms with lower protein synthesis levels − *glit-1*, *ttr-33* and *tsp-17* are sensitive to the translation inhibitor hygromycin. However, a study reported the induction of oxidative stress by hygromycin (Oung et al., 2015), so the mutants' susceptibility to hygromycin might reflect another form of oxidative stress sensitivity rather than a reaction to protein synthesis inhibition. If protein translation were indeed diminished in the mutants, they would be expected to grow slower and we found that *glit-1* mutants show a clear and *ttr-33* mutants a minor growth delay (**Figure 3C**). We can now

determine if the *glit-1* growth delay is bypassed by mutation of the UPR gene *ire-1* in the *glit-1*;*ire-1* double mutant. We note that the strongly inhibited growth of the *glit-1*(ok237) deletion mutant is likely due to the fact that *ok237* deletion also compromises the promoter of the large ribosomal subunit protein *rpl-25.1*. In summary, we have indications that the ER UPR is upregulated in in *glit-1*, *ttr-33* and *tsp-17* mutants at basal conditions. Upregulation of the UPR is likely associated with increased cellular stress, therefore it is possible that upon additional challenge with 6-OHDA, dopaminergic neuron death is triggered more readily. In line with this argument, we find a reduction in 6-OHDA-induced dopaminergic neurodegeneration when we mutate the ER UPR gene *ire-1* in *ttr-33* mutants – as well as a weaker effect in *glit-1* mutants.

7.3 Genetic interaction with MAPK stress response pathways

To test if known *C. elegans* stress response pathways are involved in the protection against 6-OHDA, we included p38 and JNK MAPK (c-Jun N-terminal kinase mitogen-activated protein kinase) mutants in the 6-OHDA assay. We found that the MAPK mutations did not lead to premature dopaminergic neurodegeneration as a mutation in *glit-1*, *ttr-33* or *tsp-17* and did not influence the extent of neuronal loss in *glit-1* mutants. However, the JNK orthologue *jnk-1* aggravates 6-OHDA-induced neurodegeneration in the *ttr-33* mutant. The seemingly specific effect of the *jnk-1* mutation on *ttr-33* mutants needs to be confirmed by testing the influence of the *jnk-1* mutation on degeneration in wild-type animals at higher concentrations of 6-OHDA. However, the protective function of *jnk-1* in the 6-OHDA assay is in agreement with literature showing its function in the resistance against oxidative stress (Neumann-haefelin et al., 2008; Oh et al., 2005).

There is a second JNK (c-Jun N-terminal kinase) family member in *C. elegans*, *kgb-1*, but we were not able to create a double mutant between *ttr-33* and *kgb-1.* We used a balancer chromosome to keep *ttr-33* in a heterozygous state in a *kgb-1* homozygous background. In the next generation, we did not find any animals that did not carry the balancer. KGB-1 is required

for resistance to the ER toxin tunicamycin (Mizuno et al., 2008) and was proposed to regulate several transthyretin-related genes (Twumasi-Boateng, 2012), so it is conceivable that *kgb-1* acts upstream of *ttr-33*. However, the *kgb-1* mutant on its own does not show enhanced 6-OHDA-induced neuronal loss as *ttr-33*, so if *kgb-1* is involved in the protection against 6-OHDA, its function must be redundant. The influence of *kgb-1* on dopaminergic degeneration in an otherwise wild-type background has to be tested still upon treatment with higher concentrations of 6-OHDA. We note however that it is likely that KGB-1 has an important role in organismal protection since the protein was reported to transmit a neuroendocrine signal upon disruptions in core cellular processes – including translation, respiration and protein turnover (Melo and Ruvkun, 2012). In summary, the JNK protein JNK-1 provides protection against 6-OHDA-induced neurodegeneration in *ttr-33* mutants and KGB-1 might genetically interact with *ttr-33*.

7.4 Transthyretins might be secreted to support organismal defence

TTR-33 might be part of an endocrine defence pathway. The nematode-specific transthyretin-related protein family is expanded and comprises 59 members, 54 of which are predicted to be secreted (Petersen et al., 2011; Wang et al., 2010). Several studies indicate that transthyretin-related genes might be induced in response to environmental challenges such as oxidative stress or pathogen exposure: Expression of *ttr-33* and other transthyretin-related genes is upregulated upon loss of *wdr-23* in neurons – leading to a dis-inhibited *skn-1* oxidative stress response (Staab et al., 2014). Furthermore, oxidative stress induced by *tert*-butyl hydrogen leads to upregulation of several transthyretin-related genes in a *skn-1*-independent manner (Oliveira et al., 2009) and treatment with the mitochondrial complex I inhibitor rotenone leads to upregulation of 42 of 59 transthyretin-related genes (Schmeisser et al., 2013b). In line with a putative role as an oxidative stress defence protein, TTR-33 possesses conserved cysteine bridges with which it could sense or scavenge ROS – similar to the antioxidant glutathione. In

addition, bacterial infection was reported to cause upregulation of *ttr-33* (Engelmann et al., 2011) and several other transthyretin-related proteins (Treitz et al., 2015). In line with a possible role in the *C. elegans* innate immune response, *ttr-33* gene expression correlates with genes that are associated with the gene ontology terms 'defence response to fungus', 'negative regulation of metalloenzyme activity' and 'neuropeptide signalling pathway'. In summary, the transthyretin-related protein family seems to be part of a hormone-like organismal defence.

7.5 Starvation protects against 6-OHDA toxicity and might induce expression of *glit-1* and *ttr-33*

C. elegans triggers diverse signalling pathways to survive periods of starvation (Larance et al., 2015). Intriguingly, dietary restriction protects against 6-OHDA-induced neurodegeneration (González-Hunt et al., 2014; Jadiya et al., 2011) and might lead to upregulation of *glit-1* and *ttr-33* transcripts: Fasting significantly induces gene expression of *glit-1* and several transthyretin-related genes (Uno et al., 2013), and protein levels of the same and additional transthyretin-related genes (Larance, Pourkarimi et al., 2015). Furthermore, according to expression data from modENCODE libraries (linked to wormbase), *ttr-33* expression is predicted to be highest in dauer stage, a larval stage that is entered upon nutrient deprivation (Hu, 2007). We still need to test this prediction with our *ttr-33* transcriptional reporter. Since starvation leads to a decrease in 6-OHDA-induced neurodegeneration, the time L1 stage larvae were incubated in liquid without food before 6-OHDA intoxication was kept the same for all experiments. However, sometimes filtering of L1 stages from unstarved plates was necessary due to the swimming defect of two strains (*tsp-17(tm4995)* and *skn-1(zu67)/*nT1). We confirmed that starvation leads to partial resistance to 6-OHDA-induced degeneration: 60% of *glit-1* mutants exhibited degeneration of all dopaminergic head neurons 72 h after intoxication with 0.75 mM 6-OHDA if worms were filtered from an unstarved plate (**Figure 10A**), but only 10% if the mutants were incubated without food (**Figure 14C**). In summary, *glit-1*, *ttr-33* and other

transthyretin-related genes might be induced in unfavourable environmental conditions including food deprivation.

7.6 Lifespan reduction and a possible connection to the insulin/insulin-like signalling pathway

Loss of genes that are important for environmental stress protection is expected to cause reduced organismal fitness and indeed, *ttr-33* mutants – as well as *glit-1* and *tsp-17* mutants – die earlier than wild-type animals. Other transthyretin-related genes could have a role in lifespan regulation as well: Expression of almost half of all transthyretin-related genes was found to be significantly higher in the long-lived insulin-like growth factor orthologue *daf-2* (*abnormal dauer function*) mutant (Halaschek-wiener et al., 2005; Rizki et al., 2011), similar to heat-shock proteins and neuropeptide-like genes (Halaschek-wiener et al., 2005). In contrast, very few transthyretin-related gene are downregulated in the *daf-2* mutants, including *ttr-1* (Rizki et al., 2011), and *ttr-1* RNAi knockdown was indeed found to extend lifespan in an independent study (Hansen et al., 2005).

The insulin/insulin-like growth factor signalling pathway might be involved in the response to 6-OHDA. DAF-2 is the only *C. elegans* insulin/insulin-like growth factor I receptor orthologue and negatively regulates the sole forkhead box O (FOXO) transcription factor homologue DAF-16. DAF-16 is a key regulator of *C. elegans* oxidative stress resistance (Baumeister et al., 2006). Recently, *ttr-33* appeared among the neuronal targets of the DAF-16-dependent insulin/insulin-like growth factor signalling pathway (Kaletsky et al., 2015). It was also shown that JNK-1, which provides protection against 6-OHDA in the *ttr-33* mutant background, acts via DAF-16 to mediate stress resistance (Neumann-haefelin et al., 2008; Oh et al., 2005). Finally, even though we found that SKN-1 does not seem to have a major role in the protection against 6-OHDA, it was reported that SKN-1 and DAF-16 can act non-redundantly to sustain mitochondrial function in response to oxidative stress (Palikaras et al., 2015). In summary,

there are strong indications that the DAF-16 insulin/insulin-like signalling pathway could have a role in the response to 6-OHDA. We will therefore test if *daf-2* and *daf-16* mutants show decreased and increased 6-OHDA-induced dopaminergic neurodegeneration, respectively. However, we note that the two functions – protection against 6-OHDA and protection against premature death – are mediated at different life cycle stages and might therefore be independent of each other: The sensitivity to 6-OHDA declines latest in L4 stage worms in *glit-1*, *ttr-33* and *tsp-17* mutants, whereas lifespan assays only start at L4 stage.

7.7 Finding interactors of *glit-1*

glit-1 is a neuroligin-like gene, however *glit-1* is unlikely to mediate protection against 6-OHDA via the common neuroligin partner neurexin. Mutations in the only *C. elegans* neurexin *nrx-1* do not phenocopy or specifically alter the 6-OHDA sensitivity of *glit-1* mutants. However, there are a few examples of neuroligin functions exerted in a neurexin-independent manner such as increase in synaptic density in cell culture (Ko et al., 2009) and stimulation of insulin secretion on the surface of pancreatic beta-cells (Suckow et al., 2012). Like mammalian neuroligins (Bemben et al., 2015), GLIT-1 possesses a C-terminal PDZ (PSD95, Dlg1, zo-1) domain-binding sequence and we used this feature to predict several alternative GLIT-1 interactors. Some of the candidate PDZ proteins were already shown to interact with *glit-1* orthologs: The mammalian homologue of SHN-1, SHANK3, was shown to bind indirectly to neuroligin and SHANK3 mutations are – similar to mutations in neuroligins and neurexins – associated with autism (Südhof, 2008). *C. elegans* SHN-1 exhibits a similar expression pattern as *glit-1* in pharynx, intestine and neurons (Jee et al., 2004). In addition to SHN-1, DLG-1 appears in the list of putative GLIT-1 interactors. The *Drosophila* homologues of GLIT-1 and DLG-1, Gliotactin and Discs Large, were reported to associate in a Ca^{2+}-dependent manner (Padash-Barmchi et al., 2013). In addition, *Drosophila* JNK was shown to act downstream of Gliotactin and Discs

Large (Padash-Barmchi et al., 2013). Strong candidates such as *shn-1* or *dlg-1* can be tested for their involvement in *glit-1*-mediated neuroprotection.

7.8 *glit-1* genetic interaction with dopamine metabolism

glit-1 might influence dopamine turnover since *glit-1* mutants exhibit signs of increased dopamine signalling, i.e. a higher degree of paralysis when put on plates with dopamine. To exclude that the *glit-1* phenotype is based on dopamine-independent effects, we will test the *glit-1*;*dop-3* double mutant: As the inhibitory dopamine receptor *dop-3* mediates the dopamine-induced paralysis (Allen et al., 2011), the *glit-1* phenotype should be rescued in the in *glit-1*;*dop-3* mutants. Importantly, higher intrinsic dopamine release might explain the 6-OHDA sensitivity of the *glit-1* mutant: Increased release of dopamine is expected to lead to increased dopamine uptake. Since dopamine and 6-OHDA enters the neurons in the same way via the dopamine transporter, more 6-OHDA might thus enter dopaminergic neurons in the *glit-1* mutant. In line with this mechanism of action, we find that decreasing the amount of dopamine that is competing with 6-OHDA for entry – i.e. by decreasing synthesis or by decreasing vesicle packing – worsens the *glit-1* neurodegeneration phenotype. We note that the dopamine paralysis assay was conducted with L4 stage worms, whereas the 6-OHDA intoxication assay is done with L1 stage larvae. In the moment we cannot be sure about the site of action of *glit-1* in L1 stage worms since the tissue-specific rescue experiments still have to be conducted. However, *glit-1* might be expressed in dopaminergic neurons mutant in adults (**Figure 17C, D**), and therefore an influence of *glit-1* on dopamine signalling is possible. Another indication that *glit-1* mutants exhibit enhanced dopamine signalling is their decreased rate of egg-laying, a behaviour which is inhibited by dopamine (Schafer and Kenyon, 1995). However, egg-laying is controlled by many different pathways (Schafer, 2005), thus it is possible that egg-laying defects of the *glit-1* mutant are not caused by increased dopamine signalling. The results from these behavioural assays could be confirmed by measuring

dopamine signalling more directly, for example with a dopamine vesicle release assay. In this assay, the recovery of GFP-tagged synaptobrevin, a synaptic vesicle marker, is followed after photobleaching (Voglis and Tavernarakis, 2008).

7.9 *glit-1* and *tsp-17* might act via partially overlapping pathways

glit-1 and *tsp-17* mutants are equally sensitive to 6-OHDA and the *glit-1*;*tsp-17* does not exhibit an increased sensitivity compared to the single mutants. Furthermore, both mutants show signs of higher dopamine signalling, suggesting that the two genes might act in the same pathway. However, in the dopamine paralysis assay the t*sp-17*;*glit-1*(*gt1981*) double shows a stronger phenotype than the respective single mutants. In addition, *tsp-17* exhibits dopamine receptor-dependent swimming-induced paralysis (SWIP), another indication for elevated dopamine signalling and a phenotype which is not shared by *glit-1* mutants. We think that it is possible that, compared to the *tsp-17(tm4995)* deletion, the *glit-1(gt1981)* point mutation might have a weaker and therefore undetectable effect in the SWIP assay. To determine epistatic effects between the *tsp-17* and *glit-1* deletion alleles, we aimed to generate the *tsp-17(tm4995)*;*glit-1*(ok237) double, but it was only possible to get to the heterozygous/homozygous stage. Due to the close proximity of *tsp-17* and *glit-1* (3 cM distance) the use of a genetic balancer covering only one of the two genes is not possible. Therefore, we conclude that the combination of the *glit-1* and *tsp-17* deletion alleles might be synthetically lethal. In summary, mutation of *tsp-17* induces similar but stronger dopamine signalling defects than mutation of *glit-1*, so the genes might act via partially overlapping mechanisms.

7.10 Increased organismal drug uptake unlikely mechanism for *glit-1* mutant

The homologue of *glit-1* in *Drosophila* is involved in the development of the invertebrate tight junction equivalent (Genova and Fehon, 2003; Schulte et al., 2003, 2006), so it is possible that *glit-1* mutants are sensitive to 6-OHDA due to higher epithelial permeability for drugs. In

addition, the transcriptional reporter indicates strong *glit-1* expression in the pharynx and in the intestine, the tissues which probably represent the main routes of 6-OHDA uptake in liquid culture. However, *glit-1* mutants show resistance to tunicamycin, so they are unlikely to show a generally increased organismal drug uptake. Also, *glit-1* mutant sensitivity to 6-OHDA is abolished by mutation of the dopamine transporter *dat-1*, so if the drug is prevented from entering the neuron it is not having an increased effect in the mutant anymore. Finally, we could not detect an effect on the development of *glit-1* mutant larvae after intoxication with 6-OHDA – as it might be expected if a greater amount of the oxidative-stress inducing drug was able to cross epithelial barriers. To define the place in which GLIT-1 protects against 6-OHDA, tissue-specific rescue experiments will be conducted by expressing GLIT-1 only in pharynx, intestine or neurons – particularly dopaminergic neurons. We find that in adult animals, *glit-1* might be expressed in neurons, in line with a study that reported *glit-1* neuronal expression in adults only (Kaletsky et al., 2015). Since 6-OHDA intoxication is conducted in the L1 larval stage, *glit-1* possibly exerts its function from non-neuronal tissue. However, even if the main function of *glit-1* is cell-adhesion, this does not necessarily imply that the mechanism of action is increased epithelial permeability. For example, neural cell adhesion molecules (NCAMs) have roles in cell-cell adhesion and oxidative stress-induced cleavage of NCAM-180 by the matrix metalloprotease MMP-9 was reported to increase neuronal damage in conditions of ischemic stress (Fujita-Hamabe and Tokuyama, 2012; Shichi et al., 2011). In summary, it cannot be excluded, but it is unlikely that the mechanism of action of *glit-1* involves a generally increased drug uptake.

Mutation of *glit-1* induces similar phenotypes as mutation in *tsp-17*, a gene which was shown to act in dopaminergic neurons (Masoudi et al., 2014). To determine the site of action of *glit-1*, expression constructs for tissue-specific rescue are required. Unfortunately, C-terminal-tagging of GLIT-1 seems to render the protein non-functional even when tagging the endogenous locus, as the *glit-1* 6-OHDA sensitivity is not rescued in a *glit-1*/GLIT-1::GFP transheterozygote.

Tagging in the unstructured and intracellular C-terminal part of GLIT-1 still seems like the best option and we will now try to place the GFP behind a linker sequence to avoid interfering with PDZ protein binding. In parallel, tissue-specific rescue constructs without fluorophores will be created to determine in which tissue *glit-1* functions to protect from 6-OHDA toxicity.

7.11 The mechanism of action of *ttr-33* is most likely different from *glit-1* and *tsp-17*

In contrast to *glit-1* and *tsp-17* mutants, the *ttr-33* mutant does not show dopaminergic signalling defects and is less sensitive to 6-OHDA and paraquat. Due to its different sensitivity window in the 6-OHDA assay, it was not possible to determine if *ttr-33* could lie in same pathway as *tsp-17* and *glit-1*. The *ttr-33(gt1983)* mutants could simply exhibit a weaker phenotype, but it is also possible that the *ttr-33* point mutation they carry does not lead to a null phenotype. We aim to treat the double mutant strains with RNAi targeting the third gene to investigate genetic interactions between *ttr-33*, *glit-1* and *tsp-17* again. We note the surprising finding that the *ttr-33* orthologue transthyretin carries thyroxine, and the precursor of thyroxine is one of the proposed *glit-1* orthologues thyroglobulin.

7.12 Evidence for and against a role of TTR-33 in protein folding

Misfolding and aggregation of transthyretin, the human TTR-33 orthologue, is linked to the development of amyloid diseases. We hypothesised that the *ttr-33* mutations could facilitate TTR-33 aggregation and thus cause increased dopaminergic neurodegeneration. Indeed, neurodegeneration in the *ttr-33* mutant is reduced in the unfolded protein response loss-of-function mutant *ire-1*. This amelioration seems to be specific for the *ttr-33* mutant since neurodegeneration in the *glit-1* mutant is largely unaffected by mutation of *ire-1*. However, we still need to investigate the effects of *ire-1* on wild-type dopaminergic neurodegeneration at higher concentrations of 6-OHDA. If TTR-33 protein aggregation was causing the hypersensitivity of dopaminergic neurons, it might also explain why injection of (an excessive

number of) *ttr-33* wildtype copies did not rescue the *gt1983* phenotype during the mapping procedure (data not shown). However, if mutated TTR-33 is more prone to aggregation than wild-type protein, it would be expected that not all TTR-33 copies need to carry a mutation before inducing a phenotype, so *ttr-33* should exhibit a 'gain-of-function', dominant phenotype. Yet, since *ttr-33(gt1983)* behaves in a recessive fashion, the mechanism of action is likely based on the loss of gene function. Hence, the physiological role of *ttr-33* might provide the key to understand its protection against 6-OHDA-induced neurodegeneration.

7.13 *ttr-33* might be involved in the engulfment of dopaminergic neurons

The only characterised member of the transthyretin-related protein family in *C. elegans* is *ttr-52*. TTR-52 serves as a 'eat me'-signal for recognition of apoptotic cells (Wang et al., 2010) and yet as a 'save me'-signal to promote regenerative axonal fusion (Neumann et al., 2014). In both cases, TTR-52 relays the information to the cell corpse engulfment pathway, yet it is not known if any other of the 59 C. elegans transthyretin-related proteins has a similar role. It is conceivable that the distinct members of the family of transthyretin-related proteins may target distinct cell types or that they may act upon different stimuli. Indeed, transthyretin-related genes seem to be secreted in different environmental conditions (see above), but in contrast to *ttr-33* mutants, *ttr-52* mutants are not hypersensitive to 6-OHDA. TTR-52 is synthesized in and secreted from the intestine and thus labels apoptotic cells far from where it was made (Wang et al., 2010). Also TTR-33 is predicted to be a secreted protein, but seems to be produced by the posterior arcade cells in the head. So could TTR-33 act as a in a hormone-like manner? There are certainly examples of proteins that are secreted to act on tissues in other parts of the worm: The growth factor SVH-1 (suppressor of vhp-1 deletion lethality) is secreted from sensory ADL neurons and regulates axon regeneration (Li et al., 2012), and the transcription factor SKN-1 is thought to trigger the secretion of hormones from a pair of neurons to promote longevity (Bishop and Guarente, 2007).

We aim to determine if TTR-33 acts in the posterior arcade cells and if it functions as a secreted protein by expressing the TTR-33 protein from a promoter that is specific for the posterior arcaded cell (P*bath*-15) with and without its secretion signal. The 6 posterior arcade cells form a syncytium and link the digestive tract to the epidermis (Portereiko and Mango, 2001), however there is not much known about their function after embryonic development. The arcade cells contain many free ribosomes and mitochondria, but very little endoplasmic reticulum (Wright and Thomson, 1981), features that was also reported for lymphocytes and antigen-presenting cells (Young et al., 2013). Antigen-presenting cells are crucial for the activation of lymphocytes – macrophages, dendritic cells and B lymphocytes – to trigger an adaptive immune response (Young et al., 2013). The similarity between the TTR-33-expressing cells and mammalian immune cells supports our hypothesis that TTR-33 could be part of a hormone-like immune response. Just prior to larval moulting, the arcade cells contain dense core vesicles and it was suggested that they could form a new cuticle by vesicle secretion (Wright and Thomson, 1981). In addition, the posterior arcade cells were reported to express *pha-4 (defective pharynx development)* – a FoxA transcription factor with a role dietary-restriction-induced longevity (Antebi, 2013), possibly *pha-1* (Kuzmanov et al., 2014), *agr-1* (Agrin (synaptic protein) – a secretion signal-containing protein with a vertebrate orthologue functioning in the development and maintenance of neuromuscular junction) (Hrus et al., 2007), and a few hedgehog-like genes (Hao et al., 2006).

To test if *ttr-33* – similar to *ttr-52* – acts via the phagocytosis pathway, we created several double mutants for epistasis experiments. It is not known how dopaminergic neurons die after exposure to 6-OHDA, but we found that inhibition of engulfment leads to a decrease in neuronal loss in wild-type animals and *ttr-33* mutants. We note that a review about mammalian 6-OHDA models (Kostrzewa and Jacobowitz, 1974) and the paper that introduced the *C. elegans* 6-OHDA model (Nass et al., 2002) indicated that after 6-OHDA intoxication, dopaminergic neurons are surrounded by microglia or phagocytes, respectively. These reports

support the ideas that dopaminergic neurons might be engulfed after being damaged by 6-OHDA. To our knowledge, it is not clear how dopaminergic neurons die in PD patients. However, it was suggested that *pdr-1* − the *C. elegans* homologue of the E3 ligase and PD risk gene parkin − tags the key phagocytosis protein CED-10 for degradation, therewith preventing engulfment of apoptotic cells (Cabello et al., 2014). This would mean that mutation of *pdr-1/*parkin could lead to increased phagocytosis. We will follow up this line of research by using the *ced-2;ced-6* double mutant. With this strain, we can investigate if inhibition of the two partially redundant engulfment pathways (here represented by *ced-2* and *ced-6*) leads to similarly strong effects as a mutation of the common target *ced-10* in wild-type and *ttr-33* mutant background. Furthermore, we can investigate if dying dopaminergic neurons expose phosphatidylserine (PS) on their surface by using the PS reporters MFG-E8::GFP, Annexin V::GFP or GFP::lactadherin (Conradt et al., 2016). Also, the only known *C. elegans* receptor on phagocytosis cells is CED-1/MEGF10, and we will determine if a CED-1::GFP fusion accumulates around dopaminergic neurons after 6-OHDA exposure. If CED-1 indeed surrounds damaged dopaminergic neurons, and if TTR-33 truly acts as a bridge between dying dopaminergic neurons and engulfing cells, we would expect that CED-1 accumulates later than TTR-33 and that the CED-1 signal is reduced in the *ttr-33* mutant. Also, if TTR-33 surrounds dying cells, it is expected that interfering with dopaminergic neuron loss – most likely a necrosis-like cell death (see below) – would diminish its localisation. We note that microglia were reported to be activated in Parkinson's disease (Heneka et al., 2014) and that the *C. elegans* 6-OHDA model might therefore indeed recapitulate important features of this disease.

7.14 The apoptosis pathway and its role in organismal protection

As stated before, it is not known how dopaminergic neurons die after 6-OHDA intoxication and they do not seem to undergo apoptosis. Mutations in the core apoptosis pathway do not prevent cell loss (Nass et al., 2002), but we find that inhibition of apoptosis rather leads to a

loss of protection against 6-OHDA. It has been reported in that the intrinsic apoptosis pathway in *C. elegans* can sense mitochondrial reactive oxygen species (mtROS) to modulate stress sensitivity and survival (Yee et al., 2014). In the same paper, *glit-1* expression was increased under three different mtROS-inducing conditions which extended *C. elegans* lifespan. Since we find increased 6-OHDA sensitivity of *ced-4, ced-3* and *ced-13* mutants, the mtROS-sensing pathway might be involved in the reaction to 6-OHDA-induced oxidative stress. However, we still need to investigate if these genes also have protective effects wild-type degeneration at higher concentrations of 6-OHDA.

7.15 Indications for a 6-OHDA-induced necrotic cell death of dopaminergic neurons

Apart from apoptosis, necrosis is a main type of cell death and there are indications that dopaminergic neurons become necrotic after 6-OHDA intoxication. Previously, it was shown that *C. elegans* dopaminergic CEP neurons undergo necrosis after heat shock and that cell loss can be alleviated by mutating the calcium-binding chaperone *crt-1* (Kourtis et al., 2012). *crt-1* was shown to be upregulated upon tunicamycin exposure and this was dependent on the UPR gene *ire-1* (Lee et al., 2007a). Since *crt-1* appears to have a role in necrosis, we tested if it also modulates the extent of 6-OHDA-induced dopaminergic neurodegeneration. We did not find greatly increased sensitivity to 6-OHDA for *crt-1* mutants, but we still need to test if the mutation influences dopaminergic neurodegeneration in wild-type animals at higher concentrations of the drug. Remarkably, *crt-1*;*glit-1* double mutants seem to be synthetic lethal and we aim to generate the *ttr-33*;*crt-1* double mutant. In addition, we want to determine if Ca^{2+} homeostasis in general has a role in 6-OHDA-induced neurodegeneration. Pharmacologically, cellular Ca^{2+} levels can be decreased with the Ca^{2+}-specific chelator EGTA, by preventing Ca^{2+} release from ER stores with dantrolene − or increased by inhibiting Ca^{2+} uptake and stimulation of Ca^{2+} release from ER stores with thapsigargin (Xu et al., 2001).

Genetically, Ca^{2+} release from the ER can be diminished by mutating the inositol triphosphate receptor *itr-1* (Xu et al., 2001).

The aspartyl proteases ASP-3 and ASP-4 and the Ca^{2+}-dependent proteases CLP-1 and TRA-3 were shown to mediate necrosis (Syntichaki et al., 2002) and could be tested for their influence on 6-OHDA-induced neurodegeneration. Furthermore, transcriptional levels of those proteases can be tested in wild-type and mutant worms with and without 6-OHDA treatment. As mentioned above, 6-OHDA-induced neurodegeneration is reduced under conditions of starvation. Furthermore, nutrient deprivation leads to drop of aspartyl protease activity to 5-10 % of that of well-fed nematodes (Hawdon et al., 1989; Jacobson et al., 1988; Syntichaki et al., 2002). Therefore, these proteases could indeed mediate a necrosis-like cell death of dopaminergic neurons upon treatment with 6-OHDA. We note that GLIT-1 possesses two aspartates in the active site of its carboxyesterase-like domain; hence GLIT-1 could possibly act as an aspartyl protease itself.

Necrosis can be facilitated by autophagy (Samara et al., 2008; Troulinaki and Tavernarakis, 2011) and autophagy was shown to contribute to 6-OHDA-induced dopaminergic cell death (Tóth et al., 2007). This further supports the idea that dopaminergic neurons might undergo a necrosis-like cell death upon treatment with 6-OHDA.

It is possible that we find that dopaminergic neurons neither undergo apoptosis nor a necrosis-like cell death after intoxication with 6-OHDA. However, there might be a third possibility such that phagocytosis itself was shown to contribute to cell killing in C. elegans (Chakraborty et al., 2015; Hoeppner et al., 2001; Reddien et al., 2001). Remarkably, the authors also found that in some cases, cell death seems to be reversible until reaching a certain stage (Hoeppner et al., 2001).

7.16 Neuronal axon regeneration might be mediated by a similar pathway as the protection against 6-OHDA

Recently, *C. elegans* has become a model for neuronal regeneration, a process which seems to involve the *ttr-33* paralogue *ttr-52*. After cutting axons in L4 stage animals with a laser, the regrowth of the processes can be followed over time. Remarkably, several aspects of axon regeneration are conserved between *C. elegans* and vertebrates (El Bejjani and Hammarlund, 2012). The *C. elegans* PS receptor PSR-1 was shown to act in a pathway with TTR-52, CED-5, NRF-5 and CED-6 to promote axon regeneration in the PLM neurons and the authors speculates that extracellular vesicle generation (see below) could play a role in this process (Neumann et al., 2014). In addition, several of the genes which we found to be involved in 6-OHDA-induced neurodegeneration also seem to have a role in axon regeneration: The apoptosis genes CED-3 and CED-4, the calreticulin CRT-1, the JNK kinase KGB-1 (Pinan-Lucarre et al., 2012) and the neuroligin NLG-1 (Nix et al., 2014) were reported to promote regeneration, whereas the JNK kinase JNK-1 (Hammarlund et al., 2009) and IRE-1 (Nix et al., 2014) seem to inhibit it. However, the studies investigated different types of neurons and a few genes seem to have an effect in some paradigms but not in others. To our knowledge, the axons of dopaminergic neurons have not been tested for regeneration, but it was suggested that the regeneration of dopaminergic dendrites depends on similar pathways (González-Hunt et al., 2014). We speculate that 6-OHDA and a laser cut might inflict a comparable injury to the dopaminergic neurons and that related protective pathways are triggered.

7.17 Could TSP-17-containing extracellular vesicles provide a 'find-me' signal stimulating the phagocytosis of dopaminergic neurons?

To faciliate cell corpse engulfment, phosphatidylserine (PS) exposed on the surface of apoptotic cells might be transmitted to phagocytes via extracellular vesicles (exosomes) and this process seems to be regulated by TTR-52, NRF-5 and CED-7 (Mapes et al., 2012). We hypothesise that TTR-33 might exert a similar function like TTR-52 and mediate the removal of

PS from the surface of necrotic dopaminergic neurons via small vesicles. Hence, loss of *ttr-33* function might lead to accumulation of the 'eat-me' mark, such that the cells are engulfed prematurely after 6-OHDA exposure.

We speculate that the previously characterised tetraspanin *tsp-17*, for which mutation also causes sensitivity to 6-OHDA (Masoudi et al., 2014), could also function in dopaminergic cell recognition and/or extracellular vesicle generation. TSP-17 acts in dopaminergic neurons (Masoudi et al., 2014) and is a transmembrane protein like GLIT-1. Tetraspanins were shown to function in the immune system and to contribute to pathogen infection and the formation of metastasis (Charrin et al., 2014). Many tetraspanins interact directly with specific proteins, including other tetraspanins, generating a network of interactions. We note that several tetraspanins contain a PDZ-binding motif (Charrin et al., 2014), similar to neuroligins. Furthermore, tetraspanins are thought to contribute to membrane compartmentalisation (Charrin et al., 2014). Tetrasspanins are the most abundant membrane protein of extracellular vesicles and have been proposed as possible exosome markers (Andreu and Yáñez-Mó, 2014). Extracellular vesicles have a defined protein signature, comprising conserved as well as cell type specific sets of proteins (Andreu and Yáñez-Mó, 2014). We hypothesise that the tetraspanin TSP-17 – and possibly the neuroligin-like gene GLIT-1 – might mediate the formation of exosomes originating from dopaminergic neurons after 6-OHDA-induced damage. The phagocytosis of a cell is promoted by a combination of released and exposed signals – 'find-me' and 'eat-me' signals, respectively. Exosomes might represent a 'find-me' signal originating from dopaminergic neurons that were damaged by 6-OHDA.

There are additional links between the tetraspanin *tsp-17*, the neuroligin-like *glit-1* and the phagocytosis pathway. Tetraspanins functionally regulate several membrane-bound proteases, including the exit of the metalloproteinase ADAM10 from the endoplasmic reticulum and its targeting to the plasma membrane (Charrin et al., 2014). This might be of importance since

this protease was shown to cleave neuroligin-1 to generate a secreted extracellular fragment (Suzuki et al., 2012). Furthermore, connections between tetraspanins and the engulfment pathway were reported: The tetraspanin CD63 was suggested to interact with the small GTPase Rac1 (Charrin et al., 2014). The *C. elegans* homologue of Rac1 is CED-10 – the protein on which the two partially redundant phagocytosis pathways merge. In addition, the tetraspanins CD9 and CD81 were shown to cooperate to negatively regulate macrophage fusion (Charrin et al., 2014).

8 MATERIAL AND METHODS

8.1 *C. elegans* strains and maintenance

Strains were grown at 20°C unless indicated otherwise and N2 Bristol and BY200 (*pdat-1::gfp*, originally generated by the Blakely lab (Nass et al., 2002)) were used as wild-type strains. *wdr-23(tm1817)*, *tsp-17(tm4994)* and *pink-1(tm1779)* mutants were generated and kindly provided by Shohei Mitani of the National Bioresource Project (NBRP) (http://shigen.nig.ac.jp/c.elegans/). Details of these alleles are described by the National Bioresource Project. Additional information about alleles in this study is provided by WormBase (www.wormbase.org). Strains from the Caenorhabditis Genetics Center (CGC) or the NBRP were outcrossed to the BY200 strain to eliminate unlinked mutations and to introduce a green fluorescent protein (GFP) marker for dopaminergic neurons. Isolated mutants were outcrossed a minimum of six times to the BY200 strain.

Table 1: List of *C. elegans* strains from this study

BY200 *vtIs1[pdat-1::gfp; rol-6]* V
TG4100 *vtIs1* V; *glit-1*(*gt1981*) X
TG4101 *vtIs1* V; *glit-1(gk384527)* X
TG4102 *vtIs1* V; *glit-1(ok237)* X
TG4103 *ttr-33(gt1983)* V; *vtIs1* V
TG4104 *ttr-33(gk567379)* V; *vtIs1* V
TG2400 *dat-1(ok157)* III; *vtIs1* V
TG4105 *dat-1(ok157)* III; *vtIs1* V*; glit-1*(*gt1981*) X
TG4106 *dat-1(ok157)* III; *ttr-33(gt1983)* V; *vtIs1* V
N2 Bristol
TG4107 *dvIs19 [(pAF15)pgst-4::gfp::NLS]* III
SJ4005 *zcIs4 [hsp-4::gfp]* V
SJ4100 *zcIs13 [hsp-6::gfp]* V
TG4108 *dvIs19* [*(pAF15)pgst-4::gfp::NLS*] III; *glit-1*(*gt1981*) X
TG4109 *zcIs4 [phsp-4::gfp]* V; *glit-1*(*gt1981*) X
TG4110 *zcIs13 [phsp-6::gfp]* V; *glit-1*(*gt1981*) X
TG4111 *skn-1(zu67) IV/nT1 [unc-?(n754) let-?]* (IV;V); *vtIs1* V;
TG4112 *skn-1(zu67) IV/nT1 [unc-?(n754) let-?]* (IV;V); *vtIs1* V; *glit-1*(*gt1981*)
TG4113 *skn-1(lax120)*; *vtIs1* V;
TG4114 *skn-1(lax120)*; *vtIs1* V; *glit-1*(*gt1981*) X
TG4115 *wdr-23(tm1817)* I; *vtIs1* V;
TG4116 *wdr-23(tm1817)* I; *vtIs1* V; *glit-1*(*gt1981*) X
TG4117 *ire-1(v33)* II; *vtIs1* V;
TG4118 *ire-1(v33)* II; *vtIs1* V; *glit-1*(*gt1981*) X
TG4119 *ire-1(v33)* II; *ttr-33*(*gt1983*) V; *vtIs1* V

TG4120 *pmk-1(km25)* IV; *vtIs1* V
TG4121 *pmk-1(km25)* IV; *ttr-33*(*gt1983*) V; *vtIs1* V
TG4122 *jnk-1(gk7)* IV; *vtIs1* V
TG4123 *jnk-1(gk7)* IV; *ttr-33*(*gt1983*) V; *vtIs1* V
TG4124 *pmk-3(ok169)* IV; *vtIs1* V
TG4125 *pmk-3(ok169)* IV; *ttr-33*(*gt1983*) V; *vtIs1* V
TG4126 *kgb-1(ok169)* IV; *vtIs1* V;
TG4127 *kgb-1(ok169)* IV; *vtIs1* V; *glit-1*(*gt1981*) X
TG4128 *pmk-1(km25)* IV; *vtIs1* V; *glit-1*(*gt1981*) X
TG4129 *jnk-1(gk7)* IV; *vtIs1* V; *glit-1*(*gt1981*) X
TG4130 *pmk-3(ok169)* IV; *vtIs1* V; *glit-1*(*gt1981*) X
TG2436 *vtIs1* V; *tsp-17(tm4995)* X
TG4131 *vtIs1* V; *tsp-17(tm4995)* X; *glit-1*(*gt1981*) X
TG4132 *ttr-33*(*gt1983*) V; *vtIs1* V; *tsp-17(tm4995)* X
TG4133 *ttr-33*(*gt1983*) V; *vtIs1* V; *glit-1*(*gt1981*) X
TG4134 *ttr-33*(*gt1983*) V; *vtIs1* V; *glit-1*(*gt1981*) X; *tsp-17(tm4995)* X
TG4135 *vtIs1* V; *nlg-1(ok259)* X
TG4136 *vtIs1* V; *glit-1*(*gt1981*) X; *nlg-1(ok259)* X
TG4137 *vtIs1* V; *nrx-1(ok1649)* X
TG4138 *vtIs1* V; *glit-1*(*gt1981*) X; *nrx-1(ok1649)* X
TG4139 *vtIs1* V; *nrx-1(wy778)* X
TG4140 *vtIs1* V; *glit-1*(*gt1981*) X; *nrx-1(wy778)* X
TG2410 *vtIs1* V; *dop-1(vs100)* X
TG4141 *vtIs1* V; *dop-1(vs100)* X; *glit-1*(*gt1981*) X
TG2412 *dop-2(vs105)* V; *vtIs1* V
TG4142 *dop-2(vs105)* V; *vtIs1* V; *glit-1*(*gt1981*) X
TG2414 *vtIs1* V; *dop-3(vs106)* X
TG4143 *vtIs1* V; *glit-1*(*gt1981*) X; *dop-3(vs106)* X
TG4144 *dop-2(vs105)* V; *vtIs1* V; *dop-1(vs100)* X
TG4145 *dop-2(vs105)* V; *vtIs1* V; *dop-1(vs100)* X; *glit-1*(*gt1981*) X
TG4146 *vtIs1* V; *dop-1(vs100)* X; *dop-3(vs106)* X
TG4147 *vtIs1* V; *dop-1(vs100)* X; *glit-1*(*gt1981*) X*; dop-3(vs106)* X
TG2466 *dop-2(vs105)* V; *vtIs1* V; *dop-3(vs106)* X
TG4148 *dop-2(vs105)* V; *vtIs1* V; *glit-1*(*gt1981*); *dop-3(vs106)* X
TG2415 *dop-2(vs105)* V; *vtIs1* V; *dop-1(vs100)* X; *dop-3(vs106)* X
TG4149 *dop-2(vs105)* V; *vtIs1* V; *dop-1(vs100)* X; *glit-1*(*gt1981*) X*; dop-3(vs106)* X
TG2396 *bas-1(ad446)* III; *vtIs1* V
TG4150 *bas-1(ad446)* III; *vtIs1* V; *glit-1*(*gt1981*) X
TG2399 *vtIs1* V; *cat-1(ok411)* X
TG4151 *vtIs1* V; *glit-1*(*gt1981*) X; *cat-1(ok411)* X
TG2395 *cat-2(e1112)* II; *vtIs1* V;
TG4152 *cat-2(e1112)* II; *vtIs1* V; *glit-1*(*gt1981*) X
TG4153 *otIs433 [dat-1::NLS::RFP ttx-3::mCh]* V; *PExglit-1::GFP*
TG4154 *ced-2(e1752)* IV; *vtIs1* V;
TG4155 *ced-2(e1752)* IV; *ttr-33*(*gt1983*) V; *vtIs1* V;
TG4156 *ced-6(n1813)* III; *vtIs1* V;
TG4157 *ced-6(n1813)* III; *ttr-33*(*gt1983*) V; *vtIs1* V;
TG4158 *ced-10(n3246)* IV; *vtIs1* V;
TG4159 *ced-10(n3246)* IV; *ttr-33*(*gt1983*) V; *vtIs1* V;
TG4160 *ttr-52(sm211)* III; *vtIs1* V;
TG4161 *ttr-52(sm211)* III; *ttr-33*(*gt1983*) V; *vtIs1* V;
TG4162 *crt-1(ok948)* V; *vtIs1* V;

TG4163 *ced-4(n1162)* III; *vtIs1* V;
TG4164 *ced-4(n1162)* III; *ttr-33*(*gt1983*) V; *vtIs1* V;
TG4165 *ced-4(n1162)* III; *vtIs1* V; *glit-1*(*gt1981*) X
TG4166 *ced-3(n717)* IV; *vtIs1* V;
TG4167 *ced-3(n717)* IV; *vtIs1* V; *glit-1*(*gt1981*) X
TG4168 *vtIs1* V; *ced-13(sv32)* X;
TG4169 *vtIs1* V; *glit-1*(*gt1981*) X*; ced-13(sv32)* X;
TG4170 *PExttr-33::GFP*
TG4171 vtIs1 V; CB4856
TG4172 *pink-1(tm1779)* II; *vtIs1* V;
TG4173 *pink-1(tm1779)* II; *vtIs1* V; *glit-1*(*gt1981*) X
TG4174 *pdr-1(gk448)* III; *vtIs1* V;
TG4175 *pdr-1(gk448)* III; *vtIs1* V; *glit-1*(*gt1981*) X

8.1 Mutagenesis and mapping

L4 and young adult staged BY200 worms in M9 buffer were mutagenised with 25 mM ethyl methanesulfonate (EMS) for 4 h at 20°C, washed and let incubated at 15°C overnight. After the first egg-laying the worms were bleached and the F1 progeny let hatch overnight in M9. This synchronised F1 were left to develop on seeded plates until they reached early adult stage. The F1 adults were washed off in M9 again to lay a synchronised population of F2 L1 larvae which was treated with 10 mM 6-OHDA and screened for dopaminergic neuron loss after 72 h. Candidates were picked on separate plates, backcrossed at least three times and re-tested for their hypersensitivity to 6-OHDA. The genomic DNA was sent for whole-genome sequencing and SNP mapping was done as previously described (Doitsidou et al., 2010; Minevich et al., 2012).

8.2 Stress assays

To obtain synchronized L1 larvae for the **paraquat and 6-OHDA assays**, 1–10 adult worms were incubated to lay eggs in 70 µl M9 without food on a benchtop shaker at 20˚C, 500 rpm for 24-30 h. Due to the swimming-defect of tsp-17(tm4995), L1 larvae for experiments including this strain were obtained by filtering a mixed population of worms that was washed off the plates.

For **6-OHDA assays**, 10 µL 200 mM ascorbic acid and 10 µL of the respective 6-OHDA 5 x stock concentration were added to 30 µL of L1-stage larvae in M9. After 1 hour incubation at 20˚C and shaking at 500 rpm, 150 µL M9 buffer was added to oxidise and inactivate the 6-OHDA. The worms were pipetted to one half of an NGM plate containing a stripe of OP50 bacteria on the opposite half of the plate and adult worms and eggs were picked off to prevent growth of animals that were not intoxicated at L1 stage. Plates were incubated at 20˚C before examining the 6-OHDA-induced degeneration in a blinded manner (i.e. without the experimentator's knowledge of the animals' genotype) using a Leica fluorescent dissecting microscope. For intoxication of different developmental stages, the respective stages were picked after 6-OHDA treatment from a mixed population of worms.

For **paraquat assays**, 10 µL of the respective 5x paraquat stock concentration was added to 40 µL of L1-stage larvae in M9. After 1 h incubation in the shaker 150 µL M9 buffer was added and the L1 larvae were counted after pipetting them to a seeded NGM plate. Surviving worms were counted again after 24 h.

For **tunicamycin assays**, gravid adults were put on seeded plates containing the indicated concentration of tunicamycin to let lay eggs for 1-2 h to get around 50 eggs per condition. The eggs were counted immediately after removing the adults. 48 h after egg-laying, the development of the larvae was determined.

For **Hygromycin B assays**, unstarved L1 stage larvae were filtered and approximately 100 worms per condition put on seeded plates containing the indicated concentration of tunicamycin. The larvae were counted immediately after plating and 48 h afterwards.

8.1 Behavioural assays

All behavioural assays were performed in a blinded manner.

For **lifespan assays**, 50 L4 worms were picked per strain and moved to new plates every day during the first 6 days and then only to avoid mixing with the progeny. Worms that did not move after touch with a platinum pick were scored as dead. Dead worms were counted and removed every day and bag of worms and dry and burst worms were censored. The data was analysed using OASIS (Online application for Survival Analysis, http://sbi.postech.ac.kr/oasis/) (Yang et al., 2011).

Dopamine paralysis assays were carried out as previously described (Sanyal et al., 2004). Staged adult animals were incubated for 20 min on a plate containing dopamine and assessed for their ability to complete body movement through minimum and maximum amplitude during a 5 s observation period. Two plates containing 25 worms each were assessed for each condition.

For the **swimming-induced paralysis (SWIP)** assay 5-15 L4 stage larvae were picked into a glass well in 40 µL water. The number of paralysed worms scored using a Leica dissecting microscope every minute for 30 minutes (McDonald et al., 2007).

Basal slowing assays were done by Eline Jongsma as previously described (Chase et al. 2004). NGM plates were prepared and half of them seeded with HB101 bacteria before incubating them at 37°C overnight. Also, mid-L4 larvae were picked on separate plates. The next day, these staged young adult animals were put in 40 µL M9 for 2 min for washing and then picked to the centre of a plate. 6 animals each were put on a plate with and without bacteria, respectively. After a 2 min adaptation time, the locomotion rates of each animal was quantified by counting the number of body bends completed in five consecutive 20 s intervals. The experiment was done twice on different days.

For each mutant in the **egg-laying assay** (done by Eline Jongsma), eggs were counted by from total of 9 adult worms on 3 different plates after 3 hours of egg-laying.

8.2 Bioinformatic analysis

GLIT-1 and TTR-33 extra- and intracellular and transmembrane domains and signal peptides were predicted with Phobius (http://phobius.sbc.su.se/) (Käll et al., 2007).

GLIT-1 and TTR-33 protein structure models were calculated in SWISS-MODEL (swissmodel.expasy.org) (Biasini et al., 2014) and visualised with Swiss-PdbViewer 4.1.0 (http://www.expasy.org/spdbv/) (Guex and Peitsch, 1997).

For **phylogenetic analysis of GLIT-1**, CLC workbench Version 7.6.4 was used to align protein sequences (Default parameters: Gap open cost 10.0, Gap extension cost 1.0, End gap cost as any other, Alignment very accurate (slow)) and create a the tree (Tree construction method: Neighbour Joining, Protein distance measure: Jukes-Cantor, Bootstrapping: 100 Replicates).

For **GLIT-1 PDZ domain binding prediction,** the webserver POW was used (http://webservice.baderlab.org/domains/POW/). Predictions are made using a support vector machine (SVM) that was trained using experimentally determined PDZ interaction data from protein microarray and phage display experiments for mouse and human. Two types of predictors were used, a sequence-based one (Hui and Bader, 2010) – which was trained using domain and peptide sequence features – and a structure-based one (Hui et al., 2013) – which was trained using domain structure and peptide sequence features.

For ***C. elegans* TTR phylogenetic alignment** Jalview Version 2.9.0b2 (www.jalview.org) was used for alignment (ClustalWS version 2.0.12 with default settings) and visualisation (Waterhouse et al., 2009). **TTR-33 secondary structure prediction** was done with JPred4 (Drozdetskiy et al., 2015) in Jalview (Troshin et al., 2011).

For ***ttr-33* correlated gene expression analysis,** SPELL (Serial Pattern of Expression Levels Locator) Version 2.0.3.r71 was used (http://spell.caltech.edu:3000/). Given a query gene, SPELL searches for genes with correlated expression patterns based on available microarray,

RNAseq and tiling array data (currently 5264 experiments in 315 datasets). The main algorithm is described in (Hibbs et al., 2007).

8.3 Statistical analysis

The **two-tailed t-test** and were performed with the Analysis ToolPak Add-In in Microsoft Excel 2010. To choose a t-test assuming equal or unequal variances, respectively, an F-test was conducted beforehand, also with the Analysis ToolPak Add-In.

To compare 6-OHDA intoxication data, a **G-Test** was performed with R Studio 1.0.44 DescTools descriptive statistics tools package. p-values were calculated for each biological replicate and for the pooled biological replicate data, and the least significant of these p-values indicated in the graphs. Unless otherwise indicated, data is only marked as significant if all replicates and the pooled replicate data were found to be significant.

8.4 DNA cloning and generation of transgenic lines

For generation of transgenic constructs, genomic DNA was amplified with PCR primers containing additional 8 base pair restriction sites to achieve the following design: *AscI* – Promoter – *SgfI* – Gene – *NotI* – Fluorescent tag – *FseI* – 3'UTR – *PacI*. The *ttr-33* translation construct (9287374654767326 H09) was acquired from *C. elegans* TransgeneOme Resource (MPI-CBG) (Sarov et al., 2012).

Table 2: Plasmids and primers.
Restriction sites are shown in italics, translation start and end sites in bold. Translation codons are separated by a space.

***glit-1* transcriptional construct (Pglit-1::GFP) for Chr IV**

AscI – Pglit-1 – *NotI* – GFP – *FseI* – 3'glit-1– *PacI*

AscI_Pglit-1	GCTA*ggcgcgcc*GTATCTGGCATTGGCTCG
Pglit-1_Not-1	GCTA *gcg gcc gc*a **CAT**TCCATGTGACGCGAT
NotI_GFP	GCTA*gc ggc cgc* AGT AAA GGA GAA GAA CTT TTC ACT GG

GFP_FseI(Glit-1)	AAG**TTA** *ggc cgg ccc* CTT GTA TGG CCG GCT AG
FseI(GFP)_3'GLIT-1	AC AAG *ggg ccg gcc* **TAA**CTTTCAAAGTTTGTAAATAATGTATAATTTA
3'GLIT-1_Pac-1	GCTA*ttaattaa*CCAGTTGCAGTGTTTTTTTG

***ttr-33* transcriptional construct (Pttr-33::GFP) for Chr IV**

AscI – Pttr-33 – *NotI* – GFP – *FseI* – 3'ttr-33 – *PacI*

AscI_Pttr-33	GCTA*ggcgcgcc*CAAAGAAACTTGCGTGTTTC
Pttr-33_NotI	GCTA *gcg gcc gc*a **CAT**TATTTTTGTCTGAAAATACAAACAC
NotI_GFP	GCTA*gc ggc cgc* AGT AAA GGA GAA GAA CTT TTC ACT GG
GFP_FseI(ttr-33)	TTA**TTA** *ggc cgg ccc* CTT GTA TGG CCG GCT AG
FseI(GFP)_3'TTR-33	AC AAG G*gg ccg gcc* **TAA**TAATTATACTTAAAAGTATTTTCAACTG
3'TTR_33-PacI	GCTA*ttaattaa*GCATGCATCTTCCCATAAAAG

8.1 Microscopy

Images were acquired using a Deltavision (Applied Precision) microscope and deconvolved using the softWoRx Suite (Applied Precision).

9 SUPPLEMENTARY INFORMATION

Table S 1: PDZ domain proteins that are predicted to interact with the *GLIT-1* PDZ binding sequence based on sequence information.
The algorithm of the POW website predicts interactors of the GLIT-1-specific C-terminal PDZ binding sequence from 85 *C. elegans*-specific PDZ proteins based on sequence information. Proteins were sorted based on the support vector machine (SVM) decision score – measure of predictor confidence in the prediction. In the last row, selected information from WormBase was added. *Asterisk denotes domains with low similarity (<0.6) to the training set domains, as measured by binding site sequence similarity. Therefore the predictions may be less reliable.

PDZ Domain Name	SVM Decision Score	Wormbase information
TAG-60-1*	0.758	NRFL-1, NHERF (mammalian Na/H Exchange Regulatory Factor) Like) – homologue of *Drosophila* SIP1 that maintains epithelial integrity, required for normal acetylcholine neurotransmission
SHN-1-1	0.551	SHaNk (SH3/ankyrin domain scaffold protein) related – sole *C. elegans* SHANK protein and orthlogue of vertebrate SHANK3
STN-2-1	0.54	SynTrophiN – encodes a gamma-syntrophin
F30F8.3-1*	0.489	GRAS-1, GRASP (General Receptor for phosphoinositides 1-Associated Scaffold Protein) homolog
TAG-60-2*	0.422	*see above*
MPZ-1-6	0.378	Multiple PDZ domain protein
CNK-1-1*	0.299	Connector/eNhancer of KSR
MICS-1-1	0.29	MItoChondrial Scaffolding protein- orthologue of human SYNJ2BP (synaptojanin 2 binding protein) – microarray and RNA sequencing studies indicate that *mics-1* is regulated by *cyc-1, sir-2.1*, *cep-1*; microarray studies indicate that *mics-1* is regulated by Paraquat;
MAGI-1-4*	0.236	MAGI (Membrane Associated Guanylate kinase Inverted) homologue – multi PDZ-domain containing tight junction-associated protein: MAGIs are members of vertebrate membrane associated guanylate-kinase (MAGUK) family; MAGI-1/S-SCAM is also a broadly conserved synaptic scaffolding molecule
MPZ-1-7*	0.161	*see above*
ZK849.2-2	0.13	GOPC-1 (GOlgi-associated PDZ and Coiled-coil motif protein) – orthologue of human GOPC
C50D2.3-1*	0.036	Microarray and RNA sequencing studies indicate that C50D2.3 is regulated by *wdr-23, isp-1*, and *nuo-6*; microarray studies indicate that C50D2.3 is regulated by Paraquat
MAGI-1-2	0.031	*see above*

Table S 2: PDZ domain proteins that are predicted to interact with the *GLIT-1* PDZ binding sequence based on structure information.
The algorithm of the POW website predicts interactors of the GLIT-1-specific C-terminal PDZ binding sequence from 64 *C. elegans*-specific PDZ proteins based on structure information. Proteins were sorted based on the support vector machine (SVM) decision score – measure of predictor confidence in the prediction. In the last row, selected information from WormBase was added.

PDZ Domain Name	SVM Decision Score	Wormbase information
DLG-1-2	1.443	Drosophila Discs LarGe homologue – MAGUK protein, DLG-1 is physically located at apical adherens junctions in all epithelia and is required for organisation of the embryonic gut epithelium into a coherent tube.
LIN-10-2	0.896	abnormal cell LINeage – homologous to mammalian Munc interacting proteins and required for polarized protein localisation
MPZ-1-4	0.865	*see table above*
F44D12.1-1	0.744	MAGU-4 (MAGUK family) – orthologue of human DLG5 (discs large 5 (Drosophila))
MICS-1-1	0.671	*see table above*
DLG-1-1	0.666	*see above*
STN-1-1	0.648	SynTrophiN – encodes a syntrophin with homology to vertebrate α and beta-syntrophins; STN-1 physically interacts with the SNF-6 acetylcholine transporter
DSH-1-1	0.599	DiSHevelled related – homologue of Drosophila DISHEVELED, functions as part of a Wnt signaling pathway that regulates ACR-16 (Acetylcholine receptor)localisation to postsynaptic regions, a key component of activity-dependent synaptic plasticity
C35D10.2-1	0.597	GIPC-1 (RGS-GAIP Interacting Protein C) homolog
NAB-1-1	0.594	NeurABin,
MPZ-1-6	0.524	*see table above*
SHN-1-1	0.512	*see table above*
MAGI-1-4	0.509	*see table above*
FRM-5-2	0.426	FERM domain (protein4.1- ezrin-radixin-moesin) family
ZOO-1-1	0.356	ZO-1 (Zonula Occludens tight junctional protein) Ortholog
TAG-60-2	0.339	*see table above*
KIN-4-1	0.264	protein KINase – orthologue of MAST (microtubule associated serine/threonine) kinases
AFD-1-1	0.253	AFaDin (actin filament binding protein) homologue – microarray and RNA sequencing studies indicate that afd-1 is regulated by cyc-1, sir-2.1, slr-2, fbf-1, isp-1, and nuo-6; RNA sequencing and microarray studies indicate that afd-1 is regulated by Rotenone and Paraquat
TAG-60-1	0.253	*see table above*

F30F8.3-1	0.251	*see table above*
PTP-1-1	0.234	Protein Tyrosine Phosphatase
F44D12.4-1	0.233	GIPC-2 (RGS-GAIP Interacting Protein C) homolog
SYD-1-1	0.231	SYnapse Defective
T19B10.5-1	0.216	protein with partial similarity to human PERIAXIN
MPZ-1-8	0.206	*see table above*
MPZ-1-10	0.203	*see table above*
FRM-5-3	0.197	FERM domain (protein4.1- ezrin-radixin-moesin) family
PAR-3-3	0.181	abnormal embryonic PARtitioning of cytoplasm
PAR-6-1	0.179	abnormal embryonic PARtitioning of cytoplasm
MAGI-1-5	0.112	*see table above*
STN2-1	0.098	*see table above*
MPZ-1-2	0.086	*see table above*
TAG-117-1	0.071	MAGU-1
MAGI-1-3	0.055	*see table above*
ZK1321.4-1	0.054	microarray, tiling array, proteomic, and RNA sequencing studies indicate that ZK1321.4 is regulated by cyc-1, daf-16;
RHGF-1-1	0.037	RHo Guanine nucleotide exchange Factor – RHGF-1 functions within cholinergic motor neurons in one of four G-protein-mediated signaling pathways that control locomotion via regulation of acetylcholine (ACh) release at neuromuscular junctions
ZOO-1-3	0.026	*see above*

Table S 3: Gene Ontology (GO) term analysis for genes for which expression pattern correlated with *ttr-33*.

Genes with expression patterns that correlated to the *ttr-33* expression pattern were predicted using SPELL – Nematodes and their GO terms are listed below sorted by P value. The number of genes that are associated with this GO term out of all genes with a similar expression pattern to *ttr-33* and out of all genes in the genome are shown in column % Query and % genome, respectively. Very specific processes that are associated with few genes in the genome are marked in red. * Similar GO terms based on the same group of genes were merged.

GO Term	P value	% Query	% Genome	Annotated Genes
neuropeptide signaling pathway	5.21E-08	7 of 41	188 of 54514	NLP-31, FLP-9, FLP-21, FLP-24, NLP-15, NLP-27, FLP-22
(negative) regulation of metalloenzyme activity, (negative) regulation of membrane protein ectodomain proteolysis*	2.73E-04	2 of 41	2 of 54514	CRI-2, K07C11.3
single-multicellular organism process*	3.79E-04	16 of 41	5401 of 54514	FLP-24, F20A1.1, NAS-36, GRD-10, FLP-12, BEST-24, LET-522, CAL-2, SNET-1, TNC-2, RPS-20, Y73F4A.2, STA-2, T26C5.4, PTR-8, F40F12.7
(defense) response to fungus *	9.53E-04	3 of 41	32 of 54514	NLP-31, CNC-6, STA-2
multi-organism process	1.51E-02	7 of 41	1212 of 54514	NLP-31, FLP-21, F20A1.1, FLP-12, CNC-6, STA-2, C18E3.5
biological regulation	1.96E-02	23 of 41	14131 of 54514	NLP-31, FLP-9, FLP-21, FLP-24, W01B11.6, NLP-15, NLP-27, GRD-10, FLP-12, BEST-24, TTR-48, CRI-2, LET-522, H05L03.3, TTR-32, SNET-1, K07C11.3, RPS-20, STA-2, PTR-8, FLP-22, RIC-4, F40F12.7
locomotion	3.28E-02	8 of 41	1873 of 54514	NAS-36, NLP-15, GRD-10, BEST-24, LET-522, TTR-32, SNET-1, Y4C6B.2

References

Aballay, A., and Ausubel, F.M. (2001). Programmed cell death mediated by ced-3 and ced-4 protects Caenorhabditis elegans from Salmonella typhimurium-mediated killing. Proc. Natl. Acad. Sci. U. S. A. *98*, 2735–2739.

Aballay, A., Drenkard, E., Hilbun, L.R., and Ausubel, F.M. (2003). Caenorhabditis elegans innate immune response triggered by Salmonella enterica requires intact LPS and is mediated by a MAPK signaling pathway. Curr. Biol. *13*, 47–52.

Abou-Sleiman, P.M., Muqit, M.M., and Wood, N.W. (2006). Expanding insights of mitochondrial dysfunction in Parkinson's disease. Nat Rev Neurosci *7*, 207–219.

Allen, A.T., Maher, K.N., Wani, K. a, Betts, K.E., and Chase, D.L. (2011). Coexpressed D1- and D2-like dopamine receptors antagonistically modulate acetylcholine release in Caenorhabditis elegans. Genetics *188*, 579–590.

Alshehri, B., D'Souza, D.G., Lee, J.Y., Petratos, S., and Richardson, S.J. (2015). The Diversity of Mechanisms Influenced by Transthyretin in Neurobiology: Development, Disease and Endocrine Disruption. J. Neuroendocrinol. *27*, 303–323.

An, J.H., and Blackwell, T.K. (2003). Specification To a Conserved Oxidative Stress Response. Genes Dev. 1–12.

Andreu, Z., and Yáñez-Mó, M. (2014). Tetraspanins in Extracellular Vesicle Formation and Function. Front. Immunol. *5*, 1–12.

Andrew, R., Watson, D.G., Best, S.A., Midgley, J.M., Wenlong, H., and Petty, R.K. (1993). The determination of hydroxydopamines and other trace amines in the urine of parkinsonian patients and normal controls. Neurochem. Res. *18*, 1175–1177.

Antebi, A. (2013). Regulation of longevity by the reproductive system. Exp. Gerontol. *48*, 596–602.

Araç, D., Boucard, A. a., Özkan, E., Strop, P., Newell, E., Südhof, T.C., and Brunger, A.T. (2007). Structures of Neuroligin-1 and the Neuroligin-1/Neurexin-1β Complex Reveal Specific Protein-Protein and Protein-Ca2+ Interactions. Neuron *56*, 992–1003.

Artal-Sanz, M., and Tavernarakis, N. (2009). Prohibitin couples diapause signalling to mitochondrial metabolism during ageing in C. elegans. Nature *461*, 793–797.

Artal-Sanz, M., Samara, C., Syntichaki, P., and Tavernarakis, N. (2006). Lysosomal biogenesis and function is critical for necrotic cell death in Caenorhabditis elegans. J. Cell Biol. *173*, 231–239.

Baumeister, R., Schaffitzel, E., and Hertweck, M. (2006). Endocrine signaling in Caenorhabditis elegans controls stress response and longevity. J. Endocrinol. *190*, 191–202.

El Bejjani, R., and Hammarlund, M. (2012). Neural regeneration in Caenorhabditis elegans. Annu. Rev. Genet. *46*, 499–513.

Bemben, M. a., Shipman, S.L., Nicoll, R. a., and Roche, K.W. (2015). The cellular and molecular landscape of neuroligins. Trends Neurosci. 1–10.

Bertoncini, C.W., Fernandez, C.O., Griesinger, C., Jovin, T.M., and Zweckstetter, M. (2005). Familial mutants of α-synuclein with increased neurotoxicity have a destabilized conformation. J. Biol. Chem. *280*, 30649–30652.

Betarbet, R., Sherer, T.B., Mackenzie, G., Garcia-osuna, M., Panov, A. V, and Greenamyre, J.T. (2000). Chronic systemic pesticide exposure reproduces features of Parkinson's disease. Nat.

Neurosci. *3*, 1301–1306.

Biasini, M., Bienert, S., Waterhouse, A., Arnold, K., Studer, G., Schmidt, T., Kiefer, F., Cassarino, T.G., Bertoni, M., Bordoli, L., et al. (2014). SWISS-MODEL: Modelling protein tertiary and quaternary structure using evolutionary information. Nucleic Acids Res. *42*, 252–258.

Bingol, B., Tea, J.S., Phu, L., Reichelt, M., Bakalarski, C.E., Song, Q., Foreman, O., Kirkpatrick, D.S., and Sheng, M. (2014). The mitochondrial deubiquitinase USP30 opposes parkin-mediated mitophagy. Nature *509*, 370–375.

Bishop, N. a, and Guarente, L. (2007). Two neurons mediate diet-restriction-induced longevity in C. elegans. Nature *447*, 545–549.

Bolan, E.A., Kivell, B., Jaligam, V., Oz, M., Jayanthi, L.D., Han, Y., Sen, N., Urizar, E., Gomes, I., Devi, L.A., et al. (2007). D 2 Receptors Regulate Dopamine Transporter Function via an Extracellular Signal-Regulated Kinases 1 and 2-Dependent and Phosphoinositide 3 Kinase-Independent Mechanism. *71*, 1222–1232.

Bolz, D.D., Tenor, J.L., and Aballay, A. (2010). A conserved PMK-1/p38 MAPK is required in Caenorhabditis elegans tissue-specific immune response to Yersinia pestis infection. J. Biol. Chem. *285*, 10832–10840.

Bové, J., and Perier, C. (2012). Neurotoxin-based models of Parkinson's disease. Neuroscience *211*, 51–76.

Brenner, C., and Moulin, M. (2012). Physiological roles of the permeability transition pore. Circ. Res. *111*, 1237–1247.

Cabello, J., Sämann, J., Gómez-Orte, E., Erazo, T., Coppa, A., Pujol, A., Büssing, I., Schulze, B., Lizcano, J.M., Ferrer, I., et al. (2014). PDR-1/hParkin negatively regulates the phagocytosis of apoptotic cell corpses in Caenorhabditis elegans. Cell Death Dis. *5*, e1120.

Calahorro, F. (2014). Conserved and divergent processing of neuroligin and neurexin genes: from the nematode C. elegans to human. Invertebr. Neurosci. *14*, 79–90.

Calahorro, F., Alejandre, E., and Ruiz-Rubio, M. (2009). Osmotic avoidance in Caenorhabditis elegans: synaptic function of two genes, orthologues of human NRXN1 and NLGN1, as candidates for autism. J. Vis. Exp. 2–6.

Cao, S., Gelwix, C.C., Caldwell, K. a, and Caldwell, G. a (2005). Torsin-mediated protection from cellular stress in the dopaminergic neurons of Caenorhabditis elegans. J. Neurosci. *25*, 3801–3812.

Cass, W.A., and Gerhardt, G.A. (1994). Direct in vivo evidence that D2 dopamine receptors can modulate dopamine uptake. Neurosci. Lett. *176*, 259–263.

Caudle, W.M., Colebrooke, R.E., Emson, P.C., and Miller, G.W. (2008). Altered vesicular dopamine storage in Parkinson's disease: a premature demise. Trends Neurosci. *31*, 303–308.

Chakraborty, S., Lambie, E.J., Bindu, S., Mikeladze-Dvali, T., and Conradt, B. (2015). Engulfment pathways promote programmed cell death by enhancing the unequal segregation of apoptotic potential. Nat. Commun. *6*, 10126.

Chandra, S., Gallardo, G., Fernández-Chacón, R., Schlüter, O.M., and Südhof, T.C. (2005). α-Synuclein cooperates with CSPα in preventing neurodegeneration. Cell *123*, 383–396.

Charmpilas, N., Daskalaki, I., Papandreou, M.E., and Tavernarakis, N. (2015). Protein synthesis as an integral quality control mechanism during ageing. Ageing Res. Rev. *23*, 75–89.

Charrin, S., Jouannet, S., Boucheix, C., and Rubinstein, E. (2014). Tetraspanins at a glance. J. Cell Sci. 1–8.

Chase, D.L., and Koelle, M.R. (2007). Biogenic amine neurotransmitters in C. elegans. WormBook 1–15.

Chaudhuri, K.R., Odin, P., Antonini, A., and Martinez-Martin, P. (2011). Parkinson's disease: The non-motor issues. Park. Relat. Disord. *17*, 717–723.

Chege, P.M., and McColl, G. (2014). Caenorhabditis elegans: A model to investigate oxidative stress and metal dyshomeostasis in Parkinson's disease. Front. Aging Neurosci. *6*, 1–15.

Chen, L., and Feany, M.B. (2005). Alpha-synuclein phosphorylation controls neurotoxicity and inclusion formation in a Drosophila model of Parkinson disease. Nat. Neurosci. *8*, 657–663.

Chen, Y.-Z., Mapes, J., Lee, E.-S., Skeen-Gaar, R.R., and Xue, D. (2013). Caspase-mediated activation of Caenorhabditis elegans CED-8 promotes apoptosis and phosphatidylserine externalization. Nat. Commun. *4*, 2726.

Choe, K.P., Przybysz, A.J., and Strange, K. (2009). The WD40 repeat protein WDR-23 functions with the CUL4/DDB1 ubiquitin ligase to regulate nuclear abundance and activity of SKN-1 in Caenorhabditis elegans. Mol. Cell. Biol. *29*, 2704–2715.

Chung, S., Gumienny, T.L., Hengartner, M.O., and Driscoll, M. (2000). A common set of engulfment genes mediates removal of both apoptotic and necrotic cell corpses in C. elegans. Nat. Cell Biol. *2*, 931–937.

Clark, I.E., Dodson, M.W., Jiang, C., Cao, J.H., Huh, J.R., Seol, J.H., Yoo, S.J., Hay, B. a, and Guo, M. (2006). Drosophila pink1 is required for mitochondrial function and interacts genetically with parkin. Nature *441*, 1162–1166.

Conradt, B., Wu, Y.C., and Xue, D. (2016). Programmed cell death during C. elegans development. Genetics *203*, 1533–1562.

Conway, K.A., Rochet, J.C., Bieganski, R.M., and Lansbury, P.T. (2001). Kinetic stabilization of the α-synuclein protofibril by a dopamine-α-synuclein adduct. Science *294*, 1346–1349.

Curtius, H.C., Wolfensberger, M., Steinmann, B., Redweik, U., and Siegfried, J. (1974). Mass fragmentography of dopamine and 6-hydroxydopamine. Application to the determination of dopamine in human brain biopsies from the caudate nucleus. J. Chromatogr. *99*, 529–540.

Darland-Ransom, M., Wang, X., Sun, C.-L., Mapes, J., Gengyo-Ando, K., Mitani, S., and Xue, D. (2008). Role of C. elegans TAT-1 protein in maintaining plasma membrane phosphatidylserine asymmetry. Science *320*, 528–531.

Derry, W.B., Putzke, A.P., and Rothman, J.H. (2001). Caenorhabditis elegans p53 : Role in Apoptosis , Meiosis , and Stress Resistance. Science (80-.). *294*, 591–596.

Doitsidou, M., Poole, R.J., Sarin, S., Bigelow, H., and Hobert, O. (2010). C. elegans mutant identification with a one-step whole-genome-sequencing and SNP mapping strategy. PLoS One *5*, e15435.

Drozdetskiy, A., Cole, C., Procter, J., and Barton, G.J. (2015). JPred4 : a protein secondary structure prediction server. Nucleic Acids Res *43*, 389–394.

Duda, J., Pötschke, C., and Liss, B. (2016). Converging roles of ion channels, calcium, metabolic stress, and activity pattern of Substantia nigra dopaminergic neurons in health and Parkinson's disease. J. Neurochem. 1–23.

Dzamko, N., Inesta-Vaquera, F., Zhang, J., Xie, C., Cai, H., Arthur, S., Tan, L., Choi, H., Gray, N., Cohen, P., et al. (2012). The IkappaB kinase family phosphorylates the Parkinson's disease kinase LRRK2 at Ser935 and Ser910 during Toll-Like Receptor signaling. PLoS One *7*.

Engelmann, I., Griffon, A., Tichit, L., Montañana-Sanchis, F., Wang, G., Reinke, V., Waterston,

R.H., Hillier, L.W., and Ewbank, J.J. (2011). A comprehensive analysis of gene expression changes provoked by bacterial and fungal infection in C. elegans. PLoS One *6*.

Eroglu, M., and Derry, W.B. (2016). Your neighbours matter – non-autonomous control of apoptosis in development and disease. Cell Death Differ. *1*, 1–9.

Ewbank, J.J. (2006). Signaling in the immune response. WormBook 1–12.

Fabrichny, I.P., Leone, P., Sulzenbacher, G., Comoletti, D., Miller, M.T., Taylor, P., Bourne, Y., and Marchot, P. (2007). Structural Analysis of the Synaptic Protein Neuroligin and Its β-Neurexin Complex: Determinants for Folding and Cell Adhesion. Neuron *56*, 979–991.

Filomeni, G., Zio, D. De, Cecconi, F., De Zio, D., and Cecconi, F. (2015). Oxidative stress and autophagy: the clash between damage and metabolic needs. Cell Death Differ. *22*, 377–388.

Finkel, T., and Holbrook, N.J. (2000). Oxidants, oxidative stress and the biology of ageing. Nature *408*, 239–247.

Fleming, C.E., Saraiva, M.J., and Sousa, M.M. (2007). Transthyretin enhances nerve regeneration. J. Neurochem. *103*, 831–839.

Fu, R., Shen, Q., Xu, P., Luo, J.J., and Tang, Y. (2014). Phagocytosis of microglia in the central nervous system diseases. Mol. Neurobiol. *49*, 1422–1434.

Fujita-Hamabe, W., and Tokuyama, S. (2012). The involvement of cleavage of neural cell adhesion molecule in neuronal death under oxidative stress conditions in cultured cortical neurons. Biol. Pharm. Bull. *35*, 624–628.

Galluzzi, L., Kepp, O., Krautwald, S., Kroemer, G., and Linkermann, A. (2014). Molecular mechanisms of regulated necrosis. Semin. Cell Dev. Biol. *35*, 24–32.

Gardai, S.J., McPhillips, K.A., Frasch, S.C., Janssen, W.J., Starefeldt, A., Murphy-Ullrich, J.E., Bratton, D.L., Oldenborg, P.A., Michalak, M., and Henson, P.M. (2005). Cell-surface calreticulin initiates clearance of viable or apoptotic cells through trans-activation of LRP on the phagocyte. Cell *123*, 321–334.

Gartner, A., Milstein, S., Ahmed, S., Hodgkin, J., and Hengartner, M.O. (2000). A conserved checkpoint pathway mediates DNA damage--induced apoptosis and cell cycle arrest in C. elegans. Mol. Cell *5*, 435–443.

Gartner, A., Boag, P.R., and Blackwell, T.K. (2008). Germline survival and apoptosis. WormBook 1–20.

Genova, J.L., and Fehon, R.G. (2003). Neuroglian, Gliotactin, and the Na+/k+ ATPase are essential for septate junction function in Drosophila. J. Cell Biol. *161*, 979–989.

Gerke, P., Keshet, A., Mertenskötter, A., and Paul, R.J. (2014). The JNK-Like MAPK KGB-1 of caenorhabditis elegans promotes reproduction, lifespan, and gene expressions for protein biosynthesis and germline homeostasis but interferes with hyperosmotic stress tolerance. Cell. Physiol. Biochem. *34*, 1951–1973.

Glinka, Y., Gassen, M., and Youdim, M.B. (1997). Mechanism of 6-hydroxydopamine neurotoxicity. J. Neural Transm. Suppl. *50*, 55–66.

González-Hunt, C.P., Leung, M.C.K., Bodhicharla, R.K., McKeever, M.G., Arrant, A.E., Margillo, K.M., Ryde, I.T., Cyr, D.D., Kosmaczewski, S.G., Hammarlund, M., et al. (2014). Exposure to Mitochondrial Genotoxins and Dopaminergic Neurodegeneration in Caenorhabditis elegans. PLoS One *9*, e114459.

Greene, J.C., Whitworth, A.J., Andrews, L.A., Parker, T.J., and Pallanck, L.J. (2005). Genetic and genomic studies of Drosophila parkin mutants implicate oxidative stress and innate immune

responses in pathogenesis. Hum. Mol. Genet. *14*, 799–811.

Guex, N., and Peitsch, M.C. (1997). SWISS-MODEL and the Swiss-PdbViewer: An environment for comparative protein modeling. Electrophoresis *18*, 2714–2723.

Guzman, J.N., Sanchez-Padilla, J., Wokosin, D., Kondapalli, J., Ilijic, E., Schumacker, P.T., and Surmeier, D.J. (2010). Oxidant stress evoked by pacemaking in dopaminergic neurons is attenuated by DJ-1. Nature *468*, 696–700.

Haddad, D., and Nakamura, K. (2015). Understanding the susceptibility of dopamine neurons to mitochondrial stressors in Parkinson's disease. FEBS Lett. *589*, 3702–3713.

Halaschek-wiener, J., Khattra, J.S., Mckay, S., Pouzyrev, A., Stott, J.M., Yang, G.S., Holt, R. a, Jones, S.J.M., Marra, M. a, Brooks-wilson, A.R., et al. (2005). Analysis of long-lived C. elegans daf-2 mutants using serial analysis of gene expression. Genome Res. 603–615.

Hall, D.H., Gu, G., García-Añoveros, J., Gong, L., Chalfie, M., and Driscoll, M. (1997). Neuropathology of degenerative cell death in Caenorhabditis elegans. J. Neurosci. *17*, 1033–1045.

Hammarlund, M., Nix, P., Hauth, L., Jorgensen, E.M., and Bastiani, M. (2009). Axon regeneration requires a conserved MAP kinase pathway. Science *323*, 802–806.

Hammarström, P., Schneider, F., and Kelly, J.W. (2001). Trans-suppression of misfolding in an amyloid disease. Science *293*, 2459–2462.

Hammarström, P., Wiseman, R.L., Powers, E.T., and Kelly, J.W. (2003). Prevention of transthyretin amyloid disease by changing protein misfolding energetics. Science *299*, 713–716.

Hansen, M., Hsu, A.-L., Dillin, A., and Kenyon, C. (2005). New Genes Tied to Endocrine, Metabolic, and Dietary Regulation of Lifespan from a Caenorhabditis elegans Genomic RNAi Screen. PLoS Genet. *1*, e17.

Hao, L., Johnsen, R., Lauter, G., Baillie, D., and Bürglin, T.R. (2006). Comprehensive analysis of gene expression patterns of hedgehog-related genes. BMC Genomics *7*, 280.

Hao, L.-Y., Giasson, B.I., and Bonini, N.M. (2010). DJ-1 is critical for mitochondrial function and rescues PINK1 loss of function. Proc. Natl. Acad. Sci. U. S. A. *107*, 9747–9752.

Hawdon, J.M., Emmons, S.W., and Jacobson, L.A. (1989). Regulation of proteinase levels in the nematode Caenorhabditis elegans. Preferential depression by acute or chronic starvation. Biochem J *264*, 161–165.

Heifetz, A., Keenan, R.W., and Elbein, A.D. (1979). Mechanism of Action of Tunicamycin on the UPD-GlcNAc:Dolichyl-Phosphate GlcNAc-1Phosphate Transferase. Biochemistry *18*, 2186–2192.

Hekimi, S., Lapointe, J., and Wen, Y. (2011). Taking a "good" look at free radicals in the aging process. Trends Cell Biol. *21*, 569–576.

Heneka, M.T., Kummer, M.P., and Latz, E. (2014). Innate immune activation in neurodegenerative disease. Nat. Rev. Immunol. *14*, 463–477.

Hengartner, M.O. (1997). Cell Death. D.L. Riddle, T. Blumenthal, B.J. Meyer, and J.R. Priess, eds. (Cold Spring Harbor (NY)), p.

Hibbs, M. a, Hess, D.C., Myers, C.L., Huttenhower, C., Li, K., and Troyanskaya, O.G. (2007). Exploring the functional landscape of gene expression: directed search of large microarray compendia. Bioinformatics *23*, 2692–2699.

Hipp, M.S., Park, S.H., and Hartl, U.U. (2014). Proteostasis impairment in protein-misfolding

and -aggregation diseases. Trends Cell Biol. *24*, 506–514.

Hoeppner, D.J., Hengartner, M.O., and Schnabel, R. (2001). Engulfment genes cooperate with ced-3 to promote cell death in Caenorhabditis elegans. Nature *412*, 202–206.

Höglinger, G.U., Carrard, G., Michel, P.P., Medja, F., Lombès, A., Ruberg, M., Friguet, B., and Hirsch, E.C. (2003). Dysfunction of mitochondrial complex I and the proteasome: interactions between two biochemical deficits in a cellular model of Parkinson's disease. J. Neurochem. *86*, 1297–1307.

Holzer, G., Morishita, Y., Fini, J.-B., Lorin, T., Gillet, B., Hughes, S., Tohmé, M., Deléage, G., Demeneix, B., Arvan, P., et al. (2016). Thyroglobulin Represents a Novel Molecular Architecture of Vertebrates. J. Biol. Chem. jbc.M116.719047.

Horvitz, H.R., Chalfie, M., Trent, C., Sulston, J.E., and Evans, P.D. (1982). Serotonin and octopamine in the nematode Caenorhabditis elegans. Science *216*, 1012–1014.

Hrus, A., Lau, G., Hutter, H., Schenk, S., Ferralli, J., Brown-Luedi, M., Chiquet-Ehrismann, R., and Canevascini, S. (2007). C. elegans agrin is expressed in pharynx, IL1 neurons and distal tip cells and does not genetically interact with genes involved in synaptogenesis or muscle function. PLoS One *2*.

Hu, P.J. (2007). Dauer. WormBook 1–19.

Hu, X., Luo, J., and Xu, J. (2015). The Interplay between Synaptic Activity and Neuroligin Function in the CNS. *2015*, 34–47.

Hu, Z., Hom, S., Kudze, T., Tong, X.-J., Choi, S., Aramuni, G., Zhang, W., and Kaplan, J.M. (2012). Neurexin and Neuroligin Mediate Retrograde Synaptic Inhibition in C. elegans. Science (80-.). *337*, 980–984.

Huang, G., Shi, L.Z., and Chi, H. (2009). Regulation of JNK and p38 MAPK in the immune system: Signal integration, propagation and termination. Cytokine *48*, 161–169.

Hui, S., and Bader, G.D. (2010). Proteome scanning to predict PDZ domain interactions using support vector machines. BMC Bioinformatics *11*.

Hui, S., Xing, X., and Bader, G.D. (2013). Predicting PDZ domain mediated protein interactions from structure. BMC Bioinformatics *14*, 27.

Hunter, J.W., Mullen, G.P., McManus, J.R., Heatherly, J.M., Duke, A., and Rand, J.B. (2010). Neuroligin-deficient mutants of C. elegans have sensory processing deficits and are hypersensitive to oxidative stress and mercury toxicity. Dis. Model. Mech. *3*, 366–376.

Ichtchenko, K., Hata, Y., Nguyen, T., Ullrich, B., Missler, M., Moomaw, C., and Südhof, T.C. (1995). Neuroligin 1: A splice site-specific ligand for β-neurexins. Cell *81*, 435–443.

Inoue, H., Hisamoto, N., An, J.H., Oliveira, R.P., Nishida, E., Blackwell, T.K., and Matsumoto, K. (2005). The C . elegans p38 MAPK pathway regulates nuclear localization of the transcription factor SKN-1 in oxidative stress response. 2278–2283.

Izquierdo, P.G., Calahorro, F., and Ruiz-Rubio, M. (2013). Neuroligin modulates the locomotory dopaminergic and serotonergic neuronal pathways of C. elegans. Neurogenetics 233–242.

Jacob, J., Vanholme, B., Haegeman, A., and Gheysen, G. (2007). Four transthyretin-like genes of the migratory plant-parasitic nematode Radopholus similis: Members of an extensive nematode-specific family. Gene *402*, 9–19.

Jacobson, L.A., Jen-jacobson, L., Hawdon, J.M., Owens, G.P., Bolanowski, M.A., Emmons, S.W., Shah, M. V, Pollock, R.A., and Conklin, D.S. (1988). Identification of a Putative Structural Gene for Cathepsin D in. *119*, 355–363.

Jadiya, P., Chatterjee, M., Sammi, S.R., Kaur, S., Palit, G., and Nazir, A. (2011). Sir-2.1 modulates "calorie-restriction-mediated" prevention of neurodegeneration in Caenorhabditis elegans: implications for Parkinson's disease. Biochem. Biophys. Res. Commun. *413*, 306–310.

Jaleel, M., Nichols, R.J., Deak, M., Campbell, D.G., Gillardon, F., Knebel, A., and Alessi, D.R. (2007). LRRK2 phosphorylates moesin at threonine-558: characterization of how Parkinson's disease mutants affect kinase activity. Biochem. J. *405*, 307–317.

Jee, C., Lee, J., Lee, J. Il, Lee, W.H., Park, B.J., Yu, J.R., Park, E., Kim, E., and Ahnn, J. (2004). SHN-1, a Shank homologue in C. elegans, affects defecation rhythm via the inositol-1,4,5-trisphosphate receptor. FEBS Lett. *561*, 29–36.

Judy, M.E., Nakamura, A., Huang, A., Grant, H., McCurdy, H., Weiberth, K.F., Gao, F., Coppola, G., Kenyon, C., and Kao, A.W. (2013). A Shift to Organismal Stress Resistance in Programmed Cell Death Mutants. PLoS Genet. *9*, e1003714.

Kaletsky, R., Lakhina, V., Arey, R., Williams, A., Landis, J., Ashraf, J., and Murphy, C.T. (2015). The C. elegans adult neuronal IIS/FOXO transcriptome reveals adult phenotype regulators. Nature 1–17.

Kaletta, T., and Hengartner, M.O. (2006). Finding function in novel targets: C. elegans as a model organism. Nat. Rev. Drug Discov. *5*, 387–398.

Käll, L., Krogh, A., and Sonnhammer, E.L.L. (2007). Advantages of combined transmembrane topology and signal peptide prediction-the Phobius web server. Nucleic Acids Res. *35*, 429–432.

Kane, L. a, Lazarou, M., Fogel, A.I., Li, Y., Yamano, K., Sarraf, S. a, Banerjee, S., and Youle, R.J. (2014). PINK1 phosphorylates ubiquitin to activate Parkin E3 ubiquitin ligase activity. J. Cell Biol. *205*, 143–153.

Kang, Y., Zhao, D., Liang, H., Liu, B., Zhang, Y., Liu, Q., Wang, X., and Liu, Y. (2012). Structural study of TTR-52 reveals the mechanism by which a bridging molecule mediates apoptotic cell engulfment. Genes Dev. *26*, 1339–1350.

Kawasaki, M., Hisamoto, N., Lino, Y., Yamamoto, M., Ninomiya-Tsuji, J., and Matsumoto, K. (1999). A Caenorhabditis elegans JNK signal transduction pathway regulates coordinated movement via type-D GABAergic motor neurons. EMBO J. *18*, 3604–3615.

Kazlauskaite, A., and Muqit, M.M.K. (2015). PINK1 and Parkin - Mitochondrial interplay between phosphorylation and ubiquitylation in Parkinson's disease. FEBS J. *282*, 215–223.

Kazlauskaite, A., Kondapalli, C., Gourlay, R., Campbell, D.G., Ritorto, M.S., Hofmann, K., Alessi, D.R., Knebel, A., Trost, M., and Muqit, M.M.K. (2014a). Parkin is activated by PINK1-dependent phosphorylation of ubiquitin at Ser65. Biochem. J. *460*, 127–139.

Kazlauskaite, A., Kelly, V., Johnson, C., Baillie, C., Hastie, C.J., Peggie, M., Macartney, T., Woodroof, H.I., Alessi, D.R., Pedrioli, P.G. a, et al. (2014b). Phosphorylation of Parkin at Serine65 is essential for activation: elaboration of a Miro1 substrate-based assay of Parkin E3 ligase activity. Open Biol. *4*, 130213.

Kazlauskaite, A., Martínez-torres, R.J., Wilkie, S., Kumar, A., Peltier, J., Johnson, C., Zhang, J., Hope, A.G., Peggie, M., Trost, M., et al. (2015). Binding to serine 65-phosphorylated ubiquitin primes Parkin for optimal PINK1-dependent phosphorylation and activation. EMBO Rep. *16*, 1–16.

Kim, D.H., Feinbaum, R., Alloing, G., Emerson, F.E., Garsin, D.A., Inoue, H., Tanaka-Hino, M., Hisamoto, N., Matsumoto, K., Tan, M.-W., et al. (2002). A conserved p38 MAP kinase pathway in Caenorhabditis elegans innate immunity. Science *297*, 623–626.

Kim, D.H., Liberati, N.T., Mizuno, T., Inoue, H., Hisamoto, N., Matsumoto, K., and Ausubel, F.M. (2004). Integration of Caenorhabditis elegans MAPK pathways mediating immunity and stress resistance by MEK-1 MAPK kinase and VHP-1 MAPK phosphatase. Proc. Natl. Acad. Sci. U. S. A. *101*, 10990–10994.

Kim, G., Weiss, S.J., and Levine, R.L. (2014). Methionine oxidation and reduction in proteins. Biochim. Biophys. Acta - Gen. Subj. *1840*, 901–905.

Kim, P.S., Hossain, S. a, Park, Y.N., Lee, I., Yoo, S.E., and Arvan, P. (1998). A single amino acid change in the acetylcholinesterase-like domain of thyroglobulin causes congenital goiter with hypothyroidism in the cog/cog mouse: a model of human endoplasmic reticulum storage diseases. Proc. Natl. Acad. Sci. U. S. A. *95*, 9909–9913.

Kitada, T., Asakawa, S., Hattori, N., Matsumine, H., Yamamura, Y., Minoshima, S., Yokochi, M., Mizuno, Y., and Shimizu, N. (1998). Mutations in the parkin gene cause autosomal recessive juvenile parkinsonism. Nature *392*, 605–608.

Klein, C., and Westenberger, A. (2012). Genetics of Parkinson's disease. Cold Spring Harb. Perspect. Med. *2*, a008888.

Ko, J., Zhang, C., Arac, D., Boucard, A. a, Brunger, A.T., and Südhof, T.C. (2009). Neuroligin-1 performs neurexin-dependent and neurexin-independent functions in synapse validation. EMBO J. *28*, 3244–3255.

Kondapalli, C., Kazlauskaite, A., Zhang, N., Woodroof, H.I., Campbell, D.G., Gourlay, R., Burchell, L., Walden, H., Macartney, T.J., Deak, M., et al. (2012). PINK1 is activated by mitochondrial membrane potential depolarization and stimulates Parkin E3 ligase activity by phosphorylating Serine 65. Open Biol. *2*, 120080.

Kostrzewa, R., and Jacobowitz, D. (1974). Pharmacological actions of 6-hydroxydopamine. Pharmacol. Rev. *26*, 200–275.

Kourtis, N., Nikoletopoulou, V., and Tavernarakis, N. (2012). Small heat-shock proteins protect from heat-stroke-associated neurodegeneration. Nature *490*, 213–218.

Koyano, F., Okatsu, K., Kosako, H., Tamura, Y., Go, E., Kimura, M., Kimura, Y., Tsuchiya, H., Yoshihara, H., Hirokawa, T., et al. (2014). Ubiquitin is phosphorylated by PINK1 to activate parkin. Nature *510*, 162–166.

Kroemer, G., Galluzzi, L., and Brenner, C. (2007). Mitochondrial Membrane Permeabilization in Cell Death. Physiol. Reveiw 99–163.

Kroemer, G., Galluzzi, L., Vandenabeele, P., Abrams, J., Alnemri, E.S., Baehrecke, E.H., Blagosklonny, M. V, El-Deiry, W.S., Golstein, P., Green, D.R., et al. (2009). Classification of cell death: recommendations of the Nomenclature Committee on Cell Death 2009. Cell Death Differ *16*, 3–11.

Krysko, D. V, Denecker, G., Festjens, N., Gabriels, S., Parthoens, E., D 'herde, K., Vandenabeele, P., D'Herde, K., and Vandenabeele, P. (2006). Macrophages use different internalization mechanisms to clear apoptotic and necrotic cells. Cell Death Differ. *13*, 2011–2022.

Kuzmanov, A., Yochem, J., and Fay, D.S. (2014). Analysis of PHA-1 reveals a limited role in pharyngeal development and novel functions in other tissues. Genetics *198*, 259–268.

Larance, M., Pourkarimi, E., Wang, B., Brenes Murillo, A., Kent, R., Lamond, A.I., and Gartner, A. (2015). Global Proteomics Analysis of the Response to Starvation in C. elegans. Mol. Cell. Proteomics *14*, 1989–2001.

Lau, L. de, and Breteler, M. (2006). Epidemiology of Parkinson's disease. Lancet Neurol. *13 Suppl 1*, 2–9.

Le, W., Sayana, P., and Jankovic, J. (2014). Animal Models of Parkinson's Disease: A Gateway to Therapeutics? Neurotherapeutics *11*, 92–110.

Lee, D., Singaravelu, G., Park, B.J., and Ahnn, J. (2007a). Differential Requirement of Unfolded Protein Response Pathway for Calreticulin Expression in Caenorhabditis elegans. J. Mol. Biol. *372*, 331–340.

Lee, F.J.S., Pei, L., Moszczynska, A., Vukusic, B., Fletcher, P.J., and Liu, F. (2007b). Dopamine transporter cell surface localization facilitated by a direct interaction with the dopamine D2 receptor. EMBO J. *26*, 2127–2136.

Lee, J., Giordano, S., and Zhang, J. (2012). Autophagy, mitochondria and oxidative stress: cross-talk and redox signalling. Harv. Bus. Rev. *441*, 523–540.

Lettre, G., and Hengartner, M.O. (2006). Developmental apoptosis in C. elegans: a complex CEDnario. Nat. Rev. Mol. Cell Biol. *7*, 97–108.

Lettre, G., Kritikou, E. a, Jaeggi, M., Calixto, A., Fraser, a G., Kamath, R.S., Ahringer, J., and Hengartner, M.O. (2004). Genome-wide RNAi identifies p53-dependent and -independent regulators of germ cell apoptosis in C. elegans. Cell Death Differ. *11*, 1198–1203.

Li, Z., and Zhou, Z. (2015). How Are Necrotic Cells Recognized by Their Predators? Worm *4054*, 00–00.

Li, C., Hisamoto, N., Nix, P., Kanao, S., Mizuno, T., Bastiani, M., and Matsumoto, K. (2012). The growth factor SVH-1 regulates axon regeneration in C. elegans via the JNK MAPK cascade. Nat. Neurosci. *15*, 551–557.

Li, Z., Venegas, V., Nagaoka, Y., Morino, E., Raghavan, P., Audhya, A., Nakanishi, Y., and Zhou, Z. (2015). Necrotic Cells Actively Attract Phagocytes through the Collaborative Action of Two Distinct PS-Exposure Mechanisms. PLoS Genet. *11*, 1–26.

Lionaki, E., and Tavernarakis, N. (2013). Oxidative stress and mitochondrial protein quality control in aging. J. Proteomics *92*, 181–194.

Liu, J., and Lin, A. (2005). Role of JNK activation in apoptosis: a double-edged sword. Cell Res. *15*, 36–42.

Liz, M.A., Faro, C.J., Saraiva, M.J., and Sousa, M.M. (2004). Transthyretin, a new cryptic protease. J. Biol. Chem. *279*, 21431–21438.

Liz, M.A., Fleming, C.E., Nunes, A.F., Almeida, M.R., Mar, F.M., Choe, Y., Craik, C.S., Powers, J.C., Bogyo, M., and Sousa, M.M. (2009). Substrate specificity of transthyretin: identification of natural substrates in the nervous system. Biochem. J. *419*, 467–474.

Lodish, H., Berk, A., and Zipursky, S. (2000). Neurotransmitters, Synapses, and Impulse Transmission. In Molecular Cell Biology, (New York: Freeman, W. H.), p.

Long-Smith, C.M., Sullivan, A.M., and Nolan, Y.M. (2009). The influence of microglia on the pathogenesis of Parkinson's disease. Prog. Neurobiol. *89*, 277–287.

López-Otín, C., Blasco, M.A., Partridge, L., Serrano, M., and Kroemer, G. (2013). The Hallmarks of Aging. Cell *153*.

Lu, J., and Holmgren, A. (2014). The Thioredoxin Superfamily in Oxidative Protein Folding. Antioxid. Redox Signal. *0*, 1–14.

Malhotra, J.D., and Kaufman, R.J. (2007). Endoplasmic reticulum stress and oxidative stress: a vicious cycle or a double-edged sword? Antioxid. Redox Signal. *9*, 2277–2293.

Mapes, J., Chen, Y.Z., Kim, A., Mitani, S., Kang, B.H., and Xue, D. (2012). CED-1, CED-7, and TTR-52 regulate surface phosphatidylserine expression on apoptotic and phagocytic cells. Curr.

Biol. *22*, 1267–1275.

Maro, G.S., Gao, S., Olechwier, A.M., Hung, W.L., Liu, M., Özkan, E., Zhen, M., and Shen, K. (2015). MADD-4/Punctin and Neurexin Organize C. elegans GABAergic Postsynapses through Neuroligin. Neuron 1–13.

Masoudi, N., Ibanez-Cruceyra, P., Offenburger, S.-L., Holmes, A., and Gartner, A. (2014). Tetraspanin (TSP-17) Protects Dopaminergic Neurons against 6-OHDA-Induced Neurodegeneration in C. elegans. PLoS Genet. *10*, e1004767.

McCutchen, S.L., Colon, W., and Kelly, J.W. (1993). Transthyretin mutation Leu-55-Pro significantly alters tetramer stability and increases amyloidogenicity. Biochemistry *32*, 12119–12127.

McCutchen, S.L., Lai, Z., Miroy, G.J., Kelly, J.W., and Colno, W. (1995). Comparison of Lethal and Nonlethal Transthyretin Variants and Their Relationship to Amyloid Disease. 13527–13536.

McDonald, P.W., Hardie, S.L., Jessen, T.N., Carvelli, L., Matthies, D.S., Blakely, R.D., and Mat (2007). Vigorous motor activity in Caenorhabditis elegans requires efficient clearance of dopamine mediated by synaptic localization of the dopamine transporter DAT-1. J. Neurosci. *27*, 14216–14227.

Melo, J. a., and Ruvkun, G. (2012). Inactivation of conserved C. elegans genes engages pathogen- and xenobiotic-associated defenses. Cell *149*, 452–466.

Minevich, G., Park, D.S., Blankenberg, D., Poole, R.J., and Hobert, O. (2012). CloudMap: a cloud-based pipeline for analysis of mutant genome sequences. Genetics *192*, 1249–1269.

Mizuno, T., Hisamoto, N., Terada, T., Kondo, T., Adachi, M., Nishida, E., Kim, D.H., Ausubel, F.M., and Matsumoto, K. (2004). The Caenorhabditis elegans MAPK phosphatase VHP-1 mediates a novel JNK-like signaling pathway in stress response. EMBO J. *23*, 2226–2234.

Mizuno, T., Fujiki, K., Sasakawa, A., Hisamoto, N., and Matsumoto, K. (2008). Role of the Caenorhabditis elegans Shc adaptor protein in the c-Jun N-terminal kinase signaling pathway. Mol. Cell. Biol. *28*, 7041–7049.

Nass, R., Miller, D.M., and Blakely, R.D. (2001). C. elegans: A novel pharmacogenetic model to study Parkinson's disease. Park. Relat. Disord. *7*, 185–191.

Nass, R., Hall, D.H., Iii, D.M.M., Blakely, R.D., and Miller, D.M. (2002). Neurotoxin-induced degeneration of dopamine neurons in Caenorhabditis elegans. Proc. Natl. Acad. Sci. U. S. A. *99*, 3264–3269.

Neumann, B., Coakley, S., Giordano-Santini, R., Linton, C., Lee, E.S., Nakagawa, A., Xue, D., and Hilliard, M. a (2014). EFF-1-mediated regenerative axonal fusion requires components of the apoptotic pathway. Nature *517*, 219–222.

Neumann-haefelin, E., Qi, W., Finkbeiner, E., Walz, G., Baumeister, R., and Hertweck, M. (2008). SHC-1 / p52Shc targets the insulin / IGF-1 and JNK signaling pathways to modulate life span and stress response in C . elegans. Genes Dev. 2721–2735.

Nguyen, T., and Südhof, T.C. (1997). Binding properties of neuroligin 1 and neurexin 1β reveal function as heterophilic cell adhesion molecules. J. Biol. Chem. *272*, 26032–26039.

Nicklas, W.J., Vyas, I., and Heikkila, R.E. (1985). Inhibition of NADH-linked oxidation in brain mitochondria by 1-methyl-4-phenyl-pyridine, a metabolite of the neurotoxin, 1-methyl-4-phenyl-1,2,5,6-tetrahydropyridine. Life Sci. *36*, 2503–2508.

Nikoletopoulou, V., and Tavernarakis, N. (2014). Necrotic cell death in Caenorhabditis elegans (Elsevier Inc.).

Nikoletopoulou, V., Markaki, M., Palikaras, K., and Tavernarakis, N. (2013). Crosstalk between apoptosis, necrosis and autophagy. Biochim. Biophys. Acta - Mol. Cell Res. *1833*, 3448–3459.

Nix, P., Hammarlund, M., Hauth, L., Lachnit, M., Jorgensen, E.M., and Bastiani, M. (2014). Axon Regeneration Genes Identified by RNAi Screening in C. elegans. J. Neurosci. *34*, 629–645.

Oh, S.W., Mukhopadhyay, A., Svrzikapa, N., Jiang, F., Davis, R.J., and Tissenbaum, H. a (2005). JNK regulates lifespan in Caenorhabditis elegans by modulating nuclear translocation of forkhead transcription factor/DAF-16. Proc. Natl. Acad. Sci. U. S. A. *102*, 4494–4499.

Oliveira, R.P., Abate, J.P., Dilks, K., Landis, J., Ashraf, J., Murphy, C.T., and Blackwell, T.K. (2009). Condition-adapted stress and longevity gene regulation by Caenorhabditis elegans SKN-1/Nrf. Aging Cell *8*, 524–541.

Ordureau, A., Sarraf, S.A., Duda, D.M., Heo, J.M., Jedrychowski, M.P., Sviderskiy, V.O., Olszewski, J.L., Koerber, J.T., Xie, T., Beausoleil, S.A., et al. (2014). Quantitative proteomics reveal a feedforward mechanism for mitochondrial PARKIN translocation and ubiquitin chain synthesis. Mol. Cell *56*, 360–375.

Oung, H.M., Lin, K.C., Wu, T.M., Chandrika, N.N.P., and Hong, C.Y. (2015). Hygromycin B-induced cell death is partly mediated by reactive oxygen species in rice (Oryza sativa L.). Plant Mol. Biol. *89*, 577–588.

Padash-Barmchi, M., Charish, K., Que, J., and Auld, V.J. (2013). Gliotactin and Discs large are co-regulated to maintain epithelial integrity. J. Cell Sci. *126*, 1134–1143.

Palikaras, K., Lionaki, E., and Tavernarakis, N. (2015). Coordination of mitophagy and mitochondrial biogenesis during ageing in C. elegans. Nature.

Park, J., Lee, S.B., Lee, S., Kim, Y., Song, S., Kim, S., Bae, E., Kim, J., Shong, M., Kim, J.-M., et al. (2006). Mitochondrial dysfunction in Drosophila PINK1 mutants is complemented by parkin. Nature *441*, 1157–1161.

Peixoto, R.T., Kunz, P. a., Kwon, H., Mabb, A.M., Sabatini, B.L., Philpot, B.D., and Ehlers, M.D. (2012). Transsynaptic Signaling by Activity-Dependent Cleavage of Neuroligin-1. Neuron *76*, 396–409.

Petersen, T.N., Brunak, S., von Heijne, G., and Nielsen, H. (2011). SignalP 4.0: discriminating signal peptides from transmembrane regions. Nat. Methods *8*, 785–786.

Pickrell, A.M., and Youle, R.J. (2015). The roles of PINK1, Parkin, and mitochondrial fidelity in parkinson's disease. Neuron *85*, 257–273.

Pinan-Lucarre, B., Gabel, C. V., Reina, C.P., Hulme, S.E., Shevkoplyas, S.S., Slone, R.D., Xue, J., Qiao, Y., Weisberg, S., Roodhouse, K., et al. (2012). The core apoptotic executioner proteins CED-3 and CED-4 promote initiation of neuronal regeneration in Caenorhabditis elegans. PLoS Biol. *10*.

Ploumi, C., Daskalaki, I., and Tavernarakis, N. (2016). Mitochondrial biogenesis and clearance: a balancing act. FEBS J.

Polymeropoulos, M.H., Lavedan, C., Leroy, E., Ide, S.E., Dehejia, A., Dutra, A., Pike, B., Root, H., Rubenstein, J., Boyer, R., et al. (1997). Mutation in the α-Synuclein Gene Identified in Families with Parkinson's Disease Mutation in the α-Synuclein Gene Identified in Families with Parkinson's Disease. Science (80-.). *276*, 2045–2047.

Portereiko, M.F., and Mango, S.E. (2001). Early morphogenesis of the Caenorhabditis elegans pharynx. Dev. Biol. *233*, 482–494.

Priyadarshi, A., Khuder, S.A., Schaub, E.A., and Priyadarshi, S.S. (2001). Environmental Risk Factors and Parkinson's Disease: A Metaanalysis. Environ. Res. *86*, 122–127.

Ravichandran, K.S. (2011). Beginnings of a Good Apoptotic Meal: The Find-Me and Eat-Me Signaling Pathways. Immunity *35*, 445–455.

Reddien, P.W., and Horvitz, H.R. (2004). The engulfment process of programmed cell death in Caenorhabditis elegans. Annu. Rev. Cell Dev. Biol. *20*, 193–221.

Reddien, P.W., Cameron, S., and Horvitz, H.R. (2001). Phagocytosis promotes programmed cell death in C. elegans. Nature *412*, 198–202.

Refai, E., Dekki, N., Yang, S.-N., Imreh, G., Cabrera, O., Yu, L., Yang, G., Norgren, S., Rossner, S.M., Inverardi, L., et al. (2005). Transthyretin constitutes a functional component in pancreatic {beta}-cell stimulus-secretion coupling. Pnas *102*, 17020–17025.

Richardson, S.J. (2015). Tweaking the Structure to Radically Change the Function: The Evolution of Transthyretin from 5-Hydroxyisourate Hydrolase to Triiodothyronine Distributor to Thyroxine Distributor. Front. Endocrinol. (Lausanne). *5*, 1–9.

Richardson, S., and Cody (Eds.), V. (2009). Recent Advances in Transthyretin Evolution, Structure and Biological Functions (Springer).

Richardson, C.E., Kinkel, S., and Kim, D.H. (2011). Physiological IRE-1-XBP-1 and PEK-1 signaling in Caenorhabditis elegans larval development and immunity. PLoS Genet. *7*, 1–10.

Rizki, G., Iwata, T.N., Li, J., Riedel, C.G., Picard, C.L., Jan, M., Murphy, C.T., and Lee, S.S. (2011). The Evolutionarily Conserved Longevity Determinants HCF-1 and SIR-2.1/SIRT1 Collaborate to Regulate DAF-16/FOXO. PLoS Genet. *7*, e1002235.

Rosenbusch, K.E., and Kortholt, A. (2016). Activation Mechanism of LRRK2 and Its Cellular Functions in Parkinson ' s Disease. *2016*.

Runkel, E.D., Liu, S., Baumeister, R., and Schulze, E. (2013). Surveillance-Activated Defenses Block the ROS–Induced Mitochondrial Unfolded Protein Response. PLoS Genet. *9*, e1003346.

Salinas, L.S., Maldonado, E., and Navarro, R.E. (2006). Stress-induced germ cell apoptosis by a p53 independent pathway in Caenorhabditis elegans. Cell Death Differ. *13*, 2129–2139.

Sämann, J., Hegermann, J., von Gromoff, E., Eimer, S., Baumeister, R., Schmidt, E., Saemann, Sa, J., and Gromoff, E. Von (2009). Caenorhabditits elegans LRK-1 and PINK-1 act antagonistically in stress response and neurite outgrowth. J. Biol. Chem. *284*, 16482–16491.

Samara, C., Syntichaki, P., and Tavernarakis, N. (2008). Autophagy is required for necrotic cell death in Caenorhabditis elegans. Cell Death Differ. *15*, 105–112.

Santos, S.D., Lambertsen, K.L., Clausen, B.H., Akinc, A., Alvarez, R., Finsen, B., and Saraiva, M.J. (2010). CSF transthyretin neuroprotection in a mouse model of brain ischemia. J. Neurochem. *115*, 1434–1444.

Sanyal, S., Wintle, R.F., Kindt, K.S., Nuttley, W.M., Arvan, R., Fitzmaurice, P., Bigras, E., Merz, D.C., Hébert, T.E., van der Kooy, D., et al. (2004). Dopamine modulates the plasticity of mechanosensory responses in Caenorhabditis elegans. EMBO J. *23*, 473–482.

Sarkar, S., Raymick, J., and Imam, S. (2016). Neuroprotective and Therapeutic Strategies against Parkinson's Disease: Recent Perspectives. Int. J. Mol. Sci. *17*.

Sarov, M., Murray, J.I., Schanze, K., Pozniakovski, A., Niu, W., Angermann, K., Hasse, S., Rupprecht, M., Vinis, E., Tinney, M., et al. (2012). A Genome-Scale Resource for In Vivo Tag-Based Protein Function Exploration in C. elegans. Cell *150*, 855–866.

Sawin, E.R., Ranganathan, R., and Horvitz, H.R. (2000). C . elegans Locomotory Rate Is Modulated by the Environment through a Dopaminergic Pathway and by Experience through a Serotonergic Pathway. Neuron *26*, 619–631.

Schafer, W.R. (2005). Egg-laying. WormBook 1–7.

Schafer, W., and Kenyon, C. (1995). A calcium-channel homologue required for adaptation to dopamine and serotonin in Caenorhabditis elegans. Nature.

Schapira, A.H., Cooper, J.M., Dexter, D., Jenner, P., Clark, J.B., and Marsden, C.D. (1989). Mitochondrial complex I deficiency in Parkinson's disease. Lancet (London, England) *1*, 1269.

Schiavi, A., Maglioni, S., Palikaras, K., Shaik, A., Strappazzon, F., Brinkmann, V., Torgovnick, A., Castelein, N., De Henau, S., Braeckman, B.P., et al. (2015). Iron-Starvation-Induced Mitophagy Mediates Lifespan Extension upon Mitochondrial Stress in C. elegans. Curr. Biol. *25*, 1810–1822.

Schmeisser, K., Mansfeld, J., Kuhlow, D., Weimer, S., Priebe, S., Heiland, I., Birringer, M., Groth, M., Segref, A., Kanfi, Y., et al. (2013a). Role of sirtuins in lifespan regulation is linked to methylation of nicotinamide. Nat. Chem. Biol. *9*, 693–700.

Schmeisser, S., Priebe, S., Groth, M., Monajembashi, S., Hemmerich, P., Guthke, R., Platzer, M., and Ristow, M. (2013b). Neuronal ROS signaling rather than AMPK/sirtuin-mediated energy sensing links dietary restriction to lifespan extension. Mol. Metab. *2*, 92–102.

Schober, A. (2004). Classic toxin-induced animal models of Parkinson's disease: 6-OHDA and MPTP. Cell Tissue Res. *318*, 215–224.

Schulte, J., Tepass, U., and Auld, V.J. (2003). Gliotactin, a novel marker of tricellular junctions, is necessary for septate junction development in Drosophila. J. Cell Biol. *161*, 991–1000.

Schulte, J., Charish, K., Que, J., Ravn, S., MacKinnon, C., and Auld, V.J. (2006). Gliotactin and Discs large form a protein complex at the tricellular junction of polarized epithelial cells in Drosophila. J. Cell Sci. *119*, 4391–4401.

Schultz, W. (2007). Multiple dopamine functions at different time courses. Annu. Rev. Neurosci. *30*, 259–288.

Schultz, W. (2016). Dopamine reward prediction error coding. Dialogues Clin. Neurosci. *18*, 23–32.

Schumacher, B., Hofmann, K., Boulton, S., and Gartner, a (2001). The C. elegans homolog of the p53 tumor suppressor is required for DNA damage-induced apoptosis. Curr. Biol. *11*, 1722–1727.

Schumacher, B., Schertel, C., Wittenburg, N., Tuck, S., Mitani, S., Gartner, A., Conradt, B., and Shaham, S. (2005). C. elegans ced-13 can promote apoptosis and is induced in response to DNA damage. Cell Death Differ. *12*, 153–161.

Sena, L.A., and Chandel, N.S. (2012). Physiological roles of mitochondrial reactive oxygen species. Mol. Cell *48*, 158–166.

Shiba-Fukushima, K., Imai, Y., Yoshida, S., Ishihama, Y., Kanao, T., Sato, S., and Hattori, N. (2012). PINK1-mediated phosphorylation of the Parkin ubiquitin-like domain primes mitochondrial translocation of Parkin and regulates mitophagy. Sci. Rep. *2*, 1002.

Shichi, K., Fujita-Hamabe, W., Harada, S., Mizoguchi, H., Yamada, K., Nabeshima, T., and Tokuyama, S. (2011). Involvement of matrix metalloproteinase-mediated proteolysis of neural cell adhesion molecule in the development of cerebral ischemic neuronal damage. J. Pharmacol. Exp. Ther. *338*, 701–710.

Shivers, R.P., Pagano, D.J., Kooistra, T., Richardson, C.E., Reddy, K.C., Whitney, J.K., Kamanzi, O., Matsumoto, K., Hisamoto, N., and Kim, D.H. (2010). Phosphorylation of the conserved transcription factor ATF-7 by PMK-1 p38 MAPK regulates innate immunity in Caenorhabditis elegans. PLoS Genet. *6*.

Sian, J., Dexter, D.T., Lees, A.J., Daniel, S., Agid, Y., Javoy-Agid, F., Jenner, P., and Marsden, C.D. (1994). Alterations in glutathione levels in Parkinson's disease and other neurodegenerative disorders affecting basal ganglia. Ann. Neurol. *36*, 348–355.

Spillantini, M.G., Schmidt, M.L., Lee, V.M., Trojanowski, J.Q., Jakes, R., and Goedert, M. (1997). α-synuclein in Lewy bodies. Nature *388*, 839–840.

Staab, T. a., Griffen, T.C., Corcoran, C., Evgrafov, O., Knowles, J. a., and Sieburth, D. (2013). The Conserved SKN-1/Nrf2 Stress Response Pathway Regulates Synaptic Function in Caenorhabditis elegans. PLoS Genet. *9*.

Staab, T. a., Egrafov, O., Knowles, J. a., and Sieburth, D. (2014). Regulation of Synaptic nlg-1/Neuroligin Abundance by the skn-1/Nrf Stress Response Pathway Protects against Oxidative Stress. PLoS Genet. *10*.

Standaert, D.G.., and Galanter, J.M. (2008). Pharmacology of Dopaminergic Neurotransmission. In Principles of Pharmacology: The Pathophysiologic Basis of Drug Therapy, D.E. Golan, A.H.J. Tashijan J, E.J. Armstrong, and A.W. Armstrong, eds. (Lippincott Williams & Wilkins), p.

Suckow, A.T., Zhang, C., Egodage, S., Comoletti, D., Taylor, P., Miller, M.T., Sweet, I.R., and Chessler, S.D. (2012). Transcellular neuroligin-2 interactions enhance insulin secretion and are integral to pancreatic β cell function. J. Biol. Chem. *287*, 19816–19826.

Südhof, T.C. (2008). Neuroligins and neurexins link synaptic function to cognitive disease. Nature *455*, 903–911.

Sullivan, P.G., Dragicevic, N.B., Deng, J.H., Bai, Y., Dimayuga, E., Ding, Q., Chen, Q., Bruce-Keller, A.J., and Keller, J.N. (2004). Proteasome inhibition alters neural mitochondrial homeostasis and mitochondria turnover. J. Biol. Chem. *279*, 20699–20707.

Sulston, J.E., and Horvitz, H.R. (1977). Post-embryonic cell lineages of the nematode, Caenorhabditis elegans. Dev. Biol. *56*, 110–156.

Sulston, J., Dew, M., and Brenner, S. (1975). Dopaminergic neurons in the nematode Caenorhabditis elegans. J. Comp. Neurol. *163*, 215–226.

Sulston, J.E., Schierenberg, E., White, J.G., and Thomson, J.N. (1983). The embryonic cell lineage of the nematode Caenorhabditis elegans. Dev. Biol. *100*, 64–119.

Suo, S., Sasagawa, N., and Ishiura, S. (2003). Cloning and characterization of a Caenorhabditis elegans D2-like dopamine receptor. J. Neurochem. *86*, 869–878.

Suzuki, J., Denning, D.P., Imanishi, E., Horvitz, H.R., and Nagata, S. (2013). Xk-Related Protein 8 and CED-8 Promote Phosphatidylserine Exposure in Apoptotic Cells. Science (80-.). *341*, 403–406.

Suzuki, K., Hayashi, Y., Nakahara, S., Kumazaki, H., Prox, J., Horiuchi, K., Zeng, M., Tanimura, S., Nishiyama, Y., Osawa, S., et al. (2012). Activity-Dependent Proteolytic Cleavage of Neuroligin-1. Neuron *76*, 410–422.

Sykiotis, G.P., and Bohmann, D. (2010). Stress-activated cap'n'collar transcription factors in aging and human disease. Sci. Signal. *3*, re3.

Syntichaki, P., and Tavernarakis, N. (2002). Death by necrosis. Uncontrollable catastrophe, or is there order behind the chaos? EMBO Rep. *3*, 604–609.

Syntichaki, P., Xu, K., Driscoll, M., and Tavernarakis, N. (2002). Specific aspartyl and calpain proteases are required for neurodegeneration in C. elegans. Nature *419*, 939–944.

Syntichaki, P., Samara, C., and Tavernarakis, N. (2005). The vacuolar H+-ATPase mediates intracellular acidification required for neurodegeneration in C. elegans. Curr. Biol. *15*, 1249–

1254.

Tabas, I., and Ron, D. (2011). Integrating the mechanisms of apoptosis induced by endoplasmic reticulum stress. Nat. Cell Biol. *13*, 184–190.

Tanner, C.M., Kame, F., Ross, G.W., Hoppin, J.A., Goldman, S.M., Korell, M., Marras, C., Bhudhikanok, G.S., Kasten, M., Chade, A.R., et al. (2011). Rotenone, paraquat, and Parkinson's disease. Environ. Health Perspect. *119*, 866–872.

Thomas, B., and Beal, M.F. (2007). Parkinson's disease. Hum. Mol. Genet. *16*, 183–194.

Tóth, M.L., Simon, P., Kovács, A.L., and Vellai, T. (2007). Influence of autophagy genes on ion-channel-dependent neuronal degeneration in Caenorhabditis elegans. J. Cell Sci. *120*, 1134–1141.

Treitz, C., Cassidy, L., Höckendorf, A., Leippe, M., and Tholey, A. (2015). Quantitative proteome analysis of Caenorhabditis elegans upon exposure to nematicidal Bacillus thuringiensis. J. Proteomics *113*, 337–350.

Troemel, E.R., Chu, S.W., Reinke, V., Lee, S.S., Ausubel, F.M., and Kim, D.H. (2006). p38 MAPK regulates expression of immune response genes and contributes to longevity in C. elegans. PLoS Genet. *2*, e183.

Troshin, P. V., Procter, J.B., and Barton, G.J. (2011). Java bioinformatics analysis web services for multiple sequence alignment-JABAWS:MSA. Bioinformatics *27*, 2001–2002.

Troulinaki, K., and Tavernarakis, N. (2011). Endocytosis and intracellular trafficking contribute to necrotic neurodegeneration in C. elegans. EMBO J. *31*, 654–666.

Tsigelny, I., Shindyalov, I.N., Bourne, P.E., Südhof, T.C., and Taylor, P. (2000). Common EF-hand motifs in cholinesterases and neuroligins suggest a role for Ca2+ binding in cell surface associations. Protein Sci. *9*, 180–185.

Tu, H., Pinan-Lucarré, B., Ji, T., Jospin, M., and Bessereau, J.-L. (2015). C. elegans Punctin Clusters GABAA Receptors via Neuroligin Binding and UNC-40/DCC Recruitment. Neuron 1–13.

Twumasi-Boateng, K. (2012). Sensing and Responding to Stress Stimuli in Caenorhabditis elegans: Implications for Aging and Immunity. University of California, Berkeley.

Uno, M., Honjoh, S., Matsuda, M., Hoshikawa, H., Kishimoto, S., Yamamoto, T., Ebisuya, M., Yamamoto, T., Matsumoto, K., and Nishida, E. (2013). A Fasting-Responsive Signaling Pathway that Extends Life Span in C. elegans. Cell Rep. *3*, 79–91.

Urra, H., Dufey, E., Lisbona, F., Rojas-Rivera, D., and Hetz, C. (2013). When ER stress reaches a dead end. Biochim. Biophys. Acta - Mol. Cell Res. *1833*, 3507–3517.

Valente, E.M., Abou-Sleiman, P.M., Caputo, V., Muqit, M.M.K., Harvey, K., Gispert, S., Ali, Z., Del Turco, D., Bentivoglio, A.R., Healy, D.G., et al. (2004). Hereditary early-onset Parkinson's disease caused by mutations in PINK1. Sci. (New York, NY) *304*, 1158–1160.

Varma, D., and Sen, D. (2015). Role of the unfolded protein response in the pathogenesis of Parkinson ' s disease. 1–26.

Varoqueaux, F., Aramuni, G., Rawson, R.L., Mohrmann, R., Missler, M., Gottmann, K., Zhang, W., Südhof, T.C., and Brose, N. (2006). Neuroligins determine synapse maturation and function. Neuron *51*, 741–754.

Vlachos, M., and Tavernarakis, N. (2010). Non-apoptotic cell death in caenorhabditis Elegans. Dev. Dyn. *239*, 1337–1351.

Voglis, G., and Tavernarakis, N. (2008). A synaptic DEG/ENaC ion channel mediates learning in C. elegans by facilitating dopamine signalling. EMBO J. *27*, 3288–3299.

Wang, X., and Yang, C. (2016). Programmed cell death and clearance of cell corpses in Caenorhabditis elegans. Cell. Mol. Life Sci. *73*, 1–16.

Wang, A., Costello, S., Cockburn, M., Zhang, X., Bronstein, J., and Ritz, B. (2011). Parkinson's disease risk from ambient exposure to pesticides. Eur. J. Epidemiol. *26*, 547–555.

Wang, X., Wang, J., Gengyo-Ando, K., Gu, L., Sun, C.-L., Yang, C., Shi, Y., Kobayashi, T., Shi, Y., Mitani, S., et al. (2007). C. elegans mitochondrial factor WAH-1 promotes phosphatidylserine externalization in apoptotic cells through phospholipid scramblase SCRM-1. Nat. Cell Biol. *9*, 541–549.

Wang, X., Li, W., Zhao, D., Liu, B., Shi, Y., Chen, B., Yang, H., Guo, P., Geng, X., Shang, Z., et al. (2010). Caenorhabditis elegans transthyretin-like protein TTR-52 mediates recognition of apoptotic cells by the CED-1 phagocyte receptor. Nat. Cell Biol. *12*, 655–664.

Wang, X., Cattaneo, F., Ryno, L., Hulleman, J., Reixach, N., and Buxbaum, J.N. (2014). The systemic amyloid precursor transthyretin (TTR) behaves as a neuronal stress protein regulated by HSF1 in SH-SY5Y human neuroblastoma cells and APP23 Alzheimer's disease model mice. J. Neurosci. *34*, 7253–7265.

Waterhouse, A.M., Procter, J.B., Martin, D.M.A., Clamp, M., and Barton, G.J. (2009). Jalview Version 2-A multiple sequence alignment editor and analysis workbench. Bioinformatics *25*, 1189–1191.

Whitworth, A.J., Theodore, D. a, Greene, J.C., Benes, H., Wes, P.D., and Pallanck, L.J. (2005). Increased glutathione S-transferase activity rescues dopaminergic neuron loss in a Drosophila model of Parkinson's disease. Proc. Natl. Acad. Sci. U. S. A. *102*, 8024–8029.

Wilhelm, M., Xu, Z., Kukekov, N. V., Gire, S., and Greene, L.A. (2007). Proapoptotic nix activates the JNK pathway by interacting with POSH and mediates death in a Parkinson disease model. J. Biol. Chem. *282*, 1288–1295.

Wojda, U., Salinska, E., and Kuznicki, J. (2008). Calcium ions in neuronal degeneration. IUBMB Life *60*, 575–590.

Wright, K.A., and Thomson, J.N. (1981). The buccal capsule of C. elegans (Nematoda: Rhabditoidea): An ultrastructural study. Can. J. Zool. *59*, 1952–1961.

Xu, K., Tavernarakis, N., and Driscoll, M. (2001). Necrotic cell death in C. elegans requires the function of calreticulin and regulators of Ca 2+ release from the endoplasmic reticulum. Neuron *31*, 957–971.

Yamashima, T. (2000). Implication of cysteine proteases calpain, cathepsin and caspase in ischemic neuronal death of primates. Prog. Neurobiol. *62*, 273–295.

Yang, J.-S.S., Nam, H.G.H.-J.J., Seo, M., Han, S.K., Choi, Y., Nam, H.G.H.-J.J., Lee, S.-J.J., and Kim, S. (2011). OASIS: Online application for the survival analysis of lifespan assays performed in aging research. PLoS One *6*, e23525.

Yee, C., Yang, W., and Hekimi, S. (2014). The intrinsic apoptosis pathway mediates the pro-longevity response to mitochondrial ROS in C elegans. Cell *157*, 897–909.

You, H., Lei, P., and Andreadis, S.T. (2013). JNK is a novel regulator of intercellular adhesion. Tissue Barriers *1*, e26845.

Young, B., Woodford, P., and O'Dowd, G. (2013). Organ systems. In Wheater's Functional Histology, A. Hall, ed. (Philadelphia: Elsevier Churchill Livingstone), p. 202.

Yue, M., Hinkle, K.M., Davies, P., Trushina, E., Fiesel, F.C., Christenson, T.A., Schroeder, A.S., Zhang, L., Bowles, E., Behrouz, B., et al. (2015). Progressive dopaminergic alterations and mitochondrial abnormalities in LRRK2 G2019S knock-in mice. Neurobiol. Dis. *78*, 172–195.

Zhang, Y., Wang, H., Kage-Nakadai, E., Mitani, S., and Wang, X. (2012). C. elegans secreted lipid-binding protein NRF-5 mediates PS appearance on phagocytes for cell corpse engulfment. Curr. Biol. *22*, 1276–1284.

Ziegler, U. (2004). Morphological Features of Cell Death. News Physiol. Sci. *19*, 124–128.

Zitvogel, L., Kepp, O., and Kroemer, G. (2010). Decoding Cell Death Signals in Inflammation and Immunity. Cell *140*, 798–804.

Zullig, S., Neukomm, L.J., Jovanovic, M., Charette, S.J., Lyssenko, N., Halleck, M.S., Reutelingsperger, C.M., Schlegel, R.A., and Hengartner, M.O. (2007). Aminophospholipid Translocase TAT-1 Promotes Phosphatidylserine Exposure during C. elegans Apoptosis. Curr. Biol. *17*, 994–999.